

KATHOLIEKE UNIVERSITEIT
LEUVEN

Arenberg Doctoral School of Science, Engineering & Technology
Faculty of Engineering
Department of Electrical Engineering

Resource Allocation in Modulation and Equalization Procedures in DSL Modems

Prabin Kumar Pandey

Dissertation presented in partial
fulfillment of the requirements for
the degree of Doctor
in Engineering

October 2011

Resource Allocation in Modulation and Equalization Procedures in DSL Modems

Prabin Kumar Pandey

Jury:
Prof. em. dr. ir. Y. Willems, president
Prof. dr. ir. M. Moonen, promotor
Prof. dr. L. Deneire (U. Nice), co-promoter
Prof. dr. ir. G. Gielen
Prof. dr. ir. I. Verbauwhede
Prof. dr. ir. G. Leus (T.U. Delft)
Prof. dr. ir. J. Louveaux (U.C.L)

Dissertation presented in partial fulfillment of the requirements for the degree of Doctor in Engineering

October 2011

© Katholieke Universiteit Leuven – Faculty of Engineering
Kasteelpark Arenberg 1/2200, B-3001 Leuven (Belgium)

Alle rechten voorbehouden. Niets uit deze uitgave mag worden vermenigvuldigd en/of openbaar gemaakt worden door middel van druk, fotocopie, microfilm, elektronisch of op welke andere wijze ook zonder voorafgaande schriftelijke toestemming van de uitgever.

All rights reserved. No part of the publication may be reproduced in any form by print, photoprint, microfilm or any other means without written permission from the publisher.

Legal depot number D/2011/7515/110
ISBN number 978-94-6018-409-3

Preface

It seems like yesterday, when I came to Leuven to start my PhD. Now it is already time to finish it and move on. It has been an incredible journey, which would not have been possible without the support of many wonderful people I met during this period.

First of all, I would like to thank Prof. Marc Moonen for giving me the opportunity to join his research group. He has been a very patient supervisor. Without his constant support, guidance and encouragement, this day would not have been possible.

I would like to thank my co-promoter Prof. Luc Deneire for all the support. I would also like to thank Prof. Geert Leus for hosting my stay at TU Delft, it was a very pleasant experience.

I would like to thank my jury members: Prof. Georges Gielen, Prof. Ingrid Verbauwhede, Prof. Geert Leus and Prof. Jerome Louveoux and Prof. Yves Willems (chairman) for agreeing to be in my examination committee. Their valuable suggestions and comments have helped to improve the quality of this dissertation.

I would like to thank my colleagues in our research group: T.J., Geert V.M., Guan ye, Sam, Imad, Paschalis, Jan, Geert R., Ann, Gert C., Simon, Vincent, Sylwester, Alex, Bram, Bruno, Rodrigo, Amir, Beier, Javier, Joseph, Pepe, Salvatore, Ludovico for making the stay enjoyable. Thanks Paschal for translating the abstract into Dutch for me. Special thanks to my good friends Kim, Romain, Deepak and Reshma for all their help, support and a lot of happy memories. Also thanks goes to Mathias, Daniele, Johan, Jean-Marc, Nuria, Mikael, Manya, Jun li for making Marie curie trips so much fun. Special thanks to my friends Akhilesh, Amit, Shambhu and his family for their support. Also thanks goes to Ilse, Ida, Lut and John for taking care of the administrative processes.

I would like to thank my parents, whose unwavering belief in me brought solace to me in difficult times and made me strong. Also special thanks to my sisters,

my brother-in-laws and my nephews and my niece for everything they have done for me.

Last but not the least, I thank my dear wife Bina for always being there for me in some of the most difficult times of my life. Without her love and support I would be lost.

Prabin Kumar Pandey
Dresden, October 2011

Abstract

Digital subscriber line (DSL) technology is a very popular broadband access technology. It uses the existing telephone infrastructure to provide broadband access. In order to cope with the increased bandwidth demand to support broadband services, such as, Video on Demand (VoD), real time multimedia streaming, it is important to further improve the DSL.

The main performance degradation of the DSL system is caused by channel impairments, such as, crosstalk and inter-symbol interference (ISI). Furthermore, the discrete Fourier transform (DFT) based discrete multitone (DMT) system has very poor spectral properties, which prohibit the use of tones at the band edges in order to meet the power spectral density (PSD) constraints of the system, thus reducing the achievable bit rate.

In order to mitigate the channel impairments as well as to combat the poor spectral properties of the DFT based DMT, sophisticated signal processing techniques are employed both in single-user DSL and multi-user DSL scenarios. These signal processing techniques increase the overall run-time complexity of the DSL system, which makes them hard to realize in practice. However, the DSL channel is a very slowly time-varying channel, which allows for offline optimization of the signal processing techniques such that their run-time complexity is reduced. This necessitates efficient algorithms to reduce the overall run-time complexity without affecting the system performance significantly.

In this dissertation, various resource allocation algorithms are investigated in order to reduce the run-time complexity of the signal processing techniques without sacrificing the performance of the system.

In the first part, resource allocation algorithms for the single-user DSL scenario are investigated. In particular, the per-tone pulse shaping filter based DMT transmitter and per-tone equalization (PTEQ) based DMT receiver will be considered. Owing to various properties of the DSL channel, the use of a constant number of non-zero filter taps in both the pulse shaping filter and the PTEQ is seen to unnecessarily increase the run-time complexity and hence an allocation

procedure for the non-zero filter taps is called for. It can be seen that the filter tap allocation problem is a combinatorial problem. In this dissertation, we propose two approaches to reduce this combinatorial complexity: The first approach is based on a contiguous filter tap selection and the second approach is based on sparse approximation based filter design. It is shown that with both of these methods the number of required non-zero filter taps and hence the run-time complexity is reduced significantly. Furthermore, it is shown that the filter tap allocation performs even better when employed in combination with transmit power allocation.

In the second part, resource allocation algorithms for the multi-user DSL scenario are investigated, where crosstalk cancellation is a crucial component. In the presence of only additive white Gaussian noise (AWGN), it has been shown that instead of performing a full so called linear zero-forcing (ZF) crosstalk cancellation only few major crosstalkers may be canceled without significant performance loss. Therefore, an optimum canceler allocation algorithm, known as partial crosstalk cancellation, only cancels the major crosstalkers per line and per tone, resulting in a significant reduction in run-time complexity. In this dissertation, we extend this partial crosstalk cancellation concept to the scenario where spatially correlated background noise is present. It is shown that in this scenario, minimum mean square error (MMSE) based cancelers outperform linear ZF cancelers. However, the optimal canceler allocation problem then has a prohibitively high complexity. In this dissertation, we propose two approaches to reduce the complexity: the first approach is based on a selection metric, which combines the information of in-domain crosstalk with information of spatially correlated background noise. Based on this selection metric the crosstalkers are ordered and selected for inclusion in the linear MMSE cancellation. This approach is then extended to include non-linear MMSE cancelers. The second approach, based on sparse approximation, directly chooses the cancelers to be taken into account by first designing a sparse linear MMSE canceler. Both of these approaches reduce the run-time complexity while performing near optimally under the resource constraint. Furthermore, it is shown that the spectrum balancing, i.e., transmit power optimization, combined with partial crosstalk cancellation further reduces the number of canceler taps required without sacrificing performance.

Korte Inhoud

Digital subscriber line' (DSL)-technologie is een zeer populaire breedbandtoegangstechnologie. Hierbij wordt gebruik gemaakt van de bestaande telefonie-infrastructuur voor het aanbieden van breedbandinternettoegang. Om echter tegemoet te komen aan de toenemende bandbreedte-vereisten van breedbanddiensten, zoals o.a. Video on Demand (VoD) en real-time multimedia streaming, is het belangrijk om DSL-technologie verder te verbeteren.

De grootste degradatie van DSL-performantie wordt veroorzaakt door kanaaldistorties zoals overspraak (crosstalk) en intersymboolinterferentie (ISI). Bovendien wordt discrete Fourier transform (DFT) gebaseerde discrete multitone (DMT) gekenmerkt door slechte spectrale eigenschappen, dat het gebruik van tonen nabij de spectrumgrenzen niet toelaat om te kunnen voldoen aan de zendvermogenbeperkingen van het systeem. Hierdoor wordt echter de maximaal bereikbare bitsnelheid beperkt.

Om de impact van de kanaaldistorties tegen te gaan en om de slechte spectrale eigenschappen van DFT gebaseerde DMT systemen aan te pakken, worden signaalverwerkingstechnieken gebruikt voor zowel enkele gebruiker als meerdere gebruiker DSL scenario's. Deze signaalverwerkingstechnieken verhogen de globale runtime complexiteit van het DSL systeem, hetgeen praktische implementatie vermoeilijkt. Het DSL kanaal is zeer traag tijdsvariÃńrend waardoor offline optimalisatie van de signaalverwerkingstechnieken mogelijk wordt, en dat toelaat om de runtime complexiteit significant te reduceren. Dit vergt efficiÃńnte algoritmes om de globale runtime complexiteit te kunnen verlagen zonder de systeemperformantie aan te tasten.

In deze thesis worden verschillende resource allocatie algoritmes onderzocht om de runtime complexiteit van signaalverwerkingstechnieken te reduceren zonder opoffering van de performantie van het systeem.

In het eerste gedeelte worden resource allocatie algoritmes onderzocht voor enkele gebruiker DSL systemen. Meer specifiek, de per-tone pulse shaping filter gebaseerde DMT transmitter en per-tone egalisatie (PTEQ) gebaseerde DMT

ontvanger worden beschouwd. Omwille van de verscheidene eigenschappen van het DSL kanaal, zorgt het gebruik van een vaste aantal niet-nul filter taps voor zowel de pulse shaping filter als de PTEQ ontvanger voor een onnodige toename in de runtime complexiteit, en daarom wordt er een selectieprocedure van de niet-nul filter taps voorgesteld. Dit filter tap selectieprobleem komt echter overeen met een combinatorisch probleem. In deze thesis stellen we twee aanpakken voor om deze combinatorische complexiteit te vereenvoudigen: De eerste aanpak is gebaseerd op een aangrenzende tap selectie en de tweede aanpak is gebaseerd op spaarse approximatie gebaseerde filterontwerp. Er wordt aangetoond dat met deze methodes het aantal vereiste niet-nul filter taps significant gereduceerd wordt. Verder wordt er aangetoond dat de filter tap allocatie een zelfs betere performantie heeft wanneer het gebruikt wordt in combinatie met zendvermogen-allocatie.

In het tweede gedeelte worden resource allocatie algoritmes onderzocht voor meerdere gebruiker DSL scenarios, waarbij crosstalk cancellatie een cruciale component vormt. In geval van additieve witte Gaussiaanse ruis (AWGN), is er aangetoond dat, in plaats van volledige lineaire zero-forcing (ZF) crosstalk cancellatie, het volstaat om enkel de grootste crosstalkers te cancellen zonder een al te grote impact op de performantie. Een optimale canceller allocatie algoritme, gekend als partiÃńle crosstalk cancellatie, zal daarom enkel de grote crosstalkers per lijn per toon cancellen, hetgeen resulteert in een significante reductie in runtime complexiteit. In deze thesis breiden wij dit partiÃńle crosstalk cancellatie concept uit tot het scenario waarbij spatiaal gecorreleerde achtergrondruis aanwezig is. Er is aangetoond dat voor dit type van scenario, minimum mean square error (MMSE) gebaseerde cancellers significant beter presteren dan lineaire ZF cancellers. Het optimale canceller allocatie probleem heeft dan echter een veel grotere complexiteit. In deze thesis stellen we twee aanpakken voor om de complexiteit te reduceren: de eerste aanpak is gebaseerd op een selectiemaat, dat de informatie van in-domein cancellatie combineert met informatie van spatiaal gecorreleerde achtergrondruis. Op basis van deze selectiemaat worden crosstalkers geÃűrdend en geselecteerd voor lineaire MMSE cancellatie. Deze aanpak wordt dan uitgebreid tot niet-lineaire MMSE cancellers. De tweede aanpak, dat gebaseerd is op spaarse approximatie, kiest de cancellers direct door eerst een spaarse lineaire MMSE canceller te ontwerpen. Beide aanpakken reduceren de runtime complexiteit met een bijna-optimale performantie onder de gegeven resource beperkingen. Verder wordt er aangetoond dat spectrum balancing (zendvermogen-optimalisatie), gecombineerd met partiÃńle crosstalk cancellatie het aantal canceller taps verder reduceert zonder opoffering van performantie.

Glossary

Mathematical notations

x	scalar term
$\mathbf{x}$	vector term
$\mathbf{X}$	matrix term
$\mathbf{x} \star \mathbf{y}$	linear convolution between $\mathbf{x}$ and $\mathbf{y}$
$\mathbf{x}^*$	complex conjugate of the vector $\mathbf{x}$
$\mathbf{X}^T$	transpose of matrix $\mathbf{X}$
$\mathbf{X}^H$	Hermitian transpose of matrix $\mathbf{X}$
$\mathbf{X}^{-1}$	inverse of matrix $\mathbf{X}$
$\|.\|$	absolute value
$\|\|.\|\|$	Euclidean norm
$\|.\|_2$	ℓ_2 norm
$\|.\|_1$	ℓ_1 norm
$\|.\|_0$	ℓ_0 pseudo norm
$[x]^+$	max(0,x)
$x \approx y$	x is approximately equal to y
$\mathbf{x} \geq \mathbf{y}$	componentwise inequality between vectors $\mathbf{x}$ and $\mathbf{y}$
$\mathcal{E}(.)$	expectation operation
$\mathcal{O}(.)$	order
diag($\mathbf{x}$)	diagonal matrix with vector $\mathbf{x}$ as diagonal
diag($\mathbf{X}$)	vector representing diagonal values of $\mathbf{X}$ as its elements

Fixed symbols

$\mathbf{I}_N$	identity matrix of size N
$\mathcal{I}_N$	$N \times N$ inverse discrete Fourier transform
$\mathcal{F}_N$	$N \times N$ discrete Fourier transform
b_k^n	bit loading of user n on tone k

s_k^n	power loading of user n on tone k
$\mathbf{H}_k$	channel matrix for tone k
$h_k^{n,n}$	direct frequency domain channel response of line n on tone k
$h_k^{n,m}$	FEXT from line m on line n
S_{budget}	total available power budget
C_{budget}	total available filter tap budget
Γ	SNR gap
x_k^n	transmitted symbol by transmitter n on tone k
y_k^n	received symbol by receiver n on tone k
$\mathbf{x}_k$	vector containing symbols of all the tranmitters on tone k
$\mathbf{y}_k$	vector containing symbols of all the receivers on tone k
z_k^n	noise signal received by receiver n on tone k
$\mathbf{z}_k$	vector containing all the received noise signal s of all receivers on tone k

Acronyms and Abbreviations

ADC	Analog-to- Digital Converter
ADSL	Asynchronous Digital Subscriber Line
AFE	Analog Front-End
ANSI	American National Standards Institute
AWGN	Additive White Gaussian Noise
BC	Broadcast Channel
BER	Bit Error Rate
BPL	Broadband Power Line
CO	Central Office
CP	Customer Premise
CPE	Customer Premise Equipment
CSA	Carrier Serving Area
DBS	Digital Broadcast Satellite
DFE	Decision Feedback Equalizer
DFT	Discrete Fourier Transform
DMT	Discrete Multi-tone
DS	Downstream
DSL	Digital Subscriber Line
DSM	Dynamic Spectrum Management
e.g.	*exempli gratia*: for example
ETSI	European Telecommunications Standards Institute
FDD	Frequency Division Duplexing
FEQ	Frequency Domain Equalizer
FEXT	Far End Croasstalk
FFT	Fast Fourier Transform

FIR	Finite Impulse Response
FTTB	Fiber to the Box
FTTC	Fiber to the Curb
FTTH	Fiber to the Home
FTTN	Fiber to the Node
GDFE	Generalized Decision Feedback Equalizer
HDTV	High Definition Television
i.e.	*id est*: that is
IC	Interference Channel
ICI	Inter carrier Interference
IDFT	Inverse Discrete Fourier Transform
IFFT	Inverse Fast Fourier Transform
ISDN	Integrated Services Digital Network
ISI	Inter Sysmbol Interference
ISP	Internet Service Provider
kbps	kilo bits per second
kHz	Kilo Hertz
LAN	Local Area Network
LOS	Line of Sight
MAC	Multiple Access Channel
Mbps	Mega bits per second
MC	Multicarrier
MHz	Megahertz
MIMO	Multi Input Multi Output
MMSE	Minimum mean squared error
MMSE-GDFE	Minimum mean squared error generalized decision feeback equalizer
NEXT	Near End crosstalk
NLOS	Non Line of Sight
OFDM	orthogonal frequency division multiplex
OLT	Optical Line termination
OSB	Optimum spectrum balancing
PCC	Partial crosstalk cancellation
PLC	Power line Communication
PSD	Power spectral density
PTEQ	Per-tone equalizer
PTPF	per-tone pulse shaping filter
QAM	Quadrature Amplitude Modulation
QoS	Quality of Service
RFI	Radio Frequency Interference
RT	Remote Terminal
SINR	Signal to interference and noise ratio
SNR	Signal to noise ratio
TEQ	Time domain equalizer

UMTS	Universal Mobile Telecommunications System
US	Upstream
VDSL	Very-high speed digital subscriber line
VoD	Video on Demand
VoIP	Voice over Internet Protocal
WiFi	Wireless Fidelity
WiMAX	Worldwide Interoperability for Microwave Access
WLL	Wireless Local Loop
ZF	Zero Forcing
ZF-GDFE	Zero Forcing Generalized decision feedback equalizer

Contents

Contents xi

1 Introduction 1

1.1 Broadband communication 1

1.1.1 Wireline broadband technologies 2

1.1.2 Wireless broadband technologies 4

1.2 Digital subscriber line (DSL) 6

1.3 DSL environment 8

1.3.1 Channel impairments 8

1.3.2 Multicarrier modulation 10

1.4 Problem statement 11

1.5 Thesis objective and approach 12

1.6 Thesis overview and contributions 13

2 Preliminaries 17

2.1 Introduction 17

2.2 Modulation schemes 17

2.2.1 Single carrier modulation 17

2.2.2 Multicarrier modulation 18

2.3 Capacity of a transmission medium 20

2.4 Discrete multitone modulation (DMT) 21
2.5 DMT transmitter 23
2.6 DMT receiver 25
2.7 Bit loading 26
2.8 Power loading 27
2.9 Equalization 29
2.9.1 Time-domain equalization 29
2.9.2 Per-tone equalization 29
2.10 Multi-user DSL 30
2.10.1 Multi-user channel model 31
2.10.2 Dynamic spectrum management (DSM) 33
2.10.3 Crosstalk cancellation 34
2.11 Sparse approximation 36
2.12 Summary 37

I SINGLE-USER RESOURCE ALLOCATION 39

3 Resource allocation in a DMT transmitter with per-tone pulse shaping filters 41

3.1 Introduction 41
3.2 System model 45
3.3 Problem formulation 46
3.3.1 Resource allocation for a fixed power loading 47
3.3.2 Joint pulse shaping filter tap and transmit power allocation 49
3.4 Resource allocation for a fixed power loading 51
3.4.1 Contiguous filter tap selection based resource allocation . . 51
3.4.2 Sparse approximation based resource allocation 53
3.5 Joint pulse shaping filter tap and transmit power allocation 56

3.5.1 Contiguous filter tap selection based resource allocation . . 56
3.5.2 Sparse approximation based resource allocation 58
3.6 Simulation results 59
3.6.1 Resource allocation for a fixed power loading 60
3.6.2 Joint pulse shaping filter tap and transmit power allocation 60
3.7 Conclusion 63

4 Resource allocation in a DMT receiver with per-tone equalization 67
4.1 Introduction 67
4.2 Preliminaries 69
4.2.1 Basic Data Model 69
4.2.2 Per-tone Equalization 70
4.2.3 Effect of PTEQ length 71
4.3 Problem formulation 72
4.3.1 Resource allocation for a fixed power loading 72
4.3.2 Joint equalizer filter tap and transmit power allocation . . . 74
4.4 Resource allocation for a fixed power loading 76
4.4.1 Contiguous filter tap selection based resource allocation . . 76
4.4.2 Sparse approximation based resource allocation 77
4.5 Joint equalizer filter tap and transmit power allocation 80
4.5.1 Contiguous filter tap selection based resource allocation . . 80
4.5.2 Sparse approximation based resource allocation 82
4.6 Simulation results 82
4.6.1 Resource allocation for a fixed power loading 84
4.6.2 Joint equalizer filter tap and transmit power allocation . . . 84
4.7 Conclusion 85

5 Joint resource allocation in DMT transceivers 89

5.1 Introduction 89
5.2 System model 90
5.3 Problem formulation 92
5.3.1 Resource allocation for a fixed power loading 93
5.3.2 Joint filter tap and transmit power allocation 95
5.4 Resource allocation for a fixed power loading 97
5.4.1 Contiguous filter tap selection based resource allocation . . 97
5.4.2 Sparse approximation based resource allocation 100
5.5 Joint filter tap and transmit power allocation 101
5.5.1 Contiguous filter tap selection based resource allocation . . 102
5.5.2 Sparse approximation based resource allocation 103
5.6 Simulation results 103
5.6.1 Resource allocation for a fixed power loading 106
5.6.2 Joint filter tap and transmit power allocation 106
5.7 Conclusion 108

II MULTI-USER RESOURCE ALLOCATION 111

6 Resource allocation in multi-user crosstalk cancellation 113

6.1 Introduction 113
6.2 System model 116
6.3 MMSE-based crosstalk cancellation 117
6.3.1 Linear MMSE canceler 117
6.3.2 Nonlinear MMSE canceler 118
6.3.3 Performance comparison 118
6.4 MMSE-based resource allocation 119
6.4.1 Computation of linear MMSE partial crosstalk canceler coefficients 120

6.4.2 Computation of MMSE-GDFE partial crosstalk canceler coefficients 121
6.5 Problem formulation 122
6.5.1 Partial crosstalk cancellation tap allocation for a fixed power loading 122
6.5.2 Joint partial crosstalk cancellation and spectrum balancing 125
6.6 Resource allocation in linear MMSE based crosstalk cancellation . 127
6.6.1 Partial crosstalk cancellation tap allocation for a fixed power loading 127
6.6.2 Joint partial crosstalk cancellation tap allocation and spectrum balancing 133
6.7 Resource allocation in MMSE-GDFE based crosstalk cancellation . 137
6.7.1 Partial crosstalk cancellation with a fixed power loading . . 137
6.7.2 Joint partial crosstalk cancellation and spectrum balancing 141
6.8 Simulation results 141
6.9 Conclusion 144

7 Conclusions and Future Work **149**
7.1 Conclusions 149
7.2 Future Work 153

Bibliography **155**

Publication List **171**

Curriculum vitae **173**

Chapter 1

Introduction

1.1 Broadband communication

Modern human life is increasingly dependent on faster and reliable information access, subsequently to broadband access. The rise in the use of bandwidth intensive applications such as real-time multimedia, streaming multimedia, voice-over-internet protocol (VoIP) etc., is fueling the demand for ever increasing data-rate and the quality of service. Furthermore, the broadband providers are trying to provide reliable " Triple Play" service to quell the need for voice, data and video services with a single connection. This has further heated the competition for faster and reliable broadband access technology. For example, in order to provide HDTV service, 15-20 Mbps downstream bandwidth is needed even after video compression [115]. This pushes the boundary of the current broadband technologies. In order to provide better broadband services, the broadband access network has been shown to be the bottleneck [117]. There are many broadband access technologies that promise much faster and reliable services if the access network is overhauled. But the cost of the deployment of the new access network has thus far proved to be prohibitive. Therefore, the broadband service providers want to increase the quality of service provided to subscribers but either without any overhaul or with minimum overhaul of the existing access network. Then in time the access network can be gradually replaced such that the cost is spread over time.

There are various competing broadband technologies, e.g., cable modem, DSL, 3G, WiMAX etc. Each technology has its advantages and disadvantages. We can broadly classify the existing broadband technologies into two categories; wireline broadband technologies and wireless broadband technologies.

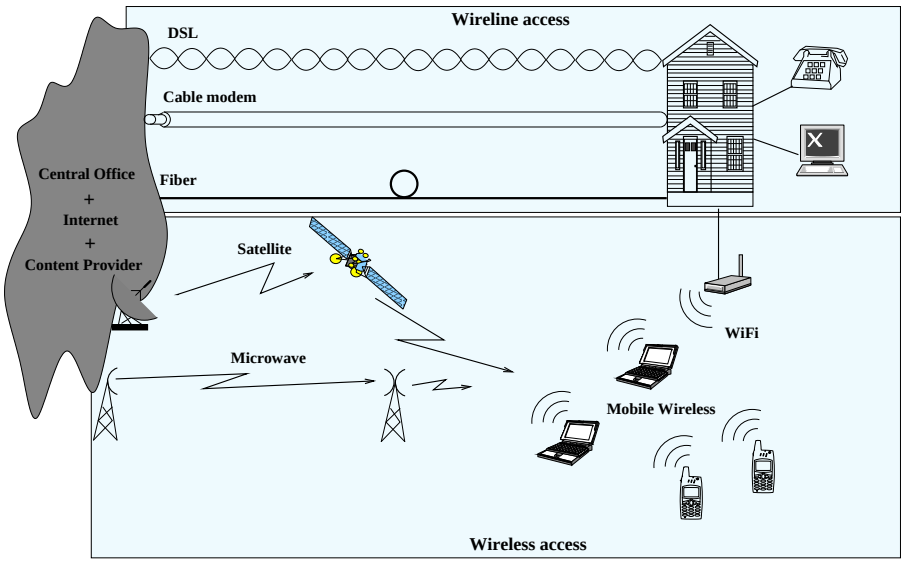


Figure 1.1: Broadband Access Network

1.1.1 Wireline broadband technologies

Wireline broadband technology relies on a physical connection to the subscriber's premise. The existing cable TV connection, telephone connection and the power line connection can all be used for this type of broadband technology. The optical fiber connection is also an example of the wireline broadband technology. The optical fiber connection promises tremendous amounts of bandwidth but the deployment of an optical fiber network in large scale has proven to be very expensive. We introduce some of the wireline broadband technologies in more detail in the following sections.

Hybrid fiber coax (HFC)

HFC uses the coaxial cable TV infrastructure to offer a broadband connection to the subscriber. Since many subscribers of broadband services already have an existing cable TV connection, this has become a popular broadband technology. The recently proposed HFC standard DOCSIS 3.0 may be able to provide 100 Mbps per channel of 8 MHz [115, 79]. However in cable modem broadband access, the bandwidth is shared because the same cable line connects several subscribers.

Therefore, the broadband experience depends on the number of subscribers sharing the same cable connection. As a consequence, the typical data rate is around 1 Mbps downstream and 128 kbps upstream [115].

Broadband power line (BPL)

BPL utilizes the existing power lines for high speed data transmission [74]. In a BPL system, data is transmitted as a low voltage high frequency signal coupled with the high voltage low frequency power signal [115]. The subscribers can plug in the modem into an ordinary wall outlet to receive broadband internet access. In practice, it has not seen a large scale deployment because it requires investment to upgrade the power transmission network to support high speed broadband services. Furthermore, the BPL environment is inherently quite noisy and the frequencies used by BPL often interfere with the amateur radio transmission. Nevertheless, BPL remains as a broadband option.

Digital subscriber line (DSL)

DSL technology uses the existing telephone network infrastructure to provide broadband connections [19, 44, 143, 64, 63]. This is achieved by splitting the voice and the data signal into distinct frequency bands. For example, frequencies up to 4 KHz carry the voice signal in traditional telephony and higher frequencies are used to carry the data stream. The frequency band carrying data can be further split into two frequency bands, namely, an upstream (US) frequency band and a downstream (DS) frequency band. DSL using equal bandwidth for upstream and downstream frequency bands is called symmetric DSL (SDSL). If the DSL uses unequal bandwidth for the upstream and downstream bands, it is known as asymmetric DSL (ADSL). However, DSL has a drawback that its performance is sensitive to the loop length i.e. the broadband data rate depends on the distance between the subscriber and the central office (CO). ADSL can provide maximum DS data rates up to 12 Mbps and US data rates up to 640 Kbps. The distance limit for ADSL is 5.4 Km, for this distance ADSL can provide approximately 500 Kbps DS data rate. In order to provide video on demand (VoD) service, the minimum DS data rate required is 15-20 Mbps, which pushes the boundary of current DSL systems. Various types of DSL, e.g., VDSL, VDSL2 etc., have been proposed in order to provide faster and more reliable broadband access. These DSL types increase the data rate by decreasing the loop length and increasing the available bandwidth, e.g. VDSL2 offers a data rate of 100-200 Mbps over a distance of 300m [116]. The variety in DSL techniques allows diversity in the service provided and can be deployed as per subscriber demand. The main features of DSL technology, its history and advances will be presented in detail in section 1.2.

Fiber to the curb/home (FTTx)

The term FTTx refers to a set of technologies that bring fiber a step closer to the subscriber [122, 115]. It uses the optical fiber to provide the broadband services. Optical fiber exhibits very low signal attenuation over long distances and do not suffer much from interference. Furthermore, it also provides much larger transmission bandwidth than any other broadband access medium. Fiber to the curb (FTTC), as the name suggests, does not connect individual subscribers to an optical fiber but the optical fiber connection is terminated near the subscriber premises. Then technologies like VDSL are used to connect the individual subscribers. The goal is to gradually move towards a fiber to the Home (FTTH) broadband access network, where all subscribers have an individual high speed physical fiber connection. But installing such a fiber access network is difficult, time-consuming, and very cost sensitive. Therefore, the existing fiber network is being gradually extended toward the end-users and then the last mile is covered by using other broadband access technologies such as DSL or BPL.

1.1.2 Wireless broadband technologies

Wireless broadband refers to the use of wireless technologies to transmit broadband signals [115]. It uses very high bandwidth relative to the carrier frequency [101]. The higher frequencies have an advantage over the lower frequencies as more spectrum is available at higher frequencies and smaller antennas can be used. However, at high frequencies signal attenuation is higher, therefore the distance over which a subscriber can be catered is limited.

The wireless technologies can be subdivided into several other categories according to different aspects of transmission. Satellite communication systems such as geostationary earth orbit satellite (GEOS) and microwave transmission links require direct line-of-sight (LOS) to be able to operate. Hence, these can be categorized as a LOS wireless broadband communication technologies. In contrast, mobile communication technologies in general do not rely on direct LOS for communication therefore can be categorized as a nonline-of-sight (NLOS) wireless broadband communication technologies. Similarly, wireless communication systems, where the transmitter and receiver are fixed (e.g. microwave links), can be categorized as a fixed wireless broadband communication technologies and when the transmitter and receiver are in relative motion, this can be categorized as a mobile wireless broadband communication technology. This includes WiFi and 3G wireless communication systems.

Satellite communication

Satellite communication entails the use of artificial satellites to provide communication links to connect different geographic locations [125, 115]. This has been primarily used to connect remote and inaccessible landscapes by using small portable terminals, e.g., Very Small Aperture Terminals (VSATs). Other uses are broadcasting TV signals (Direct Broadcast Satellites (DBS)), providing transnational communication links etc. The geostationary satellite typically has a 250ms delay, which is unacceptable for broadband services. However, the lower earth orbit satellites (LEOS) can reduce this delay significantly. But it needs significantly more satellites to offer the same coverage.

Microwave links

Microwave links are an example of fixed wireless communication technologies. It uses two fixed microwave transceivers with direct LOS [127, 115]. These have been used to connect geographically inaccessible areas, where deployment of cables is not possible. These areas can be connected with the microwave link and then the local population can be connected either with a cable network or a wireless local loop (WLL). The major drawback of the microwave link is that it relies on direct LOS, which is not always possible.

Wireless fidelity (WiFi) and Worldwide interoperability for microwave access (WiMAX)

WiFi is the wireless communication technique using a wireless local area network (WLAN) based on IEEE 802.11x standards [70]. WiFi enabled devices can connect to the internet when they are within range of a wireless network, known as access point (AP), connected to the internet. WiFi also allows communication directly from one WiFi enabled device to another WiFi enabled device without the involvement of an AP. The main disadvantages of WiFi are that the spectrum assignment is not consistent worldwide and the reach of a WiFi network is limited to 100m in general.

WiMAX is a wireless digital communications system, also known as IEEE 802.16. It is an IP based wireless broadband access technology. It has similar performance to WiFi but provides the coverage and quality of service (QoS) similar to cellular networks. It can provide broadband wireless access up to 50 km for fixed stations, and 5 - 15 km for mobile stations. WiMAX operates on both licensed and non-licensed frequencies. WiMAX network operators typically provide a WiMAX subscriber unit, which connects to the WiMAX network and then WiFi can be used to provide the connection within the house or business. The main

disadvantages of WiMAX are that LOS is needed for distant connections, bad weather conditions can affect the performance, and also other wireless equipment can cause interference.

Mobile communication (3G and beyond)

Third generation (3G) and beyond mobile communication technologies, such as UMTS, CDMA2000, LTE, feature higher data rates for internet access and real-time video [50]. Its services include voice telephony, mobile Internet access, video calls and mobile TV, all in a mobile environment. Recent 3G systems, denoted as 3.5G and 3.75G, also provide mobile broadband access of several Mbit/s to laptop computers and smartphones. Evolved high-speed packet access (HSPA+) can provide peak data rates up to 56 Mbit/s in the downlink in theory and 22 Mbit/s in the uplink. The main disadvantage of wireless mobile communication is that the channel is shared by many users, therefore the QoS depends on the number of active users at a certain time. Furthermore, the scarcity of bandwidth also is a big hindrance.

Currently, the DSL technology remains the most popular broadband access technology. The main reason for the popularity of the DSL is that it can utilize existing telephone networks to provide broadband access. It is also more cost effective than the other broadband access technologies, such as cable modem, optical fiber, satellite links etc. A recent survey has shown that the number of DSL subscribers is increasing yearly [164] and it is predicted to rise further in the coming years. Considering these trends, DSL broadband access is expected to be an important player in the field of broadband access in the future. However, it is important that the DSL continues to improve in order to remain competitive with the other broadband access techniques.

In the following section, we will introduce DSL in more detail.

1.2 Digital subscriber line (DSL)

Data communication over the telephone line started with the invention of the electric telegraph by Samuel Morse in 1844 [135] and the telephone by Alexander Graham Bell [16]. After more than a century of transmitting data in the voiceband, i.e., up to 4KHz, [105] Joseph Lechleider of Bellcore demonstrated that it is possible to transmit broadband signals over telephone lines in the late 1980s.

The integrated services digital network (ISDN) can be viewed as the first digital subscriber line (DSL) technology, which was able to provide an aggregate bit-rate of 160 kbps using a bandwidth of 80 kHz [118]. But the real broadband service

over the telephone line started with the deployment of ADSL in 1995. ADSL is specially suited for applications such as internet access and VoD. ADSL uses a bandwidth of 1.1 MHz, which is divided into multiple tones (sub-bands) using a discrete multitone (DMT) modulation scheme. The successor of ADSL is VDSL and VDSL2, which uses a bandwidth up to 30 MHz to provide a higher data rate in order to meet the increasing broadband demands. Figure 1.2 illustrates a typical DSL access network. It consists of a central office (CO), which is connected to the content provider with an optical fiber connection. From the CO twisted pair cables originate to connect to the subscribers. A pair of DSL modem is required, one at each side, to set up the DSL connection. Also, a subscriber can be connected to the CO via a remote terminal (RT). An optical network unit (ONU) can be connected to the optical line terminal (OLT) in the CO via an optical fiber connection in order to reduce the length of the twisted pair cable between the CO and the subscriber. The ONU can then use the twisted pair cable to deliver a VDSL/VDSL2 connection over a small distance.

The telephone infrastructure was originally designed to only offer voice telephony, which uses the bandwidth between 0 and 4 kHz. But in order to deliver broadband services, a higher bandwidth, up to 30 MHz, is used. This results in a DSL environment with many channel impairments. In the following section, we present various aspects of the DSL environment, which affect its performance.

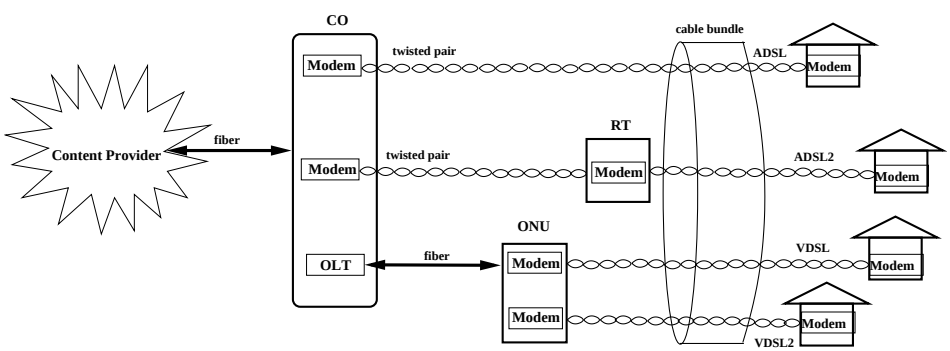


Figure 1.2: Typical DSL access network

1.3 DSL environment

1.3.1 Channel impairments

In this section, we will give an overview of some major transmission impairments in the DSL systems [43, 46, 65, 136] and its effect on the performance of the DSL system [15, 38, 83, 133, 85].

Transmission channel

The transmission channel causes distortion for any communication system. It also causes the signal to be attenuated as a function of frequency and loop length. This creates problems for subscribers that are far away from the central office and also limits the use of the higher frequencies. Furthermore, due to the dispersive nature of the channel, which can be typically represented by the impulse response of the channel, adjacent symbols overlap at the receiver. This is known as intersymbol interference (ISI). The channel dispersion and the attenuation is caused, firstly, by bridged taps [168, 39, 146], which are unterminated distribution cables. Secondly, the use of different wire gauges along a line also causes reflections due to the impedance mismatch at the junction of two line sections with different wire gauges. To mitigate the effect of the channel distortion and attenuation, a channel equalizer is employed [19, 44, 143].

Crosstalk

The twisted pairs in the wired access network are bundled within large binder groups consisting of 20 to 100 individual pairs per binder. Therefore, the pairs within a binder experience electromagnetic coupling known as crosstalk from each other [56, 58]. There are two types of crosstalks, namely, near-end crosstalk (NEXT) and far-end crosstalk (FEXT). The NEXT is caused by a neighboring transmitter on a different pair whereas the FEXT is caused by the signal originating from a remote transmitter on a different pair. Both the NEXT and the FEXT power increase with frequency e.g. NEXT $\sim f^{3/2}$ and FEXT $\sim f^2$ [63]. When the transmitters and the receivers at both ends of the binder are co-located then the NEXT is much more severe than the FEXT. This is due to the fact that the FEXT is attenuated by the channel transfer function. The effect of the NEXT can be reduced by using frequency division duplexing (FDD), where the upstream and the downstream data occupies different frequency bands [137, 139, 100]. If the FEXT originates from a remote terminal (RT) in the field then the effect might be severe, since it may be near the receiver. This is known as the near-far scenario. The effects of the FEXT can be mitigated by using power

backoff [80, 172, 163, 132], spectrum coordination [141, 30] or signal coordination [61, 60, 26, 25, 155] techniques. When the interference arises from either a line with a different DSL format or from uncoordinated DSL lines in a vectored DSL scenario, it is known as alien crosstalk [143, 131, 62]. In some cases, it might be the dominating interference in the DSL system. Mitigating the effect of the alien crosstalk is much more challenging than mitigating the effect of other interferences such as NEXT, FEXT etc. Some techniques to mitigate the effect of the alien crosstalk have been suggested in [178, 162, 62, 155, 20, 167].

Radio frequency interference (RFI)

Every telephone line acts as an antenna that emits and receives radio energy. Radio frequency signals in the same frequency range as the DSL from wireless transmitters impinge on the unshielded telephone line, which results in radio frequency interference (RFI) [144]. Since VDSL uses higher frequency bands, the RFI is specially important. There are two types of interferences, the first *egress* is caused by the DSL into a radio receiver and the second, *ingress* is the interference caused by the radio transmitter into the DSL. Techniques to suppress RFI ingress and egress are presented in [138, 104] and [14, 92, 47, 48] respectively.

Impulse noise

Sudden switching of electronic devices in the vicinity of telephone lines causes impulse noise. These are narrow pulses in time with very high level of noise compared to the received DSL signal level [84, 103, 44, 143]. It is difficult to characterize the impulse noise completely but there has been some effort to measure and model impulse noise [136, 170, 45, 71, 53, 123]. Different techniques to mitigate the impulse noise are presented in [75, 68, 95, 150].

Thermal noise

Due to the thermal agitation of the electrons in the copper wire, DSL systems experience a constant background noise known as thermal noise. The thermal noise limit is -173 dBm/Hz at room temperature but due to the quantization noise of the analog-to-digital converter (ADC) the limit is set to -140 dBm/Hz [19, 143].

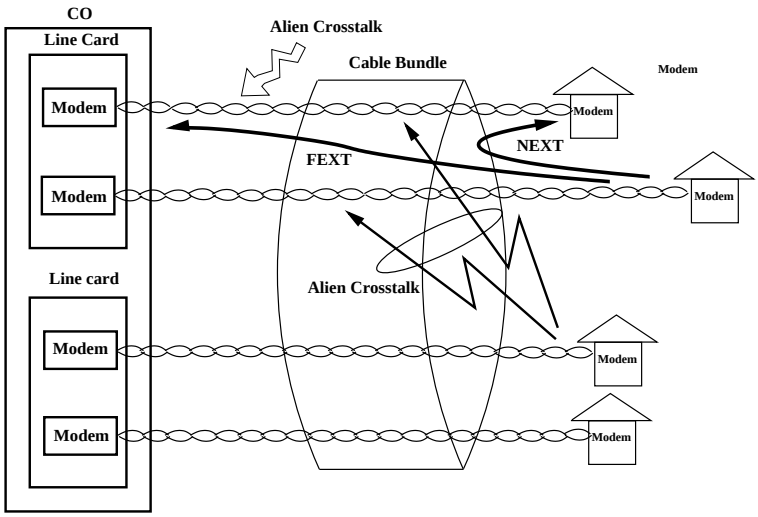


Figure 1.3: Various channel impairments in DSL

1.3.2 Multicarrier modulation

In order to deal with the frequency selectivity of the transmission channel, the channel can be divided into many sub-channels (tones), each with flat frequency response. This is known as multicarrier (MC) modulation [18]. In 1960s, the first analog multicarrier systems were implemented [31, 128] with disjoint frequency bands. In [128, 31, 72], it was shown that the spectral overlap may not result in ISI/ICI after reception. Use of discrete Fourier transform (DFT) for MC modulation was first proposed by Weinstein [169, 72, 73]. DFT based MC is the basis of popular techniques such as orthogonal frequency division multiplexing (OFDM) [3, 44]. OFDM is used in WLAN, digital video broadcast (DVB), WiMAX etc. [70, 50, 179]. The performance of the MC system can be further improved by using adaptive bit loading, which allows a different number of bits to be transmitted on different tones taking their channel state into account [19, 37, 44, 82, 88]. The modulation format used in DSL is referred to as discrete multitone modulation (DMT) and corresponds to OFDM with bit and power loading. Bit loading in WLAN/OFDM was proposed in [158]. In order to mitigate the effect of channel distortion and ISI, an OFDM system needs equalization at the receiver [19, 44, 120, 8, 2]. However, a DFT based MC system has very poor spectral characteristics, requires very stringent synchronization and also exhibit a high peak-to-average power ratio (PAPR). In order to overcome these drawbacks of the DFT based MC system, other MC modulation techniques, such as discrete wavelet multitone (DWMT) [4], filtered multitone (FMT) [34, 35, 147, 23], cosine modulated [54] and non-orthogonal pulse based systems [22, 86, 156], have been

proposed. However, due to its simple implementation using fast Fourier transform (FFT), DMT remains very popular.

1.4 Problem statement

The rise in the use of bandwidth intensive broadband applications has increased the demand for faster and more reliable broadband access. In the meantime, the rise of various broadband access technologies has increased the competition for the broadband market. To meet the demand and remain competetive, DSL technology also has to improve constantly.

Gradual decrease in the loop length and increased use of optical fiber has enabled the DSL to use higher frequencies to provide higher data rates. However, the DSL channel is highly dispersive and hence frequency selective in nature. To overcome the frequency selectivity of the DSL channel, a DFT based MC modulation technique referred to as DMT, is being used. However, a DMT transmitter has very poor spectral properties. The sidelobes are high and they decay very slowly. This causes problems while transmitting under a PSD constraint. Many tones at the band edges cannot be used because the PSD mask constraint will be violated. These unused tones are known as virtual carriers (VC). In order to improve the poor spectral properties, a transmit windowing is used. In [33], it was shown that the per-tone pulse shaping improves the spectral containment of a DFT based MC transmitter compared to time domain transmit windowing, hence reduces the number of VC's and increases the achievable data rate.

Due to the dispersive channel, block transmission based systems, such as the DMT system, suffer from inter-symbol interference and inter-carrier interference (ISI/ICI). In order to remove ISI, it was shown that a guard time known as the cyclic prefix (CP) can be added. This transforms the linear convolution between the channel input and the channel into a cyclic convolution, thus converting the corresponding channel matrix into a circulant matrix. A circulant matrix can be diagonalized by applying a DFT and an IDFT matrix. This converts the frequency selective channel into multiple parallel independent additive white Gaussian noise (AWGN) channels. These can be easily equalized by using a 1-tap equalizer. But in order for all this to work, the length of the CP should be greater than the length of the channel impulse response (CIR). Dispersive channels, such as the DSL channel, have a very long CIR, therefore an equally long CP is required. This reduces the effective throughput of the DSL system. One way to reduce the CP length is to shorten the effective CIR by using a channel shortening filter at the DSL receiver. In [2], it was shown that a minimum mean squared error per-tone equalization (MMSE-PTEQ) performs much better than the time-domain channel shortening combined with a 1-tap frequency domain equalizer (FEQ), without increasing the run-time complexity.

In the multi-user scenario, multiple lines are bundled in the same binder, which causes crosstalk. Crosstalk has been shown to be a major cause of performance degradation in DSL systems. In the literature, various techniques to mitigate the effect of crosstalk have been presented. In [61, 60, 26, 25, 30, 155], it has been shown that the effect of crosstalk can be mitigated by using various spectrum coordination and signal coordination techniques for different levels of transmit and receive coordination. When spatially correlated background noise (alien crosstalk) is also present, the crosstalk mitigation becomes much more challenging [62].

The windowing, equalization and crosstalk mitigation as described above require sophisticated signal processing techniques. These extra signal processing techniques increase the overall run-time computational complexity of the DSL system, which makes it hard to realize in practice.

However, the DSL channel is a very slowly time-varying channel. This allows for offline optimization of the signal processing techniques such that their run-time complexity is reduced. This necessitates efficient algorithms to reduce the overall run-time computational complexity without affecting the system performance significantly. This in turn enables the implementation of sophisticated signal processing algorithms to mitigate the channel effects in practice, hence increasing the achievable data rate for the DSL system.

1.5 Thesis objective and approach

The main objective of this dissertation is to provide efficient resource allocation algorithms for the DMT transceivers, which will enable them to operate at a much reduced run-time computational complexity without sacrificing performance.

For the per-tone pulse shaping based DMT transmitter, the effect of sparse per-tone filters is investigated. Since the contribution to the stopband energy from a tone depends on its position in the passband, not every pulse shaping filter needs to have the same number of non-zero filter taps. This enables us to apply efficient resource allocation algorithms to reduce the number of non-zero filter taps of the pulse shaping filters and hence reduce the run-time computational complexity

Similarly, for the per-tone equalization based DMT receiver, it can be shown that due to the frequency selective nature of the DSL channel, the use of a fixed length non-sparse equalizer wastes computational resources. This enables us to apply efficient resource allocation algorithms to reduce the number of non-zero PTEQ filter taps, hence reducing the run-time computational complexity.

It can also be seen that the per-tone operation based transmitter and receiver affect each other. Hence, the resource allocation algorithms can take this into account

to jointly optimize the resources in the DMT receiver and the DMT transmitter, thus reducing the joint run-time computational complexity.

We then move to the multi-user DSL scenario, where there are multiple lines in the same binder. In the presence of alien crosstalk, it is known that MMSE based crosstalk cancellation performs better than zero-forcing (ZF) based crosstalk cancellation. In zero-forcing based receivers, the run-time complexity can be reduced by employing a technique known as partial crosstalk cancellation. However, in MMSE based crosstalk cancellation, it is not straightforward to use the partial crosstalk cancellation technique.

1.6 Thesis overview and contributions

In this section, we will provide an overview of the thesis and its contributions.

In **Chapter 2**, the basic concept of DSL transmission is presented in detail. Different modulation schemes for DSL systems are compared. We then present the basic structure of the DMT transmitter and receiver and outline their main operations. The block transmission scheme of DMT is also presented in detail and various drawbacks of block transmission over a dispersive channel, such as inter-symbol interference (ISI) and inter-carrier interference (ICI), are also highlighted. We then present some well known techniques to mitigate these drawbacks. The multi-user scenario arises in the DSL system when multiple lines in the same binder interfere with each other. In this chapter, a system model of multi-user DSL is presented. The multi-user channel model is then presented in detail. We also explore the effect of crosstalk in such a scenario and then present various crosstalk mitigation techniques presented in literature for different levels of line coordination. Finally, some receiver structures to mitigate the crosstalk will be presented.

The resource allocation techniques devised to reduce the run-time computational complexity of different signal processing blocks can be applied in both the single-user and the multi-user DSL scenario.

Part I of this dissertation investigates resource allocation techniques for a single-user DSL scenario. The channel characteristics of the DSL system demand that different sub-channels be treated differently. Therefore, the resource allocation algorithms should try to take advantage of these characteristics to efficiently allocate the available resources such that the system performs near optimally with much reduced run-time complexity.

In **Chapter 3**, we first highlight that a DMT transmitter has poor spectral properties due to the DFT based windowing. In applications, e.g. in VDSL, the Power Spectral Density (PSD) of the transmitted signal is not allowed to exceed

a given PSD mask defining one or more pass bands and stop bands. To meet this constraint, various transmit windowing techniques have been presented in the literature. In this chapter, we focus on the per-tone pulse shaping presented in [33]. It tries to minimize the spectral leakage by shaping each tone separately by using a constant length non-sparse pulse shaping filter. This was shown to outperform time-domain based transmit windowing. In [33], per-tone transmit windowing was shown to significantly reduce the number of virtual carriers, i.e., number of null tones at the band edges. But the contribution to the out of band energy depends on the position of the tone in the band, therefore the design parameter (number of non-zero filter taps) to effectively shape each tone also varies. In this chapter, we show that the number of filter taps required to meet the PSD constraint without affecting the performance can then be reduced significantly hence reducing the run-time computational complexity. Efficient resource allocation algorithms are needed in order to allocate the non-zero filter taps. In this chapter, we present efficient algorithms to achieve this goal. The first algorithm presented uses only contiguous filter taps in order to reduce the number of combinations of non-zero filter taps, thus reducing a combinatorial search in the number of taps to a linear search in the filter order. We call this contiguous filter tap selection (CTS) approach. However, restricted sparsity pattern, such as CTS, may not result in the best sparse filters, since the optimal filter sparsity pattern may not be in that search space. To address this problem, we propose a sparse approximation based filter tap selection algorithm. This ensures that there is no restriction on the sparsity pattern of the filter and hence is shown to perform better than the CTS based resource allocation. Furthermore, it is shown that the number of non-zero filter taps can be further reduced when an optimal power allocation is performed alongside the filter tap allocation.

In **Chapter 4**, we first highlight that the dispersive nature of DSL channels results in ISI. In order to mitigate ISI, a guard interval known as cyclic prefix is added. But the length of the cyclic prefix depends on the channel impulse response. For the systems that have long channel impulse responses, e.g., DSL, channel shortening is required in order to limit the length of the cyclic prefix. To this end, several techniques have been proposed in the literature. In [2], a frequency domain based equalizer, known as per-tone equalization (PTEQ), has been proposed to equalize each tone individually. It uses a constant length non-sparse equalizer on each tone to achieve this. The PTEQ has been shown to outperform time-domain channel shortening combined with a 1-tap frequency domain equalizer without increasing the computational complexity. Due to the frequency selective nature of the DSL channel, different tones have different equalization requirements. We show that the number of non-zero equalizer taps required to equalize each tone varies over tones. Therefore, the number of non-zero equalizer taps required can be reduced without affecting the performance significantly. In this chapter, we propose efficient algorithms to this end. The first algorithm is based on selecting only contiguous filter taps in order to reduce the search space, which

is combinatorial in the filter length, to a linear search space in the filter order. We call this algorithm the contiguous filter tap selection (CTS) approach. The second algorithm is based on sparse approximation, where the sparsity pattern of the PTEQ is not restricted. This is shown to outperform the CTS approach. We also demonstrate that performing an optimal transmit power allocation alongside the filter tap allocation further reduces the number of non-zero filter taps required.

In **Chapter 5**, we then look into the DMT transceiver with per-tone pulse shaping and per-tone equalization. In chapter 3, we assumed that the channel impulse response fits in the cyclic prefix perfectly and hence ignored the effect of ISI. In this chapter, we will look into the effect of the channel impulse response in the received signal-to-noise ratio. Then the effect of channel shortening on the resource allocation in the per-tone based DMT transceiver is investigated. To this end, we analyze both the CTS based resource allocation and the sparse approximation based resource allocation. By taking the channel equalization into account we can also compensate for the filtering at the transmitter side. It can be shown that we can then minimize the overall run-time complexity of the transceiver.

The publications related to chapter 3 are [108, 107, 114].The publications related to chapter 4 are [106, 112] and the publication related to chapter 5 is [110].

Part II of this thesis investigates resource allocation for a multi-user scenario.

In **Chapter 6**, we first present the concept of crosstalk cancellation for upstream VDSL in detail. We consider the scenario where the receivers are co-located and hence receiver coordination is possible. In [25], it was shown that due to the columnwise diagonally dominant (CWDD) structure of the upstream multi-user DSL channel matrix, a simple linear zero forcing (ZF) receiver performs near optimally in the presence of AWGN background noise. In [27], it was also shown that the majority of the crosstalk originates from a very small set of lines, hence canceling only these lines would reduce the run-time computational complexity without affecting the performance significantly. This is referred to as partial crosstalk cancellation. In the presence of spatially correlated background noise, however, a prewhitening operation is required, which destroys the CWDD structure of the DSL channel matrix, therefore a linear zero-forcing canceler performs poorly. Furthermore, the partial cancellation algorithm presented in [27] also fails to achieve satisfactory results. Hence in this chapter, we first show that linear and non-linear MMSE based cancelers outperform the linear zero forcing (ZF) canceler in the presence of spatially correlated background noise. We then extend the concept of partial crosstalk cancellation to MMSE based cancelers. To this end, we propose two efficient algorithms. The first algorithm is based on metric selection, which combines the channel crosstalk information and the noise autocorrelation information to efficiently select the crosstalk line to be cancelled for both the linear as well as the non-linear MMSE based crosstalk cancelers. For the linear MMSE crosstalk canceler, we propose a second algorithm based on

sparse approximation, which searches for the best crosstalk lines to be canceled. It is further shown that the use of optimal power allocation along with the partial crosstalk cancellation further improves the performance.

The publications related to chapter 6 are [109, 113, 111].

In **Chapter 7**, conclusions are drawn and some directions for future work are discussed.

Chapter 2

Preliminaries

2.1 Introduction

In this chapter, we will provide an overview of various aspects of multicarrier modulation, DMT and DSL. In the **sections 2.2.1** and **2.2.2**, differences between a single carrier and a multicarrier communication system are highlighted. **Section 2.3** introduces the information theoretic capacity of a given channel in a multicarrier communication. In **section 2.4** the DMT modulation scheme used in DSL system is presented. The transmitter and receiver structure for the DMT system are presented in **section 2.5** and **2.6** respectively. The various equalization schemes employed in DSL is presented in **section 2.9**. Various aspects of multi-user DSL, such as the multi-user channel model, crosstalk cancelers (liner and non-linear) and dynamic spectrum balancing (DSM) are also presented in this chapter.

2.2 Modulation schemes

2.2.1 Single carrier modulation

One of the modulation schemes proposed to be used in DSL is carrierless amplitude/phase (CAP) modulation [171, 77, 76]. CAP modulation is similar to quadrature amplitude modulation (QAM) and its performance is the same [121]. The key advantage of CAP modulation is its ease of implementation [51]. In order to tackle the problem of a dispersive channel, a minimum mean squared error decision feedback equalizer (MMSE-DFE) [87, 130] has been suggested.

Furthermore, since the DSL channel varies slowly with time, precoding schemes at the transmitter can also be used [149, 69, 55]. Due to the long impulse response of the DSL channel, the equalizer filters have to be very long and are computationally complex [129].

2.2.2 Multicarrier modulation

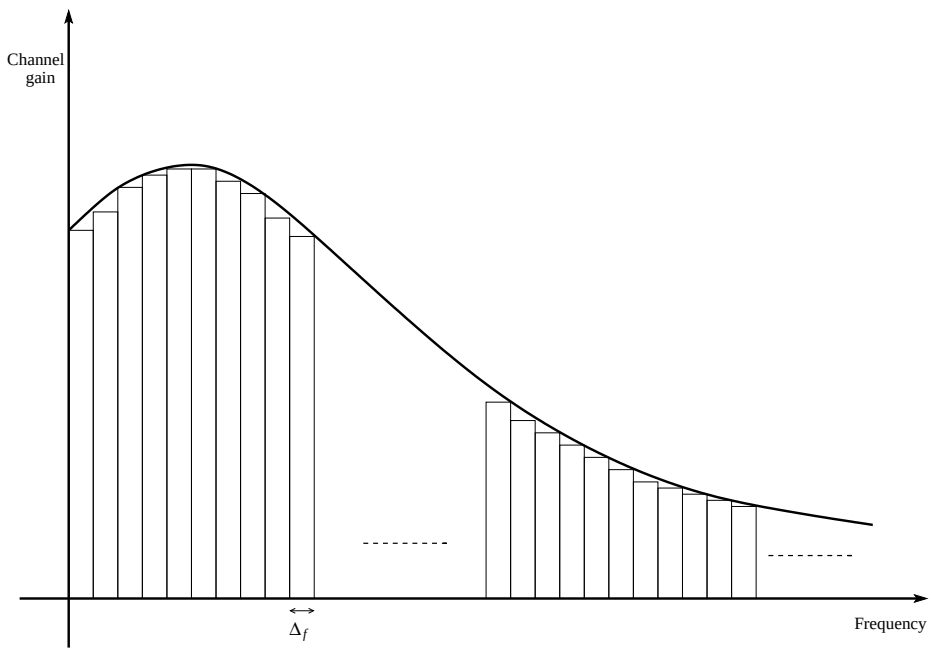


Figure 2.1: Multicarrier modulation

In the multicarrier modulation scheme, the transmission bandwidth is divided into a number of smaller parallel orthogonal frequency bands as shown in **Figure 2.1**, also known as subcarriers or tones [18, 31, 32, 128]. The transceiver structure to implement a multicarrier communication scheme is given in **Figure 2.2** [87]. The incoming bit stream acts as an input to the channel encoder. The bit stream is encoded in order to protect it from errors introduced by the channel distortion and the noise. The output of the channel encoder is then fed into the interleaver to protect it further from burst errors e.g., caused by impulse noise. The interleaver reorders the bits such that the errors are spread rather than localized hence increasing the chance of error correction. Then, the output of the interleaver is split into K parallel bit streams that are assigned to the K tones. The bit stream is then mapped to a complex-valued transmit symbol stream corresponding to

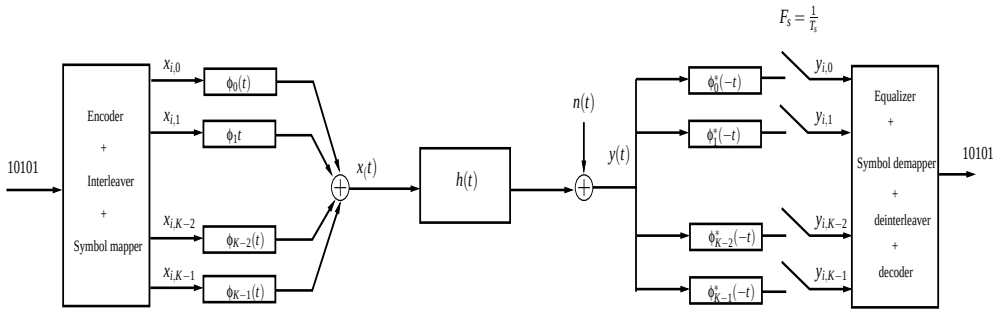


Figure 2.2: A Multicarrier transceiver

points in an M-QAM constellation. The constellation size is related to the number of bits that is represented by a symbol. In the i-th symbol period, the modulator bank is fed with the $K \times 1$ input symbol vector

$$\mathbf{x}_i = \left[x_{i,0} \cdots x_{i,K-1}\right]^T. \tag{2.1}$$

It can be assumed that the modulators use the same prototype pulse shaping filter $\phi(t)$ frequency shifted by f_k i.e., $\phi_k(t) = \phi(t)e^{j2\pi f_k t}$. The output of the multicarrier transmitter is the superposition of K QAM signals and can then be written as

$$x(t) = \sum_{i=-\infty}^{\infty} \sum_{k=0}^{K-1} x_{i,k}\phi_k(t - iT_s). \tag{2.2}$$

The symbol $x(t)$ is then transmitted over a dispersive channel with impulse response $h(t)$ and corrupted by the additive noise $n(t)$. The received signal can therefore be written as

$$y(t) = h(t) \star x(t) + n(t), \tag{2.3}$$

where $x \star y$ represents a linear convolution between x and y. At the receiver, demodulation of the received signal is performed by a bank of demodulators $\phi_k^*(-t)$, which are matched to the modulators. The ISI/ICI can be avoided by using orthogonal filters at the modulators if the channel is non-dispersive. However, the dispersive channel impulse response destroys the orthogonality and causes ISI/ICI. If the delay spread of the channel is very small as compared to the symbol time, then the tones can be considered as narrowband i.e., then there is no frequency selectivity within a tone [101]. In this case, the ISI can be ignored and each tone can be assumed to correspond to a flat frequency channel. Each tone can then be considered as a parallel AWGN channel. The discrete time data model in this case

can be written as

$$y_{i,k} = h_k x_{i,k} + n_{i,k}, \tag{2.4}$$

where $y_{i,k}$ is the ith received symbol on tone k, $h_k \triangleq h(f_k)$ is the channel frequency response at the kth tone. The sampled output of the demodulator is then equalized using a bank of simple complex valued scalars $h_k^{-1}, k \in [0, K-1]$, which are known as frequency domain equalizers.

2.3 Capacity of a transmission medium

The theoretical upper bound on the data rate that can be reliably transmitted over a transmission medium is called the capacity of the medium. Claude Shannon developed a mathematical theory of information that provides some fundamental boundaries on the performance of a communication system [134, 140]. This states that the maximum number of bits that can be transmitted over a flat AWGN channel is defined by

$$b = \log_2(1 + \text{SNR}), \tag{2.5}$$

where b is the spectral efficiency given as bits per second per Hertz bandwidth (bps/Hz), and SNR is the signal-to-noise ratio at the receiver. The overall channel capacity can then be written as

$$R = \Delta_f \log_2(1 + \text{SNR}), \tag{2.6}$$

where R is the maximum data rate supported by the channel in bps i.e., the maximum number of bits that can be transmitted reliably over the given channel, Δ_f is equal to the bandwidth of the channel.

In the case of the frequency selective channel, Shannon suggested to divide the channel into multiple narrowband AWGN subchannels [134], also called tones. The multicarrier system described in Section 2.2 is a possible practical realization of this idea. The capacity of K parallel and independent AWGN channels can be written as

$$R = \Delta_f \sum_{k=0}^{K-1} b_k = \sum_{k=0}^{K-1} \Delta_f \log_2(1 + \text{SNR}_k), \tag{2.7}$$

where b_k is the maximum number of bits that can be transmitted on the kth tone, SNR_k is the signal-to-noise ratio at the receiver on the kth tone. Under the assumption that K is large such that the discrete time data model (2.4) is valid, the true SNR_k can be given as

$$\text{SNR}_k = \frac{s_k |h_k|^2}{\sigma_k}, \tag{2.8}$$

where $s_k = \mathcal{E}\{|x_{i,k}|^2\}$ is the transmit power on tone k and $\sigma_k = \mathcal{E}\{|n_{i,k}|^2\}$ is the noise power spectral density (PSD) on tone k.

2.4 Discrete multitone modulation (DMT)

DMT is a multicarrier transmission scheme [82, 36, 126] that employs an inverse discrete Fourier transform (IDFT) to partition the channel bandwidth into parallel subchannels. The use of an IDFT and DMT for DSL was originally described in [18, 41]. One of the main advantages of using an IDFT to partition the channel bandwidth is the availability of efficient computational methods e.g. IFFT. Another advantage of using IDFT for multicarrier modulation is that the basis functions are fixed and channel independent.

Let us first consider transmission of a time domain sequence $x_{\hat{i}}^t$ through the real valued baseband continuous time channel with response $h(t)$. The total channel response typically is the convolution of the transmit filter $h_{tx}(t)$, twisted pair channel response $h_{tp}(t)$ and the receive filter $h_{rx}(t)$ and given as $h(t) = h_{tx}(t) * h_{tp}(t) * h_{rx}(t)$, where $*$ denotes linear convolution. Then for a synchronized system, the signal at the receiver can be written as

$$y(t) = \sum_{\hat{i}=-\infty}^{+\infty} x_{\hat{i}}^t h(t - \hat{i}T_s) + n(t), \tag{2.9}$$

where $n(t)$ is the continuous time additive Gaussian noise filtered by the front end filters at the receiver $h_{rx}(t)$ and T_s is the sampling period. If $y(t)$ is sampled at sample instants $t = \hat{i}T_s$, then the discrete time samples can be written as

$$y_{\hat{i}}^t = \sum_{l=0}^{L} h_l^t x_{i-l}^t + n_i^t, \tag{2.10}$$

where $y_{\hat{i}}^t = y(\hat{i}T_s)$, $h_l^t = h(lT_s)$ and the overall channel is modeled as a finite impulse response (FIR) filter of order L.

Let us now consider a block transmission, where the transmitted symbol block $\mathbf{x}$ has block length of $\bar{K} \gg L$. Then the ith transmitted symbol block can be written as

$$\bar{\mathbf{x}}_i^t = [x_{i\bar{K}}\ x_{i\bar{K}+1} \cdots x_{(i+1)\bar{K}-1}]^T \tag{2.11}$$

and the corresponding received sequence can be written as

$$\bar{\mathbf{y}}_i^t = [y_{i\bar{K}}\ y_{i\bar{K}+1} \cdots y_{(i+1)\bar{K}-1}]^T \tag{2.12}$$

From (2.10), we can model this transmission in matrix form as

$$\bar{\mathbf{y}}_i^t = \bar{\mathbf{H}}_0 \bar{\mathbf{x}}_i^t + \bar{\mathbf{n}}_i^t, \tag{2.13}$$

where $\bar{\mathbf{n}}_i^t$ is the corresponding noise vector and $\bar{\mathbf{H}}_0$ is a real Toeplitz matrix of size $\bar{K} \times \bar{K}$ and can be written as

$$\bar{\mathbf{H}}_0 = \begin{bmatrix} h_0^t & 0 & \cdots & \cdots & \cdots & 0 \\ h_1^t & h_0^t & 0 & \cdots & \cdots & 0 \\ \vdots & \ddots & \ddots & & & \vdots \\ \vdots & \ddots & \ddots & & & \vdots \\ 0 & \cdots & \cdots & h_L^t & \cdots & h_0^t \end{bmatrix} \tag{2.14}$$

Due to the dispersive nature of the channel, ISI occurs between two successive symbols. To avoid ISI, a cyclic prefix (CP) of length ν is used in each transmitted block [119, 169]. A cyclic prefix is a copy of the last ν data symbols placed at the beginning of the transmitted block. (2.13) can be rewritten to incorporate the cyclic prefix as

$$\bar{\mathbf{y}}_i^t = \bar{\mathbf{H}}_0 \mathbf{P} \mathbf{x}_i^t + \bar{\mathbf{n}}_i^t, \tag{2.15}$$

where

$$\mathbf{P} = \left[\begin{array}{c|c} \mathbf{0} & \mathbf{I}_\nu \\ \hline \multicolumn{2}{c}{\mathbf{I}_K} \end{array}\right], \tag{2.16}$$

$\mathbf{I}_x$ is the identity matrix of size x, $\mathbf{P} \in \mathbb{R}^{\bar{K} \times K}$, with $\bar{K} = K + \nu$. $\mathbf{x}_i^t$ is the input symbol block of size $K \times 1$. At the receiver, the first ν samples of $\bar{\mathbf{y}}_i^t$ are discarded by multiplying the received symbol block $\bar{\mathbf{y}}_i^t$ with the matrix $\bar{\mathbf{Q}} = [\mathbf{0}_{K \times \nu} | \mathbf{I}_K]$. The resulting output can be written as

$$\mathbf{y}_i^t = \bar{\mathbf{Q}} \bar{\mathbf{y}}_i^t = \bar{\mathbf{Q}} \bar{\mathbf{H}}_0 \mathbf{P} \mathbf{x}_i^t + \mathbf{n}_i^t, \tag{2.17}$$

where $\mathbf{y}_i^t \in \mathbb{R}^K$ and noise vector $\mathbf{n}_i^t \in \mathbb{R}^N$ with $\mathbf{n}_i^t = \bar{\mathbf{Q}} \bar{\mathbf{n}}_i^t$. $\mathbf{n}_i^t$ only retains the last K entries of $\bar{\mathbf{n}}_i^t$.

In case $L \leq \nu$, the received signal after the insertion of a cyclic prefix of length ν and then discarding the first ν samples at the receiver results in an ISI free system. Here the term $\bar{\mathbf{Q}} \bar{\mathbf{H}}_0 \mathbf{P}$ becomes a circulant matrix. Hence, the linear convolution with the channel is converted into circular convolution. The system can then be written as

$$\mathbf{y}_i^t = \mathbf{H}_c \mathbf{x}_i^t + \mathbf{n}_i^t, \tag{2.18}$$

where $\mathbf{H}_c = \bar{\mathbf{Q}}\bar{\mathbf{H}}_0\mathbf{P}$ is circulant matrix and can be written as

$$\mathbf{H}_c = \begin{bmatrix} h_0^t & 0 & \cdots & h_L^t & \cdots & h_1^t \\ h_1^t & h_0^t & \cdots & & \ddots & \vdots \\ \vdots & \ddots & \ddots & & & h_L^t \\ \vdots & & & \ddots & & \vdots \\ 0 & \cdots & h_L^t & \cdots & h_1^t & h_0^t \end{bmatrix}. \tag{2.19}$$

In order to obtain frequency domain signals, we can perform a DFT operation on both sides of (2.18). This results in

$$\underbrace{\mathcal{F}_K\mathbf{y}_i^t}_{\mathbf{y}_i} = \mathcal{F}_K\mathbf{H}_c\mathbf{x}_i^t + \underbrace{\mathcal{F}_K\mathbf{n}_i^t}_{\mathbf{n}_i}, \tag{2.20}$$

where $\mathcal{F}_K$ is the K-point DFT operation. The time-domain input symbol $\mathbf{x}_i^t$ can be written in terms of frequency domain input symbol as

$$\mathbf{x}_i^t = \mathcal{I}_K\mathbf{x}_i, \tag{2.21}$$

where $\mathcal{I}_K$ is the K-point IDFT operation. Therefore, the frequency domain data model can be written as

$$\mathbf{y}_i = \mathcal{F}_K\mathbf{H}_c\mathcal{I}_K\mathbf{x}_i + \mathbf{n}_i, \tag{2.22}$$

where $\mathbf{y}_i$, $\mathbf{x}_i$ and $\mathbf{n}_i$ are the frequency domain output symbol, frequency domain input symbol and the frequency domain additive noise. The circulant matrix is diagonalized by the IDFT and DFT operation. Therefore, we can write

$$\mathcal{F}_K\mathbf{H}_c\mathcal{I}_K = \mathbf{H}, \tag{2.23}$$

where $\mathbf{H} = diag\{h_0 \cdots h_K\}$ with the complex valued scalar frequency domain channel response in the diagonal. This can then be written as

$$\mathbf{y}_i = \mathbf{H}\mathbf{x}_i + \mathbf{n}_i. \tag{2.24}$$

Since the channel matrix $\mathbf{H}$ is a diagonal matrix, (2.24) decouples into K parallel AWGN channels as shown in **Figure 2.3**.

2.5 DMT transmitter

Figure 2.4 represents the DMT transmitter. The structure of the DMT transmitter is similar to the structure of the multicarrier transmitter in **Figure 2.2**. The DMT transmitter involves the following operations

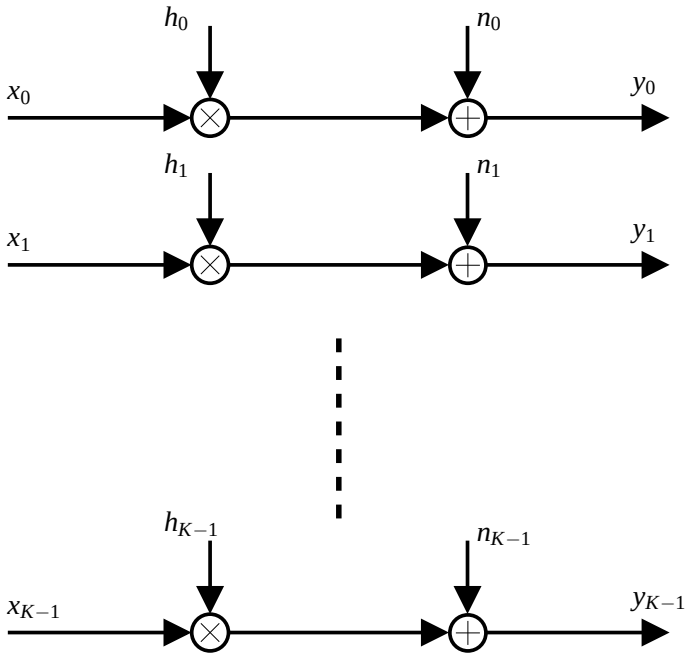


Figure 2.3: Frequency domain representation of DMT modulation

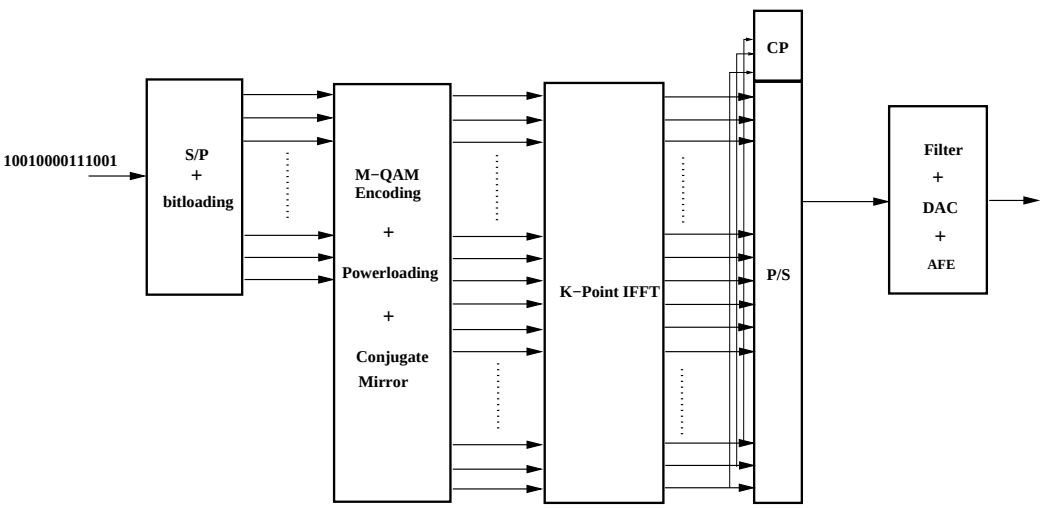


Figure 2.4: A DMT transmitter

- The incoming bit stream is encoded using a Reed-Solomon (RS) encoder [44] and the output of the encoder is then interleaved and divided into $K/2+1$ parallel streams. Each stream is assigned to a certain tone and mapped on to a complex valued M-QAM symbol.
- Then a conjugate mirror operation is performed on these $K/2+1$ M-QAM symbol such that $x_l = x_{K-l}$, where l is the sample index and output block length becomes K symbols.
- The K symbols are then modulated using a IDFT (IFFT) resulting in a real-valued time domain samples.
- A cyclic prefix of ν samples is added in front of the block to obtain $K+\nu$ time domain samples.
- The resulting time domain samples are sent through the digital front end filters, digital-to-analog converter (DAC) and the analog front end filters before transmission over the DSL channel.

2.6 DMT receiver

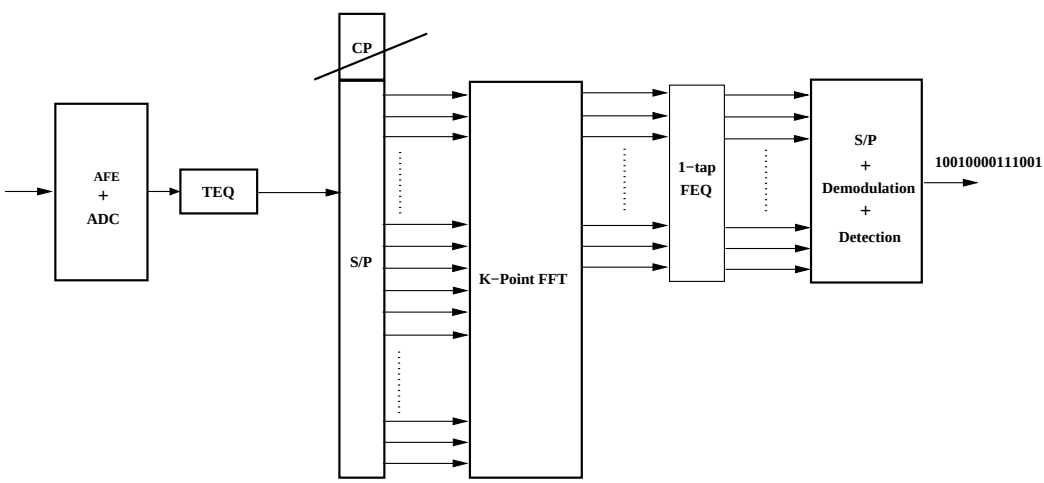


Figure 2.5: A DMT receiver

Figure 2.5 represents a typical DMT receiver structure. The DMT receiver performs the following operations

- The received analog signal is first passed through a analog front end (AFE) and an analog-to-digital converter (ADC) to get a digital output.
- Then it is provided as an input to the time-domain filter known as time domain equalizer (TEQ) so that the channel impulse response can be shortened.
- Then the output is serial-to-parallel converted and the CP is discarded
- The K remaining samples are demodulated using a DFT (FFT).
- Then the frequency domain symbols are equalized using a 1-tap frequency-domain equalizer to correct the channel distortions.
- Then the symbols are demapped, deinterleaved, and decoded to a bit stream.

2.7 Bit loading

For a noise power on a tone k, $\sigma_k \triangleq \mathcal{E}\{|n_k|^2\}$, and the transmit power $s_k \triangleq \mathcal{E}\{|x_k|^2\}$ the theoretical capacity of tone k is

$$b_k = \log_2(1 + \mathrm{SNR}_k), \tag{2.25}$$

where $\mathcal{E}\{.\}$ denotes the statistical expectation operation and the signal-to-noise ratio (SNR) on tone k is defined as

$$\mathrm{SNR}_k = \sigma_k^{-1}|h_k|^2 s_k. \tag{2.26}$$

For most practical coding schemes an SNR-gap (Γ) also has to be considered to account for the fact that most codes do not provide the theoretical capacity. Γ is a function of the coding gain, desired noise margin and target bit error probability [44, 81]. Therefore, in practice the achievable bit-rate is

$$b_k = \log_2(1 + \Gamma^{-1}\mathrm{SNR}_k), \tag{2.27}$$

In DMT based systems, the receiver estimates the SNR on each tone and reports this back to the transmitter. Then the transmitter can adapt the number of bits used on each tone by choosing a different constellation size, this is known as bit loading. This allows DMT based systems to achieve a high spectral efficiency. The number of bits transmitted on the tone is called bit loadingThe total bit-rate is then the sum of all the number of bits transmitted in all the tones and can be written as

$$R = \Delta_f \sum_k b_k = \sum_k R_k, \tag{2.28}$$

where Δ_f denotes the tone-spacing.

2.8 Power loading

DSL systems typically have to conform to a set of spectral masks which ensures that the DSL system is spectrally compatible with other communication systems that may exist in the same binder, i.e.,

$$s_k \leq s_k^{mask} \quad \forall k. \tag{2.29}$$

The modems also have to satisfy a total power constraint due to the limitations on the analog front-end

$$\sum_k s_k \leq P. \tag{2.30}$$

In order to maximize the total data rate, a modem can vary the power allocated to each tone, i.e., s_k subject to the spectral mask and the total power constraints

$$\mathbf{s}^{opt} = \underset{s_1 \cdots s_K}{\operatorname{argmax}} \sum_k R_k \tag{2.31}$$

$$\text{subject to } \sum_k s_k \leq P$$

$$s_k \leq s_k^{mask} \; \forall k,$$

where $\mathbf{s}^{opt}$ is the vector containing optimum power transmitted on each tone, i.e., $\mathbf{s}^{opt} = [s_1^{opt} \cdots s_K^{opt}]$. This adaptive distribution of power over tones is known as power loading. The objective function of (2.31) is a concave function and the constraints form a convex set and therefore the Karush-Kuhn-Tucker (KKT) conditions are sufficient for optimality. This leads to the following solution known as waterfilling [44]

$$s_k^{opt} = \left[\frac{1}{\lambda} - \frac{\Gamma\sigma_k}{|h_k|^2}\right]_0^{s_k^{mask}}, \tag{2.32}$$

where $[x]_a^b \triangleq \max(a, \min(x, b))$. The level $1/\lambda$ is chosen such that the total power constraints is satisfied. There are efficient algorithms to find the appropriate λ with complexity $\mathcal{O}(K\log K)$ [13]. With a powerful enough error correcting code, the power loading allows DMT based systems to achieve bit-rates arbitrarily close to the theoretical channel capacity. But there are always some implementation losses due to the imperfect channel coding etc. These are then accounted by using the SNR-gap Γ.

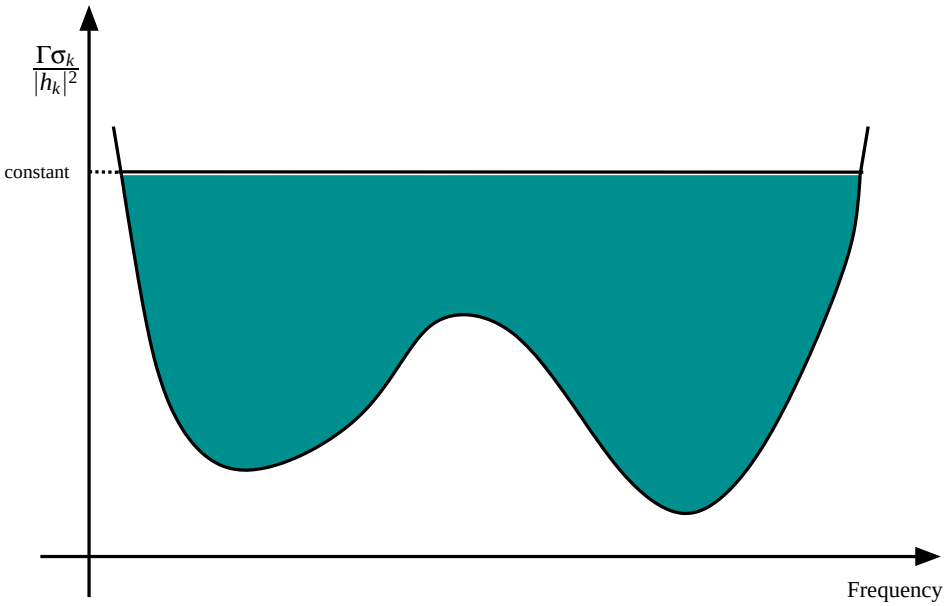


Figure 2.6: Waterfilling solution

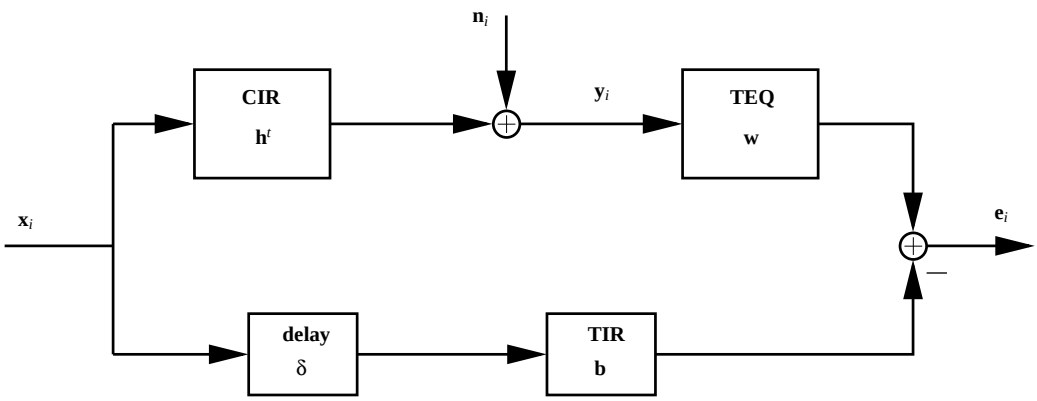


Figure 2.7: TEQ design

2.9 Equalization

2.9.1 Time-domain equalization

In order to shorten the effective length of the channel impulse response of a DSL channel, a time domain equalizer (TEQ), $\mathbf{w}$, can be used. The T-taps TEQ is generally designed based on a minimum mean square error (MMSE) criterion to shorten the channel impulse response (CIR), $\mathbf{h}^t = [h_0^t \cdots h_L^t]$, to a $\nu+1$-tap target impulse response (TIR), $\mathbf{b}$. There are a number of techniques to design the TEQ presented in the literature [7, 5, 6, 98, 161, 160, 99, 159]. One of the important parameters in TEQ design is called the decision delay. For a given CIR $\mathbf{h}^t$, it can be shortened to ν coefficients given as $b_0^t \cdots b_\nu^t \; 0 \cdots 0$ with no decision delay. With a non-zero decision delay δ, it can be shortened to $[0 \cdots b_\delta^t \cdots b_{\delta+\nu}^t \; 0 \cdots 0]$. The MMSE design procedure chooses the optimal decision delay δ as shown in **Figure 2.7** and can be written as

$$\underset{\mathbf{w},\mathbf{b},\delta}{\text{minimize}} \quad J,$$

$$\text{where} \quad J = \mathcal{E}\{\mathbf{e}_i^2\} = \mathcal{E}\left\{\left([x_{i-\delta}^t \cdots x_{i-\nu-\delta}^t | y_i^t \cdots y_{i-T+1}^t] \begin{bmatrix} -\mathbf{b} \\ \mathbf{w} \end{bmatrix}\right)^2\right\}. \quad (2.33)$$

where x_i^t and y_i^t are transmitted and received samples and i is the symbol index.

There are several disadvantages of the TEQ procedures based on MMSE channel shortening

- The MMSE based TEQ design is not related to the maximum achievable bit-rate of the DMT system.
- The obtained bit-rate is a non-smooth function of the decision delay which makes the choice of decision delay difficult.
- All the tones are equalized with the same filter, which limits the performance.
- The bit-rate maximizing TEQ is the solution of a highly non-linear cost function, which is difficult to optimize [8, 9].

2.9.2 Per-tone equalization

In the DMT receiver employing per-tone equalization (PTEQ), each tone has its own multitap equalizer after demodulation. The MMSE per-tone equalizer (MMSE-PTEQ) moves the equalization operation into the frequency domain [2] and provides large improvements with respect to time-domain equalization. The

MMSE-PTEQ bit-rate is shown to provide an upper bound for the TEQ bit-rate [2]. It has been shown in [2] that by employing a sliding DFT and difference terms, the run-time complexity of the MMSE-PTEQ is comparable to the run-time complexity of a TEQ. The details of the MMSE-PTEQ will be presented in chapter 4.

2.10 Multi-user DSL

Thus far, we have only considered a single-user scenario. However multiple DSL modems may operate and interact within a binder. This gives rise to the multi-user DSL scenario.

Consider multiple modems operating within the same binder. If the modems are synchronized and transmit simultaneously, then the discrete time received signal after sampling at rate F_s at receiver n can be written as

$$y_i^{t,n} = \sum_{l=0}^{L} \left(h_l^{t,n,n} x_{i-l}^{t,n} + \sum_{m \neq n} h_l^{t,n,m} x_{i-l}^{t,m} \right) + z_i^{t,n}, \tag{2.34}$$

where $x_i^{t,n}$ is the time-domain sequence transmitted by modem n. Also $h_l^{t,n,m} \triangleq h^{n,m}(lT_s)$, where $h^{n,m}(t)$ represents the continuous-time CIR from transmitter m to receiver n. When $m = n$ then $h^{n,n}(t)$ is known as the direct channel and when $m \neq n$ then $h^{n,m}(t)$ is known as the crosstalk channel. The $z_i^{t,n}$ denotes the total background noise, which includes additive Gaussian noise, $n_i^{t,n}$ as well as other additive noises, such as crosstalk from the lines outside the binder, impulse noise etc., experienced by receiver n. Finally, L is the order of the FIR channel response.

In the frequency domain, the channel gain on tone k from transmitter m to receiver n can be written as $h_k^{n,m}$. Since the DMT divides the frequency selective channel into parallel frequency flat subchannels (tones), $h_k^{n,m}$ is just a complex scalar value. The frequency domain channel can be obtained by performing a DFT on the time-domain channel impulse response

$$[h_1^{n,m} \cdots h_K^{n,m}]^T = \mathcal{F}_K [h_0^{t,n,m} \; \mathbf{0}_{1\times K-L-1} \; h_L^{t,n,m} \cdots h_1^{t,n,m}]^T, \tag{2.35}$$

where $\mathcal{F}_K$ denotes the K-point DFT operation. The frequency domain signal at the receiver n on tone k can then be written as

$$y_k^n = \sum_{m=1}^{N} h_k^{n,m} x_k^m + z_k^n, \tag{2.36}$$

where N is the number of lines in the binder. (2.36) can be then written in a matrix form as follows

$$\mathbf{y}_k = \mathbf{H}_k \mathbf{x}_k + \mathbf{z}_k, \tag{2.37}$$

Cable Type	TP1	TP2
diameter(mm)	0.4	0.5
$r_{0c}(\Omega/\text{km})$	286.176	174.559
a_c	0.1476962	0.0530735
$l_0(\mu\text{H/km})$	675.369	617.295
$l_\infty(\mu$ H/km)	488.952	478.971
b	0.929	1.152
f_m(kHz)	806.339	553.760
c_∞(nF/km)	49	50
g_0(n℧/km)	43	0.00023487476
g_e	0.7	1.38

Table 2.1: RLCG parameters

where $\mathbf{y}_k \triangleq [y_k^1, \cdots, y_k^N]^T$, $\mathbf{x}_k \triangleq [x_k^1, \cdots, x_k^N]^T$ contains the received and transmitted samples for all the lines on tone k. $\mathbf{z}_k = [z_k^1 \cdots z_k^N]$ contains all the noise samples for all the lines on tone k. The multi-user channel matrix $\mathbf{H}_k$ can be written as

$$\mathbf{H}_k = \begin{bmatrix} h_k^{1,1} & h_k^{1,2} & \cdots & h_k^{1,N} \\ h_k^{2,1} & h_k^{2,2} & \ddots & \vdots \\ \vdots & \ddots & \ddots & \vdots \\ h_k^{N,1} & \cdots & \cdots & h_k^{N,N} \end{bmatrix}, \tag{2.38}$$

where the diagonal elements of $\mathbf{H}_k$ contain the direct channels and the off-diagonal elements contain the crosstalk channels.

2.10.1 Multi-user channel model

The direct channel of a twisted pair cable can be modeled by using an incremental RLCG model. The RLCG model defines the resistance (R), inductance (L), capacitance (C) and the conductance (G) of the twisted pair cable per kilometer. The R, L, C, and G of a twisted pair cable can be written as follows

$$R_k = (r_{0c}^4 + a_c f_k^2)^{1/4}$$

$$L_k = (l_0 + l_\infty (f_k/f_m)^b)(1 + (f_k/f_m)^b)^{-1}$$

$$C_k = c_\infty$$

$$G_k = g_0 (f_k)^{g_e},$$

where f_k is the center frequency of tone k in Hz [11]. These models are frequency dependent and the parameters r_{0c}, a_c, l_0, l_{infty}, f_m, b, c_∞, g_0, and g_e depend on the materials and the diameter of the twisted pair cable. Typical values of these parameters are given in **Table 2.1**

The direct channel response for tone k, $h_k(d)$, of a twisted pair cable of length d km can be written as

$$h_k(d) = \frac{Z_L + Z_S}{Z_L \cosh(\gamma_k d) + Z_{0,k} \sinh(\gamma_k d) + Z_S Z_L Z_{0,k}^{-1} \sinh(\gamma_k d) + Z_S \cosh(\gamma_k d)}, \tag{2.39}$$

where γ_k is the propagation constant per unit length for the twisted pair cable at tone k and it is given as

$$\gamma_k = \sqrt{(R_k + j2\pi f_k L_k)(G_k + j2\pi f_k C_k)},$$

$Z_{0,k}$ is defined as the characteristic impedance of the line on tone k and is given as

$$Z_{0,k} \triangleq \sqrt{\frac{R_k + j2\pi f_k L_k}{G_k + j2\pi f_k L_k}},$$

Z_S is known as the source impedance of the transmitting modem and Z_L is the load impedance of the receiving modem.

Similarly, the crosstalk channels can also be modeled based on a 1% worst-case analysis. This model provides the crosstalk model such that in 99% of the cases the crosstalk is less severe than the value suggested by the model. These models ensure that the DSL modems operate for the majority of the customers. In this model, the crosstalk channel gain between two lines is given as

$$h_k^{n,m} = \alpha_{k,n,m} |h_k(d^{n,m})| \tag{2.40}$$

where

$$\alpha_{k,n,m} \triangleq K_{xf} \frac{f_k}{f_0} \sqrt{d_{\text{coupling}}^{n,m}}, \tag{2.41}$$

$f_0 = 1$ MHz and $K_{xf} = 0.0056$ [52]. If $d_{\text{coupling}}^{n,m}$ is the length of the binder segment over which there is crosstalk coupling between line m and line n, then we can write

$$d_{\text{coupling}}^{n,m} \leq \min(d_m, d_n), \tag{2.42}$$

where d_n is the length of line n in kilometers. The distance from the crosstalk source m to the crosstalk victim n is denoted as $d^{n,m}$.

The 1% worst-case model cannot be used to assess the possible gains for any particular crosstalk mitigation technique, since the gains would only be applicable

to 1% of the lines. This would give an overestimation of the performance gains. To counter this problem, full statistical models have been proposed in [91, 142]. These models could provide a more realistic assesment of the impact of crosstalk mitigation techniques in practical DSL systems.

2.10.2 Dynamic spectrum management (DSM)

The techniques to optimize the transmission for a bundle of twisted pairs are known as dynamic spectrum management (DSM). The optimization depends on the different levels of coordination between the lines in the bundle. The resources and different parameters of the DSL modems are then optimized by taking the interference of the particular DSL scenario into account. A DSL DSM infrastructure may consist of a central office (CO), where all the lines terminate and a spectrum management center (SMC). The SMC is responsible for the DSM. It collects the data from the modems e.g. transmit spectra, channel charecteristics etc. After processing the collected data, the SMC then optimizes the DSL parameters e.g. transmit spectra, data rates etc., such that the quality of service for the users is maintained. This optimization can be performed on a regular basis [42].

The DSM techniques can be classified as follows based on the level of coordination between the lines in the binder [42].

DSM level-0

DSM level 0 corresponds to no DSM coordination. No specific optimization is performed.

DSM level-1

DSM level-1 corresponds to the management of each twisted pair transmission based on estimated characteristics of the cable, i.e., each line is optimized independently.

DSM level-2

DSM level 2 corresponds to the joint coordination of the parameters of multiple DSL lines with full knowledge of the direct and crosstalk channels. It is often referred to multi-user spectrum coordination.

DSM level-3

DSM level 3 corresponds to multi-user signal coordination e.g. crosstalk precoding and/or crosstalk cancellation. It is also refered as vectored DSL.

2.10.3 Crosstalk cancellation

Linear zero forcing (ZF) crosstalk cancellation

The linear ZF canceler output can be written as [166]

$$\hat{\mathbf{x}}_k = decision\left(\mathbf{W}_k \mathbf{y}_k\right), \tag{2.43}$$

where

$$\mathbf{W}_k = \mathbf{H}_k^{-1} \tag{2.44}$$

is the $N \times N$ linear zero-forcing canceler matrix. The linear ZF canceler does not take background noise into account. Therefore, if the channel is not well conditioned, it can amplify the background noise and degrade the overall performance.

Linear MMSE crosstalk cancellation

The linear MMSE canceler output can be written as [166]

$$\hat{\mathbf{x}}_k = decision\left(\mathbf{W}_k \mathbf{y}_k\right), \tag{2.45}$$

where

$$\mathbf{W}_k = \mathbf{S}_k \mathbf{H}_k^H (\mathbf{H}_k \mathbf{S}_k \mathbf{H}_k^H + \mathbf{R}_{z,k})^{-1} \tag{2.46}$$

is the $N \times N$ linear MMSE canceler matrix. Here, $\mathbf{S}_k = diag\{s_k^1 \cdots s_k^K\}$ is the matrix containing the power on each line on tone k as its diagonal elements and $\mathbf{R}_{z,k}$ the noise correlation matrix for the bundled lines on tone k. Unlike the linear ZF canceler, the linear MMSE canceler takes the noise correlation matrix into account. This enables the linear MMSE canceler to cancel the alien crosstalk much more efficiently than the linear ZF canceler. In a high signal-to-noise ratio (SNR) AWGN scenario, the linear MMSE canceler approaches the linear ZF canceler.

Nonlinear MMSE crosstalk cancellation

The linear MMSE canceler in general performs suboptimally. A non-linear MMSE canceler such as the MMSE-GDFE [143, 61, 176, 165] and the MMSE-VBLAST [173] achieves optimal performance by feeding back the already detected symbols to remove the corresponding interference.

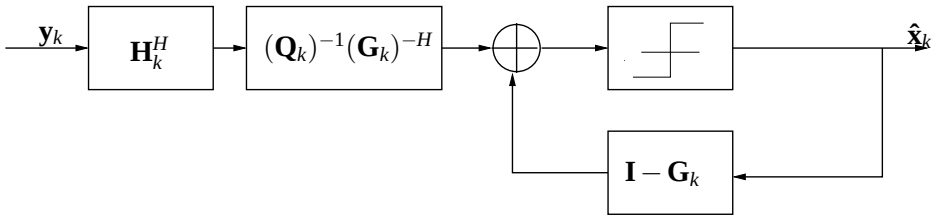


Figure 2.8: MMSE-GDFE

MMSE-GDFE

Figure 2.8 shows the MMSE-GDFE structure described in [143, 61, 176]. The feedforward filter $\mathbf{W}_{k,f}$ of the MMSE-GDFE can be written as

$$\mathbf{W}_{k,f} = (\mathbf{Q}_k)^{-1}(\mathbf{G}_k)^{-H}\mathbf{H}_k^H \tag{2.47}$$

where $\mathbf{Q}_k$ is a diagonal matrix and $\mathbf{G}_k$ is a monic lower triangular matrix. Here $\mathbf{Q}_k$ and $\mathbf{G}_k$ can be obtained from the Cholesky factorization of

$$(\bar{\mathbf{R}}_k)^{-1} = ((\mathbf{S}_k)^{-1} + \mathbf{H}_k^H(\mathbf{R}_{z,k})^{-1}\mathbf{H}_k) \tag{2.48}$$

i.e.

$$(\bar{\mathbf{R}}_k)^{-1} = \mathbf{G}_k\mathbf{Q}_k\mathbf{G}_k^H. \tag{2.49}$$

The lower triangular structure of $\mathbf{G}_k$ defines a detection order (line 1 is detected first, line N is detected last). When different lines have different priorities, the highest priority line should be detected last [155]. In [61, 176], it was shown that the MMSE-GDFE performs optimally with respect to achievable bit-rate in the spatially correlated noise scenario.

MMSE-VBLAST

In the MMSE-VBLAST [173], the interference from the already detected lines is subtracted from the received vector and then a MMSE linear canceler is applied to reduce the interference from the yet undetected lines. Let us define the channel $\mathbf{H}_k = [\mathbf{h}_k^1 \cdots \mathbf{h}_k^N]$. The MMSE-VBLAST detection algorithm is given as,

$$\text{For } n = 1 \cdots N$$

$$\hat{x}_k^n := decision\left(\mathbf{w}_{ff,k}^n(\mathbf{y}_k - \sum_{l=1}^{n-1}\mathbf{h}_k^l\hat{x}_k^l)\right) \tag{2.50}$$

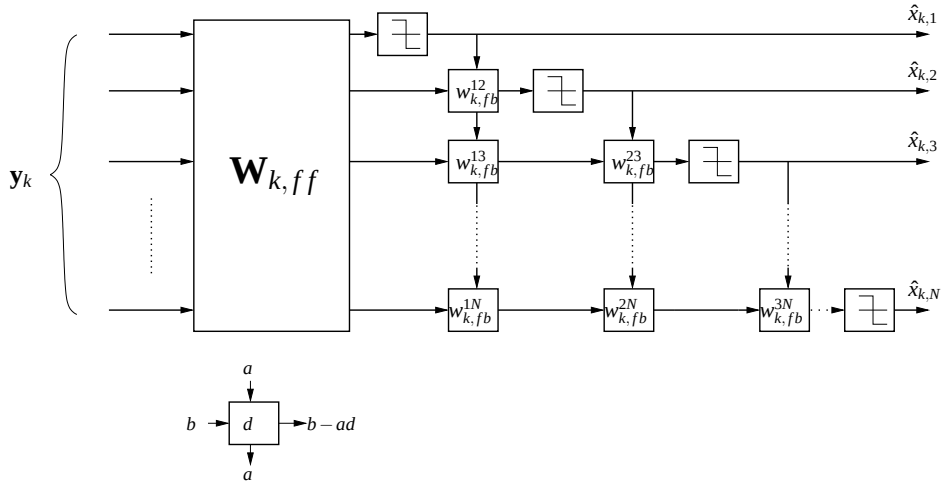


Figure 2.9: MMSE-VBLAST structure

The feedforward filter is

$$\mathbf{w}^n_{ff,k} = s^n_k \mathbf{h}^{nH}_k ([\mathbf{h}^n_k \cdots \mathbf{h}^N_k]\mathbf{S}^{N-n}_k [\mathbf{h}^n_k \cdots \mathbf{h}^N_k]^H + \mathbf{R}_{z,k})^{-1}, \tag{2.51}$$

where s^n_k is the n-th diagonal element of matrix $\mathbf{S}_k$, $\mathbf{S}^{N-n}_k$ is an $(N-n)\times(N-n)$ diagonal matrix containing the power transmitted on lines n to line N and $\hat{x}^n_k$ is the estimate of x^n_k. The formula (2.50) is equivalent to

For $n = 1 \cdots N$

$$\hat{x}^n_k := decision \left(\mathbf{w}^n_{ff,k}\, \mathbf{y}_k - \sum_{l=1}^{n-1} \underbrace{\mathbf{w}^n_{ff,k}\mathbf{h}^l_k}_{\triangleq \mathrm{w}^{ln}_{fb,k}} \hat{x}^l_k \right), \tag{2.52}$$

where the decision feedback operation is now again applied at the end as indicated in the Figure 2.9. In [59], the MMSE-GDFE and the MMSE-VBLAST were shown to be equivalent.

2.11 Sparse approximation

Sparse approximation represents a class of problems where a sparse linear combination of given input signals is preferred. The sparse solution is obtained by imposing a penalty on the non-zero coefficients. The most common applications

of sparse approximation are deconvolution, signal modelling, machine learning etc. [151, 152].

Let us assume a system with additive noise

$$\mathbf{y} = \mathbf{A}\mathbf{w} + \mathbf{n}, \tag{2.53}$$

where $\mathbf{A}$ is a known matrix, $\mathbf{w}$ is the unknown sparse coefficient vector and $\mathbf{n}$ is the additive noise. If the signal $\mathbf{y}$ is known, then our goal is to estimate vector $\mathbf{w}$ with the minimum number of non-zero elements. This has been shown to be an extremely hard problem and due to the sparsity of the vector $\mathbf{w}$ is a combinatorial problem [151, 152]. However, in the case when the vector $\mathbf{w}$ is sufficiently sparse, it has been shown that the vector $\mathbf{w}$ can be accurately and efficiently approximated from the noisy observation $\mathbf{y}$ [151, 152].

The approximation problem can be written as

$$\min_{\mathbf{w}} \quad \|\mathbf{w}\|_0 \qquad \text{subject to} \quad \|\mathbf{y} - \mathbf{A}\mathbf{w}\|_2 \leq \epsilon, \tag{2.54}$$

where the ℓ_0 quasi-norm $\|.\|_0$ counts the number of non-zero elements in its argument. In order to solve (2.54), an exhaustive search through all the possible combinations of non-zero elements in $\mathbf{w}$ has to be performed. This is in general intractable since the search space can be very large.

One way to tackle the intractability of (2.54) is to replace the ℓ_0 quasi-norm with the ℓ_1 norm to obtain a convex optimization problem. Then we can write (2.54) as

$$\min_{\mathbf{w}} \quad \|\mathbf{w}\|_1 \qquad \text{subject to} \quad \|\mathbf{y} - \mathbf{A}\mathbf{w}\|_2 \leq \delta, \tag{2.55}$$

where δ is the error bound and related to ϵ. It has been shown that solving (2.55) is equivalent to solving a closely related convex problem known as the ℓ_1-penalty problem, which is given as

$$\min_{\mathbf{w}} \quad \frac{1}{2}\|\mathbf{y} - \mathbf{A}\tilde{\mathbf{w}}\|_2^2 + \gamma\|\tilde{\mathbf{w}}\|_1, \tag{2.56}$$

where γ is the tradeoff parameter which trades off between the approximation error and the sparsity of $\mathbf{w}$. It has been shown that if $\mathbf{w}$ is sufficiently sparse then the vector $\tilde{\mathbf{w}}$ can be recovered exactly for a sufficiently small γ [151, 152].

For more details on sparse approximation, we refer to the literature [151, 152, 153, 49, 57, 157]

2.12 Summary

In this chapter, we have provided an introduction to various aspects of a DSL system. This comprises the important building blocks of a DSL transceiver. A

brief overview of the different modulation schemes considered for the DSL system has been given and the motivation towards using multicarrier modulation has then been presented. A mathematical model of a DMT based system has also been introduced and DMT transmitter and receiver structures have been described. Various techniques in order to increase the capacity of the DMT system, such as bit loading and power loading have also been discussed in detail. Furthermore, some techniques, to mitigate the effect of channel impairments, such as time domain equalization and per-tone equalization have also been introduced.

In the multi-user DSL scenario, the effect of crosstalk on the system performance has been discussed and then a simple multi-user channel modelling technique has also been presented. Various techniques to optimize the transmission in this scenario are also discussed in order to either avoid the crosstalk or cancel it. Various receiver structures to cancel the effect of crosstalk have then been presented. Finally a short introduction to sparse approximation has been given.

In the following chapters, we will develop various efficient algorithms to reduce the run-time complexity of the signal processing blocks used to mitigate transmission impairments discussed in this chapter.

Part I

SINGLE-USER RESOURCE ALLOCATION

Chapter 3

Resource allocation in a DMT transmitter with per-tone pulse shaping filters

3.1 Introduction

DSL modems use DMT modulation [44]. DMT divides the available spectrum into smaller parallel sub-bands or tones. Each tone corresponds to an orthogonal carrier. The input bit-stream is divided into independent parallel streams, which then QAM-modulate the different carriers. These QAM modulations are implemented based on an IDFT [18].

The IDFT filters used to implement the DMT have a poor frequency response as shown in Figure 3.1. Firstly, their first side lobe is only 13 dB below the main lobe and secondly, the rate of decay of the side lobe energy is only inversely proportional to frequency. In some applications e.g. in VDSL, the Power Spectral Density (PSD) of the transmitted signal is not allowed to exceed a given PSD mask defining one or more pass bands and stop bands. To satisfy this constraint, many tones near the band edges cannot be used, which are known as virtual carriers (VCs). This significantly reduces the available bandwidth for data transmission. An example of the effect of not using enough VCs is shown in Figure 3.2. One of the attempted approaches to improve the spectral characteristics of the transmit signal is to use alternative transmit and receive filters instead of the IDFT filters [156, 22, 86], but this is found to make the equalization at the receiver more complicated. Another approach is to use time domain windowing of the transmit signal [10] either with

or without extending the cyclic prefix and possibly an additional cyclic suffix [40]. Inter-symbol windowing, in which only the cyclic prefix and cyclic suffix is multiplied with the window function to preserve the orthogonality was presented in [94]. Similarly, intra-symbol windowing where the window function is applied to the transmit block was proposed in [90, 47, 93]. However, this approach destroys the orthogonality and needs a post processing at the receiver. The idea of spectral compensation was considered in [17, 14, 92]. Theoretically, one of the simplest approaches is to filter the transmit signal [101].

A per-tone pulse shaping procedure to reduce the energy in the stop bands was proposed in [33]. It uses a filter to shape the spectrum for each tone separately. These filters can be designed using many techniques [96, 124, 148]. In [33], a simple filter design procedure was proposed, where a pulse shaping filter is designed for each tone such that its stop band energy contribution is minimized. The method allows for asymmetric filters which helps to reduce the stop band energy contribution of the tones at the band edges. This in turn helps to increase the number of tones that can be used for data transmission without violating the PSD mask constraint compared to a time domain windowing, as shown in Figure 3.3. The resulting transmitter structure was derived in [33] and shown to be a dual of the per-tone equalization structure proposed in [2]. It is noted that the transmit signal filtering has the same effect as the time dispersive channel and therefore the cyclic prefix length has to be increased accordingly in order to mitigate the ISI/ICI [92, 101].

In the DMT transmitter using per-tone pulse shaping as described in [33], every tone is shaped using a constant length non-sparse pulse shaping filter and each tone has the same transmit power, i.e., no specific power loading scheme used. However for a given per-tone transmit power, tones in the middle of a pass band contribute less to the overall stop band energy. Therefore, a sparse pulse shaping filter, i.e., with fewer non-zero filter taps and hence lower run-time complexity, may be used for such tones without affecting the overall performance significantly. A better alternative is thus to consider variably sparse pulse shaping filters, where each tone can use a pulse shaping filter with a different degree of sparsity. Furthermore, the number of used tones can also be increased by using a lower transmit power at the band edges. Using a lower transmit power on a larger number of tones may help to increase the achievable data rate without violating the PSD mask constraint. In conclusion, there is a need for efficient methods to optimally allocate the non-zero filter taps as well as transmit power over tones, such that a maximum data rate is achieved with the available resources, i.e., for a given power budget and filter tap (run-time complexity) budget, and without violating the PSD mask constraint.

The Lagrange multipliers method is often used to convert a constrained optimization problem into a dual unconstrained problem [102, 24]. In this chapter, we propose two algorithms to optimally allocate the non-zero filter taps and transmit power over tones by solving the dual problem. The first approach is based on an

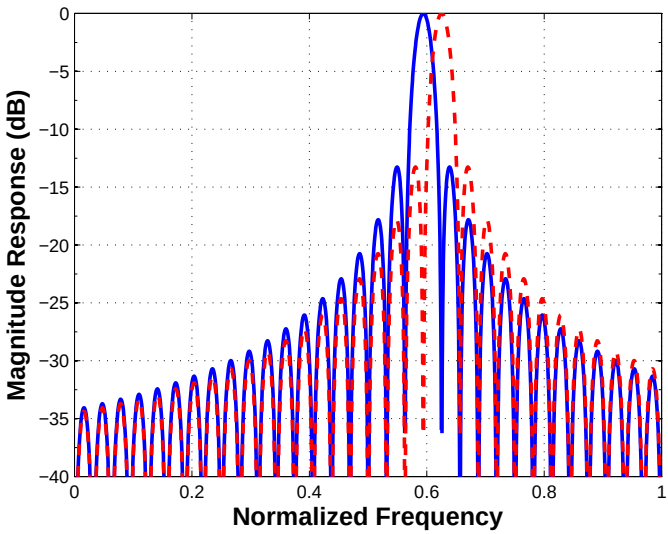


Figure 3.1: Spectrum of two adjacent tones in a DFT based multicarrier system

exhaustive search over all the pulse shaping filter orders and is referred to as the contiguous filter tap selection (CTS) based approach. The second approach uses sparse approximation to compute the sparse pulse shaping filters, hence we refer to it as the sparse approximation based approach.

The chapter is organized as follows: In **section 3.2**, the filter design criteria for a per-tone pulse shaping filter are presented. Additionally, an efficient DMT transmitter structure to incorporate the effect of per-tone pulse shaping filter is also given.

In **section 3.3**, the optimization problem to allocate pulse shaping filter taps for a constant power loading scenario as well as for a joint pulse shaping filter tap and transmit power allocation scenario is formulated. In each case, it is shown that the dual problem formulation decouples the optimization problem over tones, hence reducing the computational complexity of the solution of the optimization problem.

In **section 3.4**, we then present algorithms to further reduce the computational complexity of the optimization problem derived in section 3.3 under fixed power loading.

In **section 3.5**, the two algorithms presented in section 3.4 are extended to include both pulse shaping filter taps and transmit power allocation.

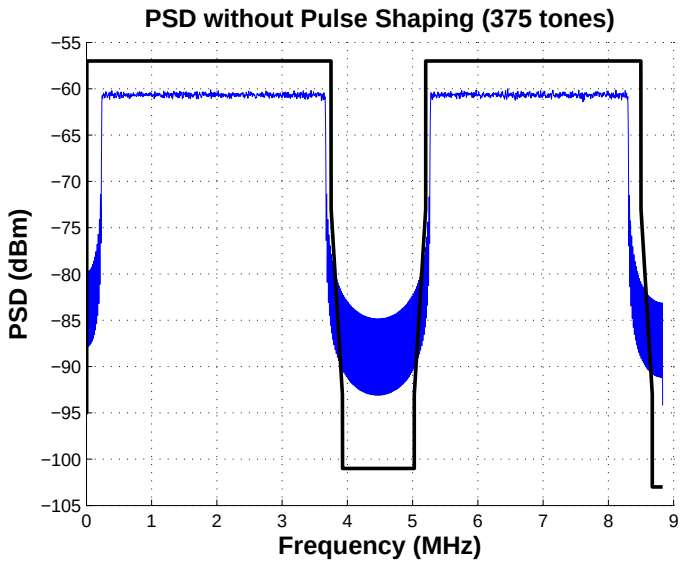
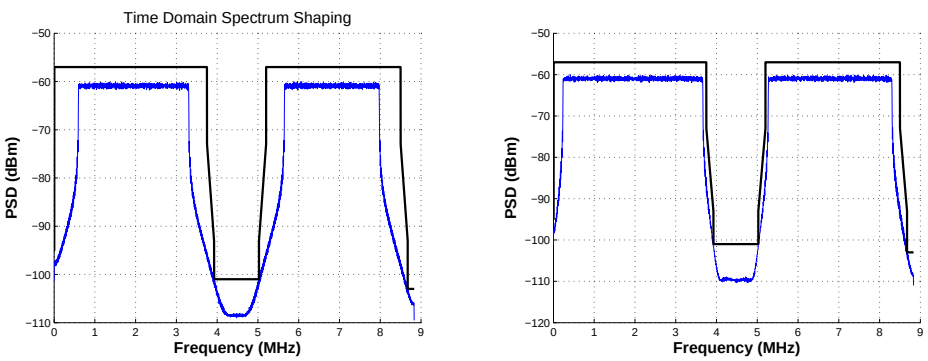


Figure 3.2: PSD of a VDSL system without any transmit pulse shaping, violating the spectral mask constraints



(a) (b)

Figure 3.3: PSD of a VDSL system satisfying the spectral mask constraints (a) with time domain pulse shaping (b) with per-tone pulse shaping

In **section 3.6**, the simulation results are shown and conclusions are drawn in **section 3.7**.

3.2 System model

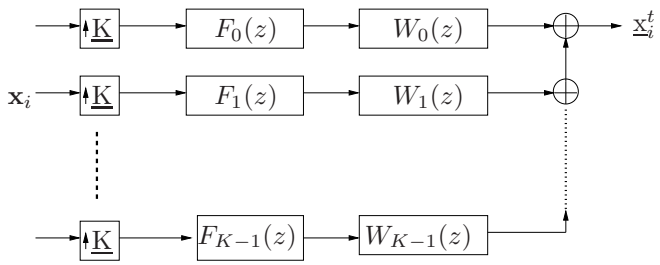


Figure 3.4: DMT transmitter with per-tone pulse shaping

The following notation is adopted in the description of the DMT system. K is the IDFT-size and k denotes the tone index, C_{max} is the order of the pulse shaping filters, ν is the cyclic prefix length. $\underline{\mathrm{x}}_i^t$ is the output of the transmitter i.e. a vector of length $\underline{\mathrm{K}} = K + C_{max} + \nu$, corresponding to one transmitted symbol at time i.

Figure 3.4 shows the DMT transmitter structure with the per-tone pulse shaping as derived in [33]. The filters $F_k(z)$ are the DFT filters defined as

$$F_k(z) = \mathbf{e}^H(z)\mathbf{f}_k, \tag{3.1}$$

where $\mathbf{e}^H(z) = [1\ z^{-1} \cdots z^{K+\nu-1}]$, $\mathbf{f}_k = [f_k^0 \cdots f_k^{K+\nu-1}]$ and $f_k^l = e^{-j\omega_k(\nu-l)}$ for $l = 0 \cdots (N+\nu-1)$, $\omega_k = \frac{2\pi k}{K}$. The pulse shaping filters, $W_k(z)$, are designed using a minimum stop band energy criterion. For simplicity we will use FIR per-tone pulse shaping filters and adopt the following design criterion, presented in [33], for every filter $W_k(z)$:

$$\begin{aligned} &\underset{\mathbf{w}_k}{\text{minimize}} \quad (1-\beta)\int_{\omega\in\Omega_1} |F_k(e^{j\omega})W_k(e^{j\omega})|^2 d\omega + \beta\int_{\omega\in\Omega_2} |F_k(e^{j\omega})W_k(e^{j\omega})|^2 d\omega \\ &\text{subject to} \qquad W_k(e^{j\omega_k}) = 1 \end{aligned} \tag{3.2}$$

where Ω_1 represents the stop band frequencies, Ω_2 represents the pass band frequencies as defined by the PSD mask, $W_k(z) = \hat{\mathbf{e}}^H(z)\mathbf{w}_k$, $\hat{\mathbf{e}}^H(z) = \left[1\ z^{-1} \cdots z^{-C_{max}}\right]$, $\mathbf{w}_k = [w_k^0\ w_k^1\ \cdots\ w_k^{C_{max}}]^T$, $F_k(e^{j\omega})$ is the frequency response of the DFT filter $F_k(z)$ at frequency ω, $W_k(e^{j\omega})$ is the frequency response of the per-tone pulse shaping filter $W_k(z)$ at frequency ω_k and β is a small constant $0 < \beta \ll 1$. The pass band term is included as a regularization term[33]. The design criterion can be restated as

$$\min_{\mathbf{w}_k} \quad \mathbf{w}_k^H \mathbf{Q}_k \mathbf{w}_k \quad \text{subject to} \quad W_k(e^{j\omega_k}) = 1 \tag{3.3}$$

where,

$$\mathbf{Q}_k = (1-\beta)\int_{\omega\in\Omega_1} |F_k(e^{j\omega})|^2 \hat{\mathbf{e}}(e^{j\omega})\hat{\mathbf{e}}^H(e^{j\omega})\, d\omega + \beta\int_{\omega\in\Omega_2} |F_k(e^{j\omega})|^2 \hat{\mathbf{e}}(e^{j\omega})\hat{\mathbf{e}}^H(e^{j\omega})\, d\omega$$

with $\hat{\mathbf{e}}^H(e^{j\omega}) = [1\ e^{-j\omega}\cdots\ e^{-jC_{max}\omega}]$.

We will design a pulse shaping filter under additional sparsity constraints, i.e, we will complement (3.2) or (3.3) with constraints

$$w_k^j = 0 \quad \text{if} \quad C_{kj} = 0 \quad \text{for } j = 0\cdots C_{max}, \tag{3.4}$$

where the C_{kj}'s define the sparsity pattern, see section 3.3. The filter design problem given by (3.2) or (3.3) and (3.4) corresponds to a linearly constrained least squares problem, which is easily solved.

From **Figure 3.4** we can see that the transmitter output is

$$\underline{\mathrm{x}}_i = \sum_{k=0}^{K-1} x_{ik}\mathbf{f}_k \star \mathbf{w}_k \tag{3.5}$$

where, $\star$ denotes the convolution operation and x_k is the input symbol for tone k. In [33] it has been shown that this transmitter output can be generated cheaply based on

$$\underline{\mathrm{x}}_i^t = \begin{pmatrix} \mathbf{0} & \mathbf{I}_\nu \\ \mathbf{I}_K & \\ \mathbf{0}_{C_{max}\times K} & \end{pmatrix} \mathcal{I}_K\mathbf{D}\mathbf{x}_i + \sum_{k=0}^{K-1} \begin{pmatrix} -\alpha^{k(\nu+1)}\bar{\mathbf{v}}_k \\ \mathbf{0}_{(K+\nu-C_{max})\times 1} \\ \alpha^k\bar{\mathbf{v}}_k \end{pmatrix} x_{ik}. \tag{3.6}$$

Here $\mathbf{I}_k$ is the k by k identity matrix, $\mathcal{I}_K$ is the IDFT matrix of size $K\times K$, $\mathbf{x}_i = [x_{i0}\cdots x_{i(K-1)}]^T$ is the input symbol vector, $\alpha = e^{-j2\pi/K}$, $\mathbf{v}_k = \mathbf{U}_k\mathbf{w}_k$ and can be written as $[v_{k,0}\ \bar{\mathbf{v}}_k^T]^T$, $\mathbf{U}_k$ is an $(C_{max}+1)$ by $(C_{max}+1)$ upper triangular Toeplitz matrix whose first row is $[1\ \alpha^k\cdots\alpha^{kC_{max}}]$, $\mathbf{D}$ is a diagonal matrix with diagonal elements $[v_{0,0}\ v_{1,0}\cdots v_{K-1,0}]$ consisting of the first element of $\mathbf{v}_k$ for each k.

3.3 Problem formulation

In section 3.3.1, we first consider the problem of pulse shaping filter taps allocation under fixed power loading. In Section 3.3.2, we then consider the problem of joint pulse shaping filter tap allocation and transmit power allocation, to maximize the data rate under the PSD mask constraints.

3.3.1 Resource allocation for a fixed power loading

When the collection of tones to be used for transmission and the powers are fixed, the tap allocation in the pulse shaping filters does not affect the achievable bit-rate (cfr. the constraint in problem (3.2) and (3.3)). Hence, in this case we only need a procedure to optimally allocate the filter taps, such that the PSD mask constraints are fulfilled. For a given tap budget C_{budget}, we can write the resource allocation problem as

$$\begin{aligned} \max_{\mathbf{C}} \quad & 0 \\ \text{subject to} \quad & \sum_{k\in\mathcal{K}} \sum_{j=0}^{C_{max}} C_{kj} \leq C_{budget} \\ & \mathbf{t}_{spec} \leq \mathbf{t}_{mask} \end{aligned} \tag{3.7}$$

where $\mathcal{K}$ is the set containing the indices of the used tones, $C_{kj} \in \{0,1\}$ defines the tap allocation i.e. C_{kj} is 1 if the j-th tap of the pulse shaping filter for tone k is selected i.e., can be non-zero and 0 otherwise, $\mathbf{c}_k = [C_{k0} \cdots C_{kC_{max}}]$ is the vector that represents the position of the non-zero pulse shaping filter taps for tone k and is referred to as the sparsity pattern of the pulse shaping filter, $\mathbf{C}$ is a matrix that has $\mathbf{c}_k$ as its kth row, C_{budget} is the predefined maximum total number of non-zero pulse shaping filter taps for all used tones, $\mathbf{t}_{mask}$ is the vector containing $\bar{M}$ sample points of the PSD mask at different frequencies and $\mathbf{t}_{spec}$ is the vector containing the similarly sampled PSD of the transmitter output. It is seen that (3.7) merely checks if the PSD mask constraint can be met with the given filter tap budget. This type of problem is known as a feasibility problem, which tests whether the constraints are mutually exclusive. Problem (3.7), amounts to a combinatorial selection and therefore is a non-convex problem. This problem is further complicated by the fact that the second constraint is coupled over tones. In order to simplify the optimization problem presented in (3.7) let us write it as the following equivalent constrained optimization problem

$$\boxed{\begin{aligned} \max_{\mathbf{C}} \quad & -\sum_{k\in\mathcal{K}} \sum_{j=0}^{C_{max}} C_{kj} \\ & \text{subject to} \quad \mathbf{t}_{spec} \leq \mathbf{t}_{mask} \end{aligned}} \tag{3.8}$$

If $\sum_{k\in\mathcal{K}} \sum_{j=0}^{C_{max}} C_{kj}$ is larger than C_{budget} after the maximization then the problem is considered infeasible. This optimization problem is still combinatorial and the constraint is still coupled over tones. The computational complexity of (3.8) is $\mathcal{O}(2^{K(C_{max}+1)})$, where K is the cardinality of the set $\mathcal{K}$ and denotes the total

number of used tones. This is intractable for practical values of K and C_{max}. In order to solve this problem let us write the dual of the problem in (3.8) as

$$\min_{\Lambda}\left\{\max_{\mathbf{C}}\left(\hat{\Psi}\right)\right\} \quad \text{subject to } \lambda_m \geq 0 \quad \text{for} \quad m = 1 \cdots \bar{M}, \tag{3.9}$$

where

$$\hat{\Psi} = -\sum_{k\in\mathcal{K}}\sum_{j=0}^{C_{max}} C_{kj} - \sum_{m=1}^{\bar{M}} \lambda_m (t_{mask,m} - t_{spec,m}), \tag{3.10}$$

Λ is a vector containing all λ_ms, m is the index for the frequency samples, i.e. $t_{mask,m}$ and $t_{spec,m}$ correspond to the PSD samples at frequency ω_m and $\bar{M}$ is the total number of frequency samples taken into consideration.

With,

$$\begin{aligned} t_{spec,m} &= \sum_{k\in\mathcal{K}} s_k |F_k(e^{j\omega_m}) W_k(e^{j\omega_m})|^2 \\ &= \sum_{k\in\mathcal{K}} s_k |F_k(e^{j\omega_m}) \hat{\mathbf{e}}^H(e^{j\omega_m}) \mathbf{w}_k|^2, \end{aligned} \tag{3.11}$$

where $s_k = E\{|x_k|^2\}$, and $\mathbf{w}_k$ is computed from the sparsity pattern $\mathbf{c}_k$ based on (3.3) and (3.4), we can rewrite equation (3.10) as,

$$\hat{\Psi} = -\sum_{k\in\mathcal{K}}\sum_{j=0}^{C_{max}} C_{kj} + \sum_{m=1}^{\bar{M}} \lambda_m \sum_{k\in\mathcal{K}} s_k |F_k(e^{j\omega_m}) \hat{\mathbf{e}}^H(e^{j\omega_m}) \mathbf{w}_k|^2 - \sum_{m=1}^{\bar{M}} \lambda_m t_{mask,m} \tag{3.12}$$

which is equivalent to

$$\hat{\Psi} = \sum_{k\in\mathcal{K}} \left\{ -\sum_{j=0}^{C_{max}} C_{kj} + \sum_{m=1}^{\bar{M}} \lambda_m s_k |F_k(e^{j\omega_m}) \hat{\mathbf{e}}^H(e^{j\omega_m}) \mathbf{w}_k|^2 \right\} - \underbrace{\sum_{m=1}^{\bar{M}} \lambda_m t_{mask,m}}_{\text{constant for a given } \lambda_m} \tag{3.13}$$

For fixed Lagrange multipliers λ_m, the term $\sum_{m=1}^{\bar{M}} \lambda_m t_{mask,m}$ is constant and therefore the maximization problem in (3.9) is effectively decoupled over tones, and can be written for each tone $k \in \mathcal{K}$ as,

$$\boxed{\max_{\mathbf{c}_k} \quad \hat{\psi}_k(\Lambda)}$$

$$\hat{\psi_k}(\Lambda) = -\sum_{j=0}^{C_{max}} C_{kj} + \sum_{m=1}^{\bar{M}} \lambda_m s_k |F_k(e^{j\omega_m})\hat{\mathbf{e}}^H(e^{j\omega_m})\mathbf{w}_k|^2 \tag{3.14}$$

This per-tone optimization problem can be solved by exhaustively searching over all possible $\mathbf{c}_k$'s. The Lagrange multipliers can then be updated until all the PSD constraints are met. Even though the problem is now decoupled over tones, it is still combinatorial for each tone. The computational complexity now is $\mathcal{O}(K2^{(C_{max}+1)})$ per update of the Lagrange multipliers, which is still very high for practical values of C_{max}. In section 3.4, we will present efficient algorithms to reduce this complexity.

In the following section, optimal transmit power allocation will also be considered along with the pulse shaping filter taps allocation.

3.3.2 Joint pulse shaping filter tap and transmit power allocation

To maximize the data rate of a single-user DMT system under a total power constraint, the optimal per-tone transmit power can be calculated by using the water filling procedure [40]. With additional PSD constraints this is no longer applicable. In the previous section, the pulse shaping filter tap allocation problem was formulated when the collection of used tones and their transmit powers are known for a system with PSD constraints. However, the number of used tones can possibly be increased if a lower transmit power at the band edges is used. Therefore by also allocating the appropriate amount of transmit power for each tone the total achievable data rate can be maximized for a given total transmit power budget. This then requires a procedure to allocate the available resources, i.e., transmit power and pulse shaping filter taps, efficiently over tones such that the achievable bit-rate is maximized and the PSD mask constraints are met. The

corresponding constrained optimization problem can be written as

$$\begin{aligned} \underset{\mathbf{C},\mathbf{s}}{\text{maximum}} \quad & \sum_{k\in\mathcal{K}} R_k \\ \text{subject to} \quad & \mathbf{t}_{spec} \leq \mathbf{t}_{mask} \\ & \sum_{k\in\mathcal{K}} \sum_{j=0}^{C_{max}} C_{kj} \leq C_{budget} \\ & \sum_{k\in\mathcal{K}} s_k \leq S_{budget} \\ & 0 \leq s_k \leq S_{max,k} \end{aligned} \tag{3.15}$$

where R_k is the achieved bit-rate for tone k which is given as

$$R_k = \Delta_f log_2(1 + \frac{s_k^n |h_k|^2}{\sigma_k \Gamma}),$$

$\frac{s_k^n |h_k|^2}{\sigma_k \Gamma}$ is the signal-to-noise ratio of tone k, Γ is the SNR gap, $\mathbf{s} = [s_1 \cdots s_K]$ is the vector containing the transmit powers, S_{budget} is the total transmit power budget, $s_k \in \mathcal{S}$ is the transmit power allocated to tone k, $\mathcal{S}$ is the set containing all the allowed discrete power levels, $S_{max,k}$ is the maximum transmit power allowed for tone k. All the other quantities are as in section 3.3.1. Optimization problem (3.15) is coupled over tones and is a combinatorial problem. It has a computational complexity of $\mathcal{O}(\tilde{L}^K 2^{K(C_{max}+1)})$, where $\tilde{L}$ is the cardinality of set $\mathcal{S}$ and K is the cardinality of set $\mathcal{K}$. This is intractable even for moderate $K, \tilde{L}$ and C_{max}. In the previous section, it was shown that the dual problem formulation leads to a decoupling of the problem over tones. Therefore, in order to reduce the computational complexity, we will also formulate a dual problem of (3.15). The dual optimization problem can be written as

$$\min_{\gamma,\alpha,\Lambda} \left\{ \max_{\mathbf{C},\mathbf{s}} (\Psi) \right\} \qquad \text{subject to} \quad \gamma, \alpha, \Lambda \geq 0$$

where,

$$\Psi = \sum_{k\in\mathcal{K}} R_k + \gamma\left(C_{budget} - \sum_{k\in\mathcal{K}}\sum_{j=0}^{C_{max}} C_{kj}\right) + \alpha\left(S_{budget} - \sum_{k\in\mathcal{K}} s_k\right)$$

$$+ \sum_{m=1}^{\bar{M}} \lambda_m(t_{mask,m} - t_{spec,m}) \tag{3.16}$$

$$\tag{3.17}$$

The last constraint in (3.15) may be excluded from the dual formula since it can be implicitly imposed by reducing $\mathcal{S}$ in each per-tone minimization problem.

For fixed Lagrange multipliers the maximization problem in (3.16) is again decoupled over tones, and by substituting (3.11), can be written for each tone as,

$$\max_{\mathbf{c}_k, s_k} \quad \psi_k(\gamma, \alpha, \Lambda),$$

where

$$\psi_k(\gamma, \alpha, \Lambda) = R_k - \gamma \sum_{j=0}^{C_{max}} C_{kj} - \alpha s_k - \sum_{m=1}^{\bar{M}} \lambda_m s_k |F_k(e^{j\omega_m})\hat{\mathbf{e}}^H(e^{j\omega_m})\mathbf{w}_k|^2, \tag{3.18}$$

The computational complexity now reduces to $\mathcal{O}(K\tilde{L}_s 2^{(C_{max}+1)})$ per update of the Lagrange parameters which is still very high for practical values of C_{max}.

In section 3.5, we will present efficient algorithms to reduce this complexity.

3.4 Resource allocation for a fixed power loading

3.4.1 Contiguous filter tap selection based resource allocation

Here we present an approach that is based on (3.14) to further reduce the computational complexity. Let us restate (3.14) again for convenience as

$$\boxed{\max_{\mathbf{c}_k} \quad \hat{\psi}_k(\Lambda)}$$

$$\hat{\psi_k}(\Lambda) = -\sum_{j=0}^{C_{max}} C_{kj} + \sum_{m=1}^{\bar{M}} \lambda_m s_k |F_k(e^{j\omega_m})\hat{\mathbf{e}}^H(e^{j\omega_m})\mathbf{w}_k|^2 \tag{3.19}$$

The computational complexity of (3.19) is $\mathcal{O}(K2^{C_{max}+1})$. The computational complexity can be reduced by restricting the sparsity pattern of the pulse shaping filters such that only contiguous taps can be non-zero i.e., $\mathbf{c}_k$ always takes the form

$$\mathbf{c}_k = [\underbrace{1\cdots1}_{L_k+1}|\ \underbrace{0\cdots0}_{C_{max}-L_k}\ ] \tag{3.20}$$

We will refer to this as the *contiguous filter tap selection* (CTS) approach. Thus the combinatorial search over all the sparsity patterns is reduced to a linear search in the filter order. This can be written as

$$\boxed{\max_{L_k} \quad \hat{\psi_k}(\Lambda)} \tag{3.21}$$

$$\hat{\psi_k}(\Lambda) = -L_k - \sum_{m=1}^{\bar{M}} \lambda_m s_k |F_k(e^{j\omega_m})\hat{\mathbf{e}}^H(e^{j\omega_m})\mathbf{w}_k|^2, \tag{3.22}$$

where L_k is the filter order on tone k. The values of the Lagrange multipliers can then be updated until all the PSD constraints are met.

An algorithm description is given below in **Alg.** 3.1. The computational complexity is thus reduced to $\mathcal{O}(K(C_{max}+1))$ from $\mathcal{O}(K2^{C_{max}+1})$. The Lagrange multipliers, λ_m are updated based on the difference between the PSD mask and the output PSD, i.e.

$$\lambda_m \Leftarrow [\lambda_m - \mu_m(t_{mask,m} - t_{spec,m})]^+ \tag{3.23}$$

where μ_m is the step size for the update which is always positive. The μ_m can be varied in order to drop the energy at a frequency point quickly if the output spectrum at that frequency exceeds the PSD mask and to cautiously increase it if the output spectrum is under the PSD mask. A typical initialization value for $\mathbf{\Lambda} = \{\lambda_m\}$ is $\mathbf{0}$ and then $\mu = \{\mu_m\}$ can be initialized with a value generally much larger than 1 as we need to establish a very high value for $\mathbf{\Lambda}$ in order to make the $\sum_{m=1}^{\bar{M}} \lambda_m s_k |F_k(\omega_m)\mathbf{e}^H(\omega_m)\mathbf{w}_k|^2$ comparable to the value L_k. The algorithm stops when the number of taps stops updating.

Algorithm 3.1 Contiguous filter tap selection based pulse shaping filter tap allocation

Initialize $\mathbf{\Lambda}$,μ
repeat
  for tone $k \in \mathcal{K}$ **do**
    for filter order $L_k = 0 \cdots C_{max}$ **do**
      $\mathbf{c}_k = [\underbrace{1 \cdots 1}_{L_k+1} | \underbrace{0 \cdots 0}_{C_{max}-L_k}]$
      compute $\mathbf{w}_k$ (equation (3.3)-(3.4))
      $\hat{\psi}_k \underset{\text{argmax}}{\Leftarrow} \{-L_k - \sum_{m=1}^{\bar{M}} \lambda_m s_k |F_k(e^{j\omega_m}) \hat{\mathbf{e}}^H(e^{j\omega_m}) \mathbf{w}_k(e^{j\omega_m})|^2\}$
    end for
  end for
  compute $\mathbf{t}_{spec}$
  for $m = 1 \cdots \bar{M}$ **do**
    $\lambda_m = [\lambda_m - \mu_m(t_{mask,m} - t_{spec,m})]^+$
  end for
until (change in filter taps)

It is important to note that an analytical expression for the duality gap will be difficult to obtain. Therefore, it should be noted that the solution obtained from the dual problem formulation after the constraint relaxation may not be the globally optimal solution of the primal problem but nevertheless the procedure is found to provide practically relevant solutions (see section 3.6).

3.4.2 Sparse approximation based resource allocation

Computing sparse pulse shaping filters

From the previous section, it is clear that if we can somehow control the possible sparsity patterns of the pulse shaping filters, the computational complexity of the per-tone optimization problem will be reduced significantly. In section 3.4.1, the sparsity pattern of the pulse shaping filter was restricted to combinations where only contiguous taps can be non-zero, thus reducing the computational complexity from the combinatorial search to a linear search in the filter orders. However, restricting the sparsity pattern may not be the best approach, since the best sparsity pattern may not be in the restricted search space. In order to find a better way to control the sparsity pattern, let us write the problem of designing a pulse shaping filter (3.3) as a sparse approximation problem[152], i.e.

$$\min_{\mathbf{w}_k} \quad \mathbf{w}_k^H \mathbf{Q}_k \mathbf{w}_k + \tau \left\|\mathbf{w}_k\right\|_0 \quad \text{subject to} \quad W_k(e^{j\omega_k}) = 1, \tag{3.24}$$

Here $\|.\|_0$ is known as the ℓ_0 quasi-norm, which basically counts the number of non-zero elements of the vector in the argument, τ controls the trade off between the sparsity and the quadratic term. Problem (3.24) is however known to be NP hard in general. To simplify (3.24) the non-convex ℓ_0 quasi-norm is often replaced by the convex ℓ_1 norm [152]. This can be written as

$$\min_{\{\tilde{\mathbf{w}}_k} \quad \tilde{\mathbf{w}}_k^H \mathbf{Q}_k \tilde{\mathbf{w}}_k + \bar{\tau} \left\|\tilde{\mathbf{w}}_k\right\|_1 \quad \text{subject to} \quad \tilde{W}_k(e^{j\omega_k}) = 1, \tag{3.25}$$

where $\tilde{\mathbf{w}}_k$ is an approximation of $\mathbf{w}_k$, $\bar{\tau}$ controls the trade off between the sparsity and the quadratic term. (3.25) is a convex problem and can be solved using any generic solver in polynomial time [24]. If the underlying system admits a sparse solution, it has been shown that solving (3.25) is equivalent to solving (3.24) [152]. In our case, the underlying system does not necessarily admit a sparse solution, therefore we can not obtain a sparse pulse shaping filter by just solving (3.25). One way to obtain a sparse pulse shaping filter is to adopt a two step procedure. Firstly, we use (3.25) for a given $\bar{\tau}$ to obtain a nearly-sparse pulse shaping filter and then force the coefficients below a certain threshold level ρ to zero. Secondly, we use the sparsity pattern so obtained and we compute the pulse shaping filter using (3.3) and (3.4). It is clear that the choice of the trade off parameter $\bar{\tau}$ and the threshold ρ_k is important for the algorithm to work properly. An efficient update rule for these parameters is based on the difference between the total available system resources and the used system resources for the current value of $\bar{\tau}$. This can be written as

$$\bar{\tau} \Leftarrow \left[\bar{\tau} - \mu(C_{\text{budget}} - \sum_{k\in\mathcal{K}} \|\mathbf{w}_k\|_0)\right]^+, \tag{3.26}$$

where μ is a step size parameter and $[a]^+$ is max(0,a). We can either use a fixed threshold or we can also update the threshold in order to speed up the algorithm. The update formula for the threshold can be written as

$$\rho \Leftarrow \left[\rho - \bar{\mu}(C_{\text{budget}} - \sum_{k\in\mathcal{K}} \|\mathbf{w}_k\|_0)\right]^+, \tag{3.27}$$

In (3.27), the threshold is same for pulse shaping filter on all the tones. However, the pulse shaping filters which do not contribute much to the stop-band energy can have higher threshold than other filters. The performance of the algorithm can be further improved by using the weighted version of ρ for each tone. The correction in the threshold value for each tone is first weighted by the stop-band energy and can be written as

$$\rho_k \Leftarrow \left[\rho_k - \bar{\mu}_k(C_{\text{budget}} - \sum_{k\in\mathcal{K}} \|\mathbf{w}_k\|_0)\right]^+, \tag{3.28}$$

where $\bar{\mu}_k$ can be given as

$$\bar{\mu}_k = \bar{\mu} \sum_{m=1}^{\bar{M}} s_k |F_k(e^{j\omega_m}) \hat{e}^H(e^{j\omega_m}) \mathbf{w}_k| \tag{3.29}$$

Sparse approximation based pulse shaping filter tap allocation

The power at the various sample points in the spectral mask stop-band of a pulse shaping filter contribute differently to the overall optimization function. This information can be used to design a better filter by weighting different frequency sample points with the Lagrange multipliers. The Lagrange multipliers can thus be incorporated into the nearly-sparse filter design by modifying (3.25) into

$$\min_{\tilde{\mathbf{w}}_k} \quad \tilde{\mathbf{w}}_k^H \mathbf{Q}_k \tilde{\mathbf{w}}_k + \bar{\tau} \left\| \tilde{\mathbf{w}}_k \right\|_1 \quad \text{subject to} \quad \tilde{W}_k(e^{j\omega_k}) = 1$$

where,

$$\begin{aligned} \mathbf{Q}_k =& (1-\beta) \sum_{m \in \mathcal{M}_{sb}} \lambda_m |F_k(e^{j\omega_m})|^2 \hat{\mathbf{e}}(e^{j\omega_m}) \hat{\mathbf{e}}^H(e^{j\omega_m}) \\ &+ \beta \sum_{m \in \mathcal{M}_{pb}} |F_k(e^{j\omega_m})|^2 \hat{\mathbf{e}}(e^{j\omega_m}) \hat{\mathbf{e}}^H(e^{j\omega_m}), \end{aligned} \tag{3.30}$$

where $\mathcal{M}_{sb}$ and $\mathcal{M}_{pb}$ are the sets containing the indices of frequency samples in the stop-band and the pass-band of the spectral mask respectively. Similarly, the weighting of the frequency samples can also be incorporated in the sparse filter design using a given sparsity pattern using (3.3) and (3.4), where again the integral is replaced by a summation and $\mathbf{Q}_k$ is rewritten to incorporate the Lagrange multipliers, i.e.,

$$\min_{\mathbf{w}_k} \quad \mathbf{w}_k^H \mathbf{Q}_k \mathbf{w}_k \quad \text{subject to} \quad W_k(e^{j\omega_k}) = 1 \tag{3.31}$$

where,

$$\begin{aligned} \mathbf{Q}_k =& (1-\beta) \sum_{m \in \mathcal{M}_{sb}} \lambda_m |F_k(e^{j\omega_m})|^2 \hat{\mathbf{e}}(e^{j\omega_m}) \hat{\mathbf{e}}^H(e^{j\omega_m}) \\ &+ \beta \sum_{m \in \mathcal{M}_{pb}} |F_k(e^{j\omega_m})|^2 \hat{\mathbf{e}}(e^{j\omega_m}) \hat{\mathbf{e}}^H(e^{j\omega_m}) \end{aligned}$$

$$w_k^j = 0 \quad \text{if} \quad C_{kj} = 0 \quad \text{for } j = 0 \cdots C_{max}, \tag{3.32}$$

Since the sparsity pattern $\mathbf{c}_k$ computed from the solution of (3.25) and then applying the threshold already provides us the number of non-zero pulse shaping filter taps and their position, there is no need to compute any other objective functions. For given λ_m, $\bar{\tau}$ and ρ, the problem reduces to computing $\mathbf{w}_k$ for different $k \in \mathcal{K}$ and then checking if the PSD mask constraints and the filter tap budget constraint are met. An algorithm description is given in **Alg.** 3.2. The complexity of the proposed algorithm is then $O(K * \kappa)$ per update of the Lagrange multipliers, where κ is the cost associated with computing the nearly-sparse filter and then a sparse filter for one tone. For large C_{max}, $\kappa \approx C_{max}$, therefore the computational complexity for sparse approximation based pulse shaping filter tap allocation under fixed power loading is similar to the exhaustive search based CTS approach in section 3.4.1. The Lagrange multipliers, λ_m are updated based on the difference between the PSD mask and the output PSD, i.e.

$$\lambda_m \Leftarrow [\lambda_m - \mu_m(t_{mask,m} - t_{spec,m})]^+ \tag{3.33}$$

where $\hat{\mu}_m$ is the step size parameter for the update, which is always positive. The $\hat{\mu}_m$ can be varied in order to speed up the algorithm. A typical initialization value for $\mathbf{\Lambda} = \{\lambda_m\}$ is $\mathbf{0}$ and then $\hat{\mu} = \{\hat{\mu}_m\}$ can be initialized with a value generally much larger than 1. The algorithm stops when the number of taps stops updating.

In the next section, the algorithms discussed in this section will be extended in order to jointly allocate the pulse shaping filter taps and transmit power.

3.5 Joint pulse shaping filter tap and transmit power allocation

3.5.1 Contiguous filter tap selection based resource allocation

Here, we present an approach that is based on the dual problem formulation presented in (3.16).

We can restrict the sparsity pattern of the pulse shaping filters as suggested for the CTS procedure in the previous section. Therefore, we can rewrite (3.16) as

$$\boxed{\max_{L_k, s_k} \quad \psi_k(\gamma, \alpha, \Lambda)} \tag{3.34}$$

$$\psi_k(\gamma, \alpha, \Lambda) = R_k - \gamma L_k - \alpha s_k - \sum_{m=1}^{\bar{M}} \lambda_m s_k |F_k(e^{j\omega_m}) \hat{\mathbf{e}}^H(e^{j\omega_m}) \mathbf{w}_k|^2 \tag{3.35}$$

Algorithm 3.2 Sparse approximation based per-tone pulse shaping filter tap allocation with fixed power loading

Initialize $\mathbf{\Lambda}$, $\bar{\tau}$, ρ_k, $\hat{\mu}$, μ, $\bar{\mu}$
repeat
  for tone $k \in \mathcal{K}$ **do**
    compute nearly-sparse $\tilde{\mathbf{w}}_k$ solving
    $\min_{\tilde{\mathbf{w}}_k} \quad \tilde{\mathbf{w}}_k^H \mathbf{Q}_k \tilde{\mathbf{w}}_k + \bar{\tau} \left\| \tilde{\mathbf{w}}_k \right\|_1 \quad \text{subject to} \quad \tilde{W}_k(e^{j\omega_k}) = 1$
    apply threshold ρ and obtain sparsity pattern $\mathbf{c}_k$
    compute sparse $\mathbf{w}_k$ solving
    $\min_{\mathbf{w}_k} \quad \mathbf{w}_k^H \mathbf{Q}_k \mathbf{w}_k \quad \text{subject to} \quad W_k(e^{j\omega_k}) = 1$
    with
    $w_k^j = 0 \quad \text{if} \quad C_{kj} = 0 \quad \text{for } j = 0 \cdots C_{max}$
    $\bar{\mu}_k = \bar{\mu} \sum_{m=1}^{\tilde{M}} s_k |F_k(e^{j\omega_m}) \hat{e}^H(e^{j\omega_m}) \mathbf{w}_k|$
  end for
  compute $\mathbf{t}_{spec}$
  for $m \in \mathcal{M}_{sb}$ **do**
    update $\lambda_m \Leftarrow [\lambda_m - \hat{\mu}_m (t_{mask,m} - t_{spec,m})]^+$
  end for
  update $\bar{\tau} \Leftarrow \left[\bar{\tau} - \mu (C_{\text{budget}} - \sum_{k \in \mathcal{K}} \left\| \mathbf{w}_k \right\|_0)\right]^+$
  for $k \in \mathcal{K}$ **do**
    update $\rho_k \Leftarrow \left[\rho_k - \bar{\mu}_k (C_{\text{budget}} - \sum_{k \in \mathcal{K}} \left\| \mathbf{w}_k \right\|_0)\right]^+$
  end for
until (change in filter taps)

This per-tone optimization problem can be solved (for fixed Lagrange multipliers) by exhaustively searching over all possible values of L_k and s_k. The values of the Lagrange multipliers can then be updated until all the constraints are met. An algorithm description is given in **Alg.** 3.3. The complexity of the proposed algorithm is $O(K * \tilde{L} * (C_{max} + 1))$.

The Lagrange multipliers (γ, α and λ) are updated based on the difference between the obtained values for the corresponding resources and their target values, i.e.

$$\lambda_m \Leftarrow \lambda_m - \mu_j (t_{mask,m} - t_{spec,m})$$

$$\gamma \Leftarrow \gamma - \hat{\mu} (C_{budget} - \sum_{k \in \mathcal{K}} L_k)$$

$$\alpha \Leftarrow \alpha - \bar{\mu} (S_{budget} - \sum_{k \in \mathcal{K}} s_k)$$

where μ_m, $\hat{\mu}$ and $\bar{\mu}$ are the step sizes for the updates which are always positive.

Algorithm 3.3 Contiguous filter tap selection based joint resource allocation algorithm

Initialize $\mathbf{\Lambda}$, α, γ, μ_m, $\bar{\mu}$, $\hat{\mu}$
repeat
  for tone $k \in \mathcal{K}$ **do**
    for filter order $L_k = 0 \cdots L_{max}$ **do**
      $\mathbf{c}_k = [\underbrace{1 \cdots 1}_{L_k} | \underbrace{0 \cdots 0}_{C_{max}-L_k}]$
      compute $\mathbf{w}_k$ using(equation (3.3)-(3.4))
      for power level $s_k = 0 \cdots s_{max}$ **do**
        $\psi_k \underset{\text{argmax}}{\Leftarrow} \{R_k - \gamma L_k - \alpha s_k - \sum_{m=1}^{\bar{M}} \lambda_m s_k |F_k(e^{j\omega_m})\hat{\mathbf{e}}^H(e^{j\omega_m})\mathbf{w}_k|^2\}$
      end for
    end for
  end for
  compute $\mathbf{t}_{spec}$
  for $m = 1 \cdots \bar{M}$ **do**
    $\lambda_m \Leftarrow [\lambda_m - \mu_m(t_{mask,j} - t_{spec,j})]^+$
  end for
  $\gamma \Leftarrow [\gamma^t - \hat{\mu}(C_{budget} - \sum_k L_k)]^+$
  $\alpha \Leftarrow [\alpha - \bar{\mu}(s_{budget} - \sum_k s_k)]^+$
until (change in filter taps and used power)

3.5.2 Sparse approximation based resource allocation

We can rewrite the per-tone optimization problem for the joint per-tone pulse shaping filter tap allocation and power loading given in (3.18) as

$$\psi_k(\gamma, \alpha, \Lambda) = R_k - \gamma||\mathbf{w}_k||_0 - \alpha s_k - s_k \underbrace{\sum_{m=1}^{\bar{M}} \lambda_m |F_k(e^{j\omega_m})\mathbf{e}^H(e^{j\omega_m})\mathbf{w}_k|^2}_{a} \quad (3.36)$$

Since, we fix the sparsity pattern of $\mathbf{w}_i$ using (3.25) and then applying the threshold, for fixed Lagrange multipliers Λ, α and γ, the per-tone optimization problem (3.36) can be solved by exhaustively searching over all possible discrete power levels s_k. Since a in (3.36) is not power dependent, we need to compute the sparse filter only once at the beginning. The per-tone objective function in (3.36) for a given sparse per-tone pulse shaping filter can be rewritten as

$$\psi_k(\alpha, \Lambda) = R_k - (\alpha + a)s_k. \quad (3.37)$$

Here $\|\mathbf{w}_k\|_0$ is a constant, hence it can be removed from the optimization problem. By fixing the sparsity pattern using the sparse approximation technique, the

total computational complexity is $\mathcal{O}(K\tilde{L}+\kappa)$ per Lagrange multiplier iteration in contrast to $\mathcal{O}(K\tilde{L}(C_{max}+1))$ per Lagrange multiplier iteration. For large C_{max} this is a significant reduction in computational complexity. The values of the Lagrange multipliers can then be updated until all the constraints are met. An algorithm description is given below in **Alg.** 3.4. The Lagrange multiplier λ_m could be updated using (3.23) and Lagrange multiplier α can be updated based on the difference between the obtained values for the corresponding resources and their target values, i.e.

$$\alpha_k^{t+1} = \left[\alpha_k^t - \tilde{\mu}(S_{budget} - \sum_{k\in\mathcal{K}} s_k)\right]^+ \tag{3.38}$$

where $\tilde{\mu}$ is a positive step size.

Algorithm 3.4 Sparse approximation based joint resource allocation algorithm

Initialize $\mathbf{\Lambda}$, α, $\bar{\tau}$, ρ_k $k \in \mathcal{K}$, $\bar{\mu}$, $\hat{\mu}$, $\tilde{\mu}$
repeat
  for tone $k \in \mathcal{K}$ **do**
    compute a sparse $\mathbf{w}_k$ using (3.25), ρ, and (3.3)
    compute $a = \sum_{m=1}^{\bar{M}} \lambda_m |F_k(e^{j\omega_m})\mathbf{e}^H(e^{j\omega_m})\mathbf{w}_k|^2$
    for power level $s_k = 0 \cdots s_k^{mask}$ **do**
      $S_k^{opt} \underset{\text{argmax}}{\Leftarrow} \{R_k - s_k(\alpha + a)\}$
    end for
    $\bar{\mu}_k = \bar{\mu}\sum_{m=1}^{\bar{M}} s_k |F_k(e^{j\omega_m})\hat{e}^H(e^{j\omega_m})\mathbf{w}_k|$
  end for
  compute $\mathbf{t}_{spec}$ using S_k^{opt}
  update $\lambda_{\bar{\mathbf{M}}}$ using $\lambda_m \Leftarrow [\lambda_m - \mu_m(t_{mask,m} - t_{spec,j})]^+$
  update α using $\alpha_k \Leftarrow \left[\alpha_k - \tilde{\mu}(S_{budget} - \sum_{k\in\mathcal{K}} s_k)\right]^+$
  update $\bar{\tau}$ using $\bar{\tau} \Leftarrow \left[\bar{\tau} - \mu(C_{\text{budget}} - \sum_{k\in\mathcal{K}} \|\mathbf{w}_k\|_0)\right]^+$
  update ρ_k using $\rho_k \Leftarrow \left[\rho_k - \bar{\mu}_k(C_{\text{budget}} - \sum_{k\in\mathcal{K}} \|\mathbf{w}_k\|_0)\right]^+$
until (change in filter taps and used power)

3.6 Simulation results

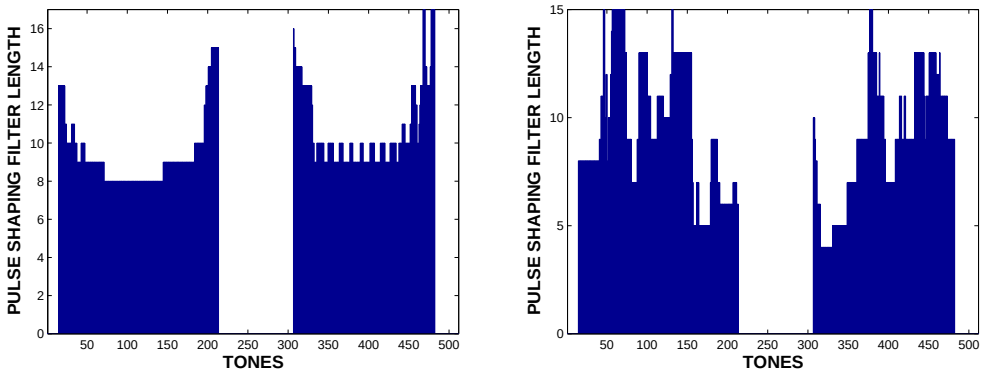
In our simulations, we consider VDSL downstream transmission with a PSD mask corresponding to the FTTCab M1 deployment scenario [10]. The size of the IDFT is 1024, the cyclic prefix length plus the overhead due to the maximum pulse shaping filter order per tone C_{max} is 80 samples and the SNR gap $\Gamma = 9.8$ dB. We use $C_{max} = 17$ to be able to compare our results to [33]. The initial values are $\lambda_j = 0$, $\alpha = 0$, $\hat{\mu}_m = 1e8$, $\bar{\mu} = 1$ and $\hat{\mu} = 1e-7$, $\bar{\tau} = 0$ and $\rho_k = 0$.

3.6.1 Resource allocation for a fixed power loading

In the first simulation, the channel under consideration is a 400m twisted pair cable in a bundle of 8 with an interference channel of 400m. We fix the tones used for transmission as suggested in [33], i.e., 375 predefined tones. **Figure 3.5(a)** shows the pulse shape filter tap distribution by using the CTS based approach. It can be seen that the tones at the band edges use filters with higher order than the tones in the middle of the band. **Figure 3.6(a)** shows that the total number of pulse shaping filter taps can be reduced significantly without violating the PSD mask constraint by using the CTS based pulse shaping filter tap allocation. In **Figure 3.6(a)**, in the initial iterations the main effort is to reduce the number of non-zero filter taps. This is achieved by using larger step size to update the Lagrange parameter but after some iteration the PSD mask constraints are violated therefore the algorithm tries to meet the PSD constraints by using smaller step size. After a few iterations, the number of non-zero filter taps stabilizes and the PSD mask constraint is also met. The total required number of pulse shaping filter taps reduces from 6735 (17*375) taps to 3787 taps corresponding to a 40% reduction. In **Figure 3.6(b)**, it is seen that the number of pulse shaping filter taps can be further reduced by using the sparse approximation based approach, namely to 3509 taps. From **Figure 3.6(a)** and **b**, it can be seen that the sparse approximation based approach also converges faster than the CTS based approach. Therefore, we can conclude that sparse approximation based approach provides a better solution at a lower computational complexity. The sparse approximation problem as formulated in (3.25) is solved using the `CVX` software for solving convex programs [67]. The distribution of pulse shaping filter taps over the 375 used tones for both algorithms is shown in **Figure 3.5(b)**. **Figure 3.7** shows the corresponding transmit PSD and the PSD mask.

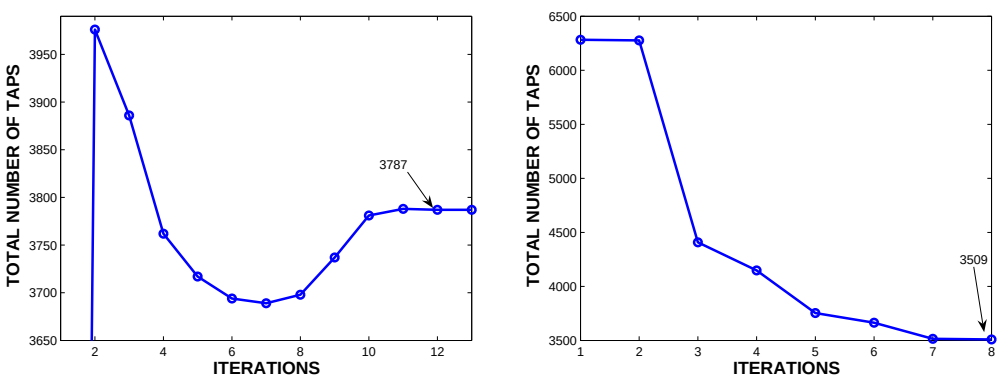
3.6.2 Joint pulse shaping filter tap and transmit power allocation

The channel under consideration is identical to the fixed power loading scenario. However, we now make all 428 tones available for transmission (instead of only 375 tones). The total available power is 11.5 dBm [10], which is larger than the total power needed to transmit maximum power -60 dBm/Hz on all tones, i.e., 8.682 dBm, hence the power constraint is not active. **Figure 3.8** shows the observed transmit PSD for the case of 5000 pulse shaping filter taps for the CTS based approach and the sparse approximation based approach. It can be seen that both the CTS based approach and the sparse approximation based approach can use the tones at the band edges more efficiently. However the sparse approximation based approach outperforms the CTS based approach. The tap distribution over tones for both approaches is presented in **Figure 3.9**. **Table 3.1** shows that the number of iterations taken for the algorithm to converge for the different pulse



(a) (b)

Figure 3.5: Distribution of number of pulse shaping filter taps over tones using (a) the CTS based approach (b) the sparse approximation based approach

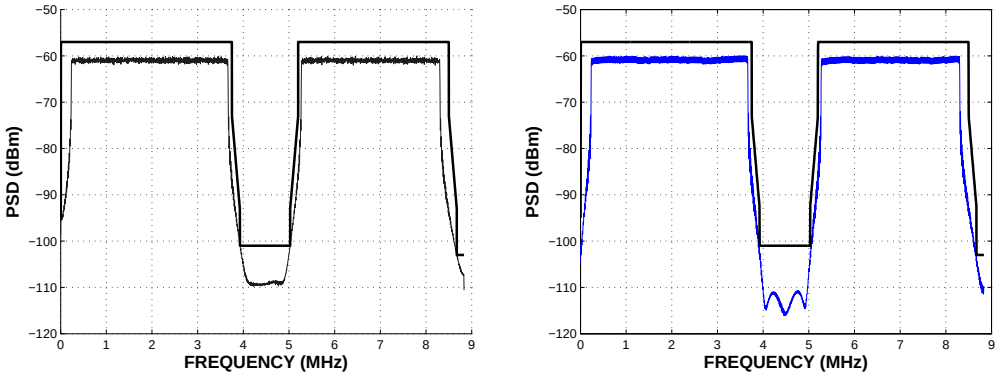


(a) (b)

Figure 3.6: Convergence of total number of pulse shaping filter taps using (a) the CTS based approach (b) the sparse approximation based approach

shaping filter tap budgets are similar for both approaches. Hence we can conclude that the overall complexity for the sparse approximation based approach is smaller than for the CTS based approach. It is obvious that if the resources are scarce, the algorithm requires a larger number of iterations, as it is then harder to distribute the resources optimally.

In **Figure 3.10** we compare the achieved bit-rates. Since the total available transmit power is larger than the total transmit power needed, we compare our



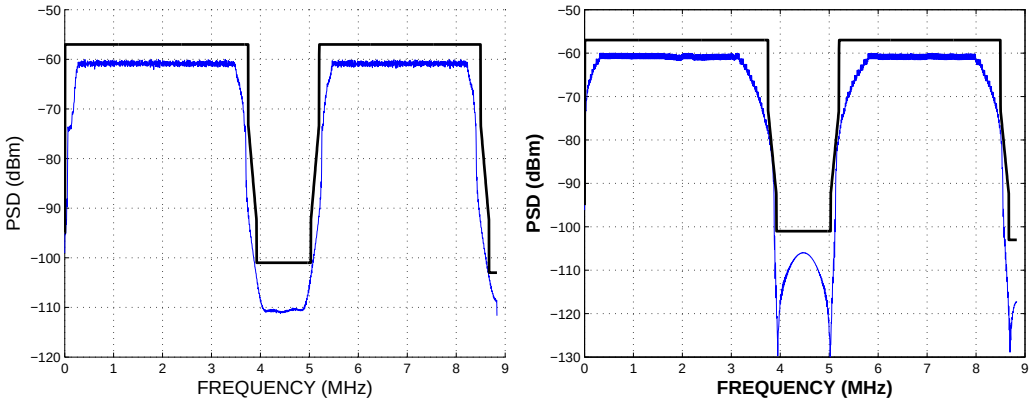
(a) (b)

Figure 3.7: Transmit PSD for (a) the CTS based approach (b) the sparse approximation based approach

Total filter taps	CTS based approach	SA based approach
5000	12	10
1000	20	21

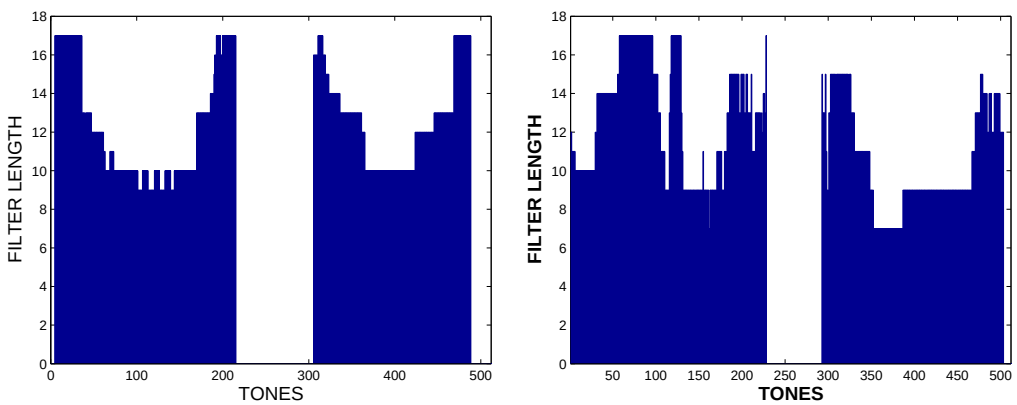
Table 3.1: Number of outer iterations taken to converge to the solution

results only for different total pulse shaping filter taps constraints, i.e., the power constraint is not active. We can see that the sparse approximation based approach performs better than the CTS based approach. It can be seen that the sparse approximation based approach utilizes the tones at the band edges more efficiently and hence the overall performance is increased. We also compare our results with two extreme cases. The first case is when there are no resource constraints (i.e. maximum allowed transmit power and maximum pulse shaping filter taps on all 428 used tones), which results in the dotted line in the **Figure 3.10**. The spectral mask constraints are not satisfied in this case. The second case is when only 375 tones are used and maximum transmit power is used for all these tones as in [33] (dashed line with + marker in the **Figure 3.10**). It can also be seen that the achieved rate for the sparse approximation based approach is consistently larger than for the CTS based approach. Furthermore, the sparse approximation based approach achieves the performance of case 2 [33] with much less (3000 vs 37*17=6325 taps) resources.



(a) (b)

Figure 3.8: Transmit PSD (5000 filter taps) for(a) the CTS based approach, (b) the sparse approximation based approach



(a) (b)

Figure 3.9: Pulse shaping filter tap distribution (5000 taps) for (a) the CTS based approach, (b) the sparse approximation based approach

3.7 Conclusion

In this chapter, it has been shown that the use of per-tone pulse shaping decreases the number of VCs on the band edges, thus increasing the achievable bit-rate of the DMT system. Furthermore, it has also been shown that using a constant length non-sparse pulse shaping filter on every tone unnecessarily increases the run-time

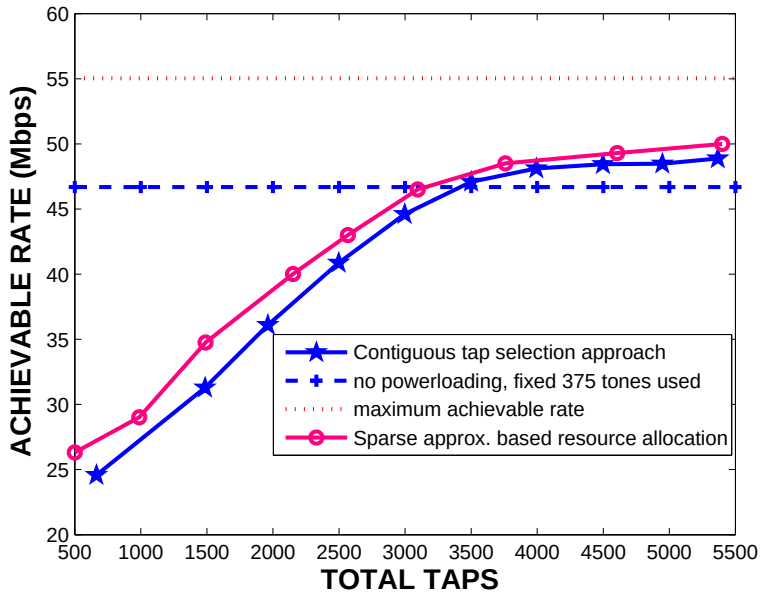


Figure 3.10: Relation of data rate and the total number of available resources

complexity of the system. Therefore, using a variably sparse pulse shaping filter on each tone reduces the run-time complexity without affecting the performance significantly.

To this end, we have proposed efficient resource allocation algorithms to distribute the available resources (total transmit power budget and total per-tone pulse shaping filter tap budget) over tones in a DMT transmitter with per-tone pulse shaping. We have shown that a dual problem formulation leads to an unconstrained optimization problem that is decoupled over tones but due to the combinatorial nature of the filter tap allocation the resulting optimization problem is still NP hard.

We have proposed two approaches to further simplify the problem. First, by restricting the filter sparsity pattern such that only contiguous taps are allowed to be non-zero, the combinatorial search in the sparsity pattern is reduced to a linear search in filter order. Second, by using sparse approximation techniques to design the sparse pulse shaping filter directly using a convex relaxation of the sparsity constraints, the sparse filter design problem can be written as a convex problem and solved efficiently. Furthermore, the techniques have also been extended to jointly allocate pulse shaping filter taps and transmit power.

A VDSL simulation has demonstrated that under a fixed power loading, the number of pulse shaping filter taps can be reduced to approximately 40% compared to the fixed length non-sparse cases without sacrificing performance. Furthermore, we have also shown that the sparse approximation based per-tone pulse shaping filter tap allocation approach performs better than the CTS based approach. When combined with transmit power loading these approaches can further reduce the number of per-tone pulse shaping filter taps needed to achieve the same bit-rate performance.

Chapter 4

Resource allocation in a DMT receiver with per-tone equalization

4.1 Introduction

Dispersive channels such as the DSL channel introduce ISI. In order to remove ISI a guard period is inserted between two DMT symbols known as the cyclic prefix (CP). The CP allows for an easy channel equalization at the DMT receiver. However, if the CP is shorter than the channel impulse response (CIR) then this results in ISI and ICI. Highly dispersive channels such as the DSL channel have a very long CIR, hence to mitigate ISI/ICI a very long CP is needed. As a long CP results in a large transmission overhead, channel equalization is used to shorten the effective length of the CIR [44] [18]. The usual time domain equalization (TEQ) [8] then corresponds to a joint equalization of all the tones and hence cannot optimize the performance in each and every tone. An alternative frequency domain equalization technique, known as per-tone equalization (PTEQ), was proposed in [2] in order to equalize each tone separately. It is then possible to optimize the bit-rate performance of the receiver using a suitable multitap equalizer for every tone, even without increasing the overall run-time computational complexity. For a detailed comparison of several equalizer architectures, we refer to [98, 97].

In a PTEQ based DSL system, typically every tone is equalized using a constant length non-sparse equalizer. However the DSL channel is frequency selective, therefore the channel gain varies for different tones, and so for a tone with a

low channel gain using a long equalizer does not improve its bit-rate performance significantly. Furthermore, due to the presence of transmit and receiver filtering effects, tones at the band edges require longer equalizers [1]. Therefore, using a constant length non-sparse equalizer for all tones may correspond to an increase in run-time complexity without much performance improvement. A better approach is then to consider variably sparse PTEQ filters, where each tone employs a PTEQ filter with different degree of sparsity. One of the main challenges then is to allocate the non-zero PTEQ filter taps for each tone without affecting the overall performance. In [174, 175], the order of the equalizer is determined by minimizing the MSE (Mean Squared Error) of the equalizer outputs. While the method tries to minimize the MSE for every tone, it does not provide a way to incorporate global resource constraints in the algorithm. Hence an alternative method is needed to distribute the non-zero equalizer taps which incorporates global resource constraints in the optimization problem.

For given resources (total number of equalizer taps and total power), the overall bit-rate optimization problem can be written as a dual problem using Lagrange multipliers. In this chapter, we will propose two algorithms to determine the optimal equalizer tap and transmit power allocation over the tones by solving this dual problem. The first approach is based on exhaustive search over all possible PTEQ filter orders and is referred to as the contiguous tap selection (CTS) based approach. The second approach is based on sparse approximation and is referred to as the sparse approximation based approach.

The chapter is organized as follows:

In **section 4.2**, a basic data model of the received DMT signal is described and per-tone equalization in DSL is reviewed.

In section **4.3**, the optimization problem for allocating the resources under a global resource constraint (total number of equalizer taps and total transmit power) is formulated for both a constant power loading scenario and with optimal power loading. It is then shown that the original optimization problem can be decoupled into per-tone optimization problems using a dual problem formulation.

In **section 4.4**, algorithm to solve the per-tone dual optimization problem for PTEQ filter tap allocation under a fixed power is presented. We present two different approaches to solve the per-tone dual problem.In **section 4.5**, the per-tone dual optimization problem for PTEQ filter tap allocation and power loading is solved. Two approaches to solve the problem is presented in this section.

In **section 4.6** the simulation results are presented. Finally conclusions are drawn in section **4.7**.

4.2 Preliminaries

4.2.1 Basic Data Model

The following notation is adopted in the description of the DMT system. K is the size of the (I)DFT and ν represents the length of the cyclic prefix, $\bar{K} = K + \nu$, and k, $\tilde{i}$ denote the tone index and DMT symbol index respectively, $\mathcal{F}_K$ and $\mathcal{I}_K$ are the K-point DFT and IDFT matrices where $\mathcal{F}_K(k,:)$ is the k-th row of $\mathcal{F}_K$. T is the length of the PTEQ filter and the equalizer coefficients vector for tone k is $\mathbf{v}_k$. $\mathbf{I}_Q$ and $\mathbf{0}_Q$ are the $Q \times Q$ identity and zero matrix respectively. $x_{k,\tilde{i}}$ is a complex subsymbol on tone k ($k = 1 \cdots K$) in symbol $\tilde{i}$. $\mathbf{x}_{\tilde{i}} = [x_{1,\tilde{i}} \cdots x_{K,\tilde{i}}]^T$. $y_{\tilde{i}}$ represents the received signal and $n_{\tilde{i}}$ represents the additive noise at time $\tilde{i}$, $\mathbf{h} = [h_L \cdots h_0 \cdots h_{-K}]$ is the channel impulse response in reverse order, $\{.\}^T$ denotes the transpose, $\{.\}^*$ denotes the conjugate.

The received signal can be modeled as

$$
\begin{aligned}
&\overbrace{\begin{bmatrix} y_{\tilde{i}.\bar{K}+\nu-T+2+\delta} \\ \ddots \\ y_{(\tilde{i}+1).\bar{K}+\delta} \end{bmatrix}}^{\mathbf{y}} \Big\updownarrow K+T-1 \\
&= \left[\begin{array}{c|ccc|c} & \mathbf{h} & 0 & \cdots & \\ \mathbf{0} & \ddots & \ddots & \ddots & \mathbf{0} \\ & 0 & \cdots & \mathbf{h} & \end{array}\right] . \begin{bmatrix} \mathbf{P} & \mathbf{0} & \mathbf{0} \\ \mathbf{0} & \mathbf{P} & \mathbf{0} \\ \mathbf{0} & \mathbf{0} & \mathbf{P} \end{bmatrix} \\
&\quad . \begin{bmatrix} \mathcal{I}_K & \mathbf{0} & \mathbf{0} \\ \mathbf{0} & \mathcal{I}_K & \mathbf{0} \\ \mathbf{0} & \mathbf{0} & \mathcal{I}_K \end{bmatrix} . \overbrace{\begin{bmatrix} \mathbf{x}_{\tilde{i}-1} \\ \mathbf{x}_{\tilde{i}} \\ \mathbf{x}_{\tilde{i}+1} \end{bmatrix}}^{\mathbf{x}} \\
&\quad + \overbrace{\begin{bmatrix} n_{\tilde{i}.\bar{K}+\nu-T+2+\delta} \\ \vdots \\ n_{(\tilde{i}+1).\bar{K}+\delta} \end{bmatrix}}^{\mathbf{n}} \\
&= \mathbf{H}.\mathbf{x} + \mathbf{n}
\end{aligned}
\tag{4.1}
$$

Here, δ is the synchronization delay and is a design parameter. Matrix $\mathbf{P}$ adds the cyclic prefix and is given as

$$
\mathbf{P} = \left[\begin{array}{c|c} \mathbf{0} & \mathbf{I}_\nu \\ \hline & \mathbf{I}_K \end{array}\right]
$$

In (4.1), the $\tilde{i}$-th symbol is the symbol of interest, the $(\tilde{i}-1)$-th and the $(\tilde{i}+1)$-th symbol have been used to fully describe the ISI. $\mathbf{y}$ is the input at the front end of the receiver. For further details on the used data model we refer to chapter 2.

4.2.2 Per-tone Equalization

Time domain equalization, together with demodulation for tone k can be written as

$$Z_k^{(\tilde{i})} = D_k \text{row}_k(\mathcal{F}_K)(\mathbf{Y}\mathbf{w}) \tag{4.2}$$

where $\mathbf{w}$ is the vector representing the T-tap time domain equalizer (TEQ) and D_k is the single tap frequency domain equalizer (FEQ) coefficient for tone k, $Z_k^{(\tilde{i})}$ is the equalizer output for tone k at symbol $\tilde{i}$. $\mathbf{Y}$ is the $K \times T$ Toeplitz matrix given as

$$\mathbf{Y} = \begin{bmatrix} y_{\tilde{i}.\bar{K}+\nu+1} & y_{\tilde{i}.\bar{K}+\nu} & \cdots & y_{\tilde{i}.\bar{K}+\nu-T+2} \\ y_{\tilde{i}.\bar{K}+\nu+2} & y_{\tilde{i}.\bar{K}+\nu+1} & \cdots & y_{\tilde{i}.\bar{K}+\nu-T+3} \\ \ddots & \ddots & \ddots & \ddots \\ y_{(\tilde{i}+1).\bar{K}} & y_{(\tilde{i}+1).\bar{K}-1} & \cdots & y_{(\tilde{i}+1).\bar{K}+\nu-T+1} \end{bmatrix},$$

where we have set $\delta = 0$ for conciseness.

The PTEQ moves the equalization operation into the frequency domain and can be derived from (4.2) as follows [2]

$$Z_k^{(\tilde{i})} = \text{row}_k \underbrace{(\mathcal{F}_K.\mathbf{Y})}_{\text{T FFTs}}. \underbrace{\mathbf{w}.D_k}_{\text{T-tap FEQ}} . \tag{4.3}$$

In (4.3), it can be seen that T FFT operations are needed to calculate one output symbol compared to one FFT operation per output symbol when time domain equalization is used. However it was shown in [2] that (4.3) can first be written in terms of a sliding FFT and then eventually only one FFT and T-1 difference terms are needed to calculate one output symbol, as shown in (4.4) and (4.5).

$$Z_k^{(\tilde{i})} = \mathbf{w}^T.D_k. \begin{bmatrix} \mathcal{F}_K(k,:) & 0 & \cdots \\ \vdots & \ddots & \vdots \\ 0 & \cdots & \mathcal{F}_K(k,:) \end{bmatrix} .\mathbf{y} \tag{4.4}$$

$$Z_k^{(\tilde{i})} = \mathbf{v}_k^T . \underbrace{\left[\begin{array}{c|c|c} \mathbf{I}_{T-1} & \mathbf{0} & -\mathbf{I}_{T-1} \\ \hline \mathbf{0} & \mathcal{F}_K(k,:) & \end{array} \right]}_{\mathbf{F}_k} . \mathbf{y} \tag{4.5}$$

The first block row in matrix $\mathbf{F}_k$ in (4.5) extracts the difference terms, while the last row corresponds to the single FFT. **Figure 4.1** shows a general structure for a per-tone equalizer as given by (4.5).

For each used tone a minimum mean squared error PTEQ (MMSE-PTEQ) can then be found by minimizing the cost function $J(\mathbf{v}_k)$ in (4.6). This MMSE-PTEQ optimizes the SNR for each tone separately.

$$\begin{aligned} \underset{\mathbf{v}_k}{\text{minimize}} \;\; J(\mathbf{v}_k) &= \underset{\mathbf{v}_k}{\text{minimize}} \; \mathcal{E}\left\{ \left| \mathbf{v}_k^T . \mathbf{F}_k . \mathbf{y} - x_k^{(\tilde{i})} \right|^2 \right\} \\ &= \underset{\mathbf{v}_k}{\text{minimize}} \left\| \underbrace{\left[\begin{array}{c} {\mathbf{R_x}}^{1/2} \mathbf{H}^H \mathbf{F}_k^H \\ \hline {\mathbf{R_n}}^{1/2} \mathbf{F}_k^H \end{array} \right]}_{\mathbf{A}_k} \mathbf{v}_k^* - \underbrace{\left[\begin{array}{c} {\mathbf{R_x}}^{1/2} \mathbf{e}_k^{(\tilde{i})H} \\ \hline \mathbf{0} \end{array} \right]}_{\mathbf{b}_k} \right\|_2^2 \\ &= \underset{\mathbf{v}_k}{\text{minimize}} \;\; \|\mathbf{A}_k \mathbf{v}_k^* - \mathbf{b}_k\|_2^2 , \end{aligned} \tag{4.6}$$

where $\mathcal{E}\{.\}$ is the expectation operation, $\mathbf{R_x} = \mathcal{E}\{\mathbf{x}\mathbf{x}^H\}$ and $\mathbf{R_n} = \mathcal{E}\{\mathbf{n}\mathbf{n}^H\}$ and $\mathbf{e}_k^{(\tilde{i})H}$ is a column vector with 1 as the k-th position and 0's elsewhere.

We will design a pulse shaping filter under additional sparsity constraints, i.e, we will complement (4.6) with constraints

$$v_k^j = 0 \quad \text{if} \quad C_{kj} = 0 \quad \text{for } j = 0 \cdots T, \tag{4.7}$$

where the C_{kj}'s define the sparsity pattern.

4.2.3 Effect of PTEQ length

The general PTEQ structure uses a constant length non-sparse equalizer for all the tones. The higher frequency part in the DSL spectrum has lower channel gains, therefore using longer equalizers does not result in a significant performance gain at these high frequencies. This is shown in **Figure 4.2**. In most of the tones a shorter equalizer can achieve almost the same performance as a longer equalizer. This highlights that a significant portion of the system resources is wasted without any performance gain.

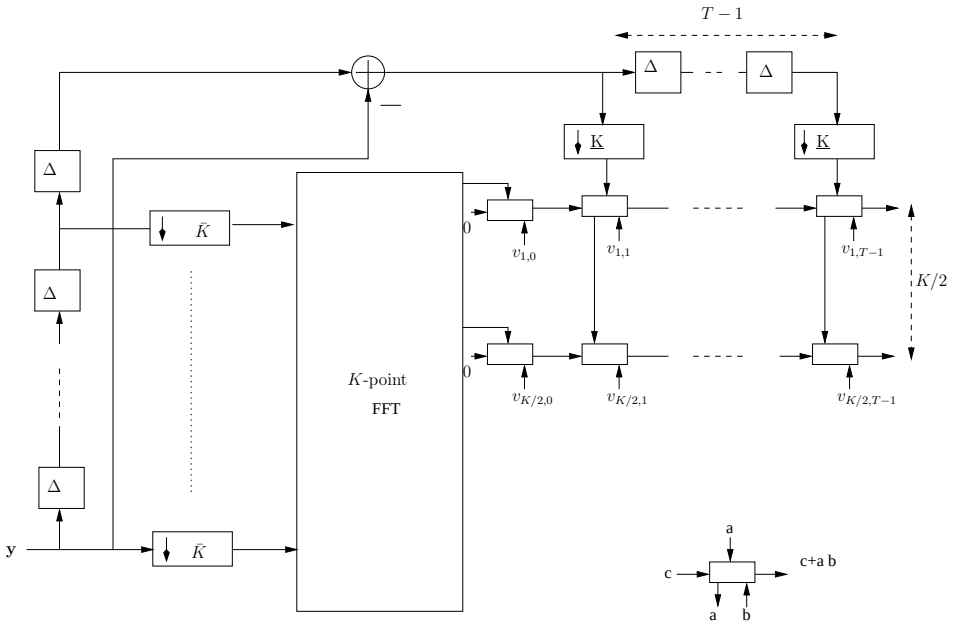


Figure 4.1: T-tap per-tone equalizer model [2]

4.3 Problem formulation

In section 4.3.1, an optimization problem for the MMSE-PTEQ tap allocation for a constant power loading is formulated. In section 4.3.2, we then extend the problem formulation to accommodate the joint MMSE-PTEQ tap and transmit power allocation.

4.3.1 Resource allocation for a fixed power loading

In the previous section, the motivation for the use of variably sparse MMSE-PTEQ filters without affecting the overall performance was presented. The main challenge then is to allocate the non-zero equalizer taps over tones such that the performance is optimal.

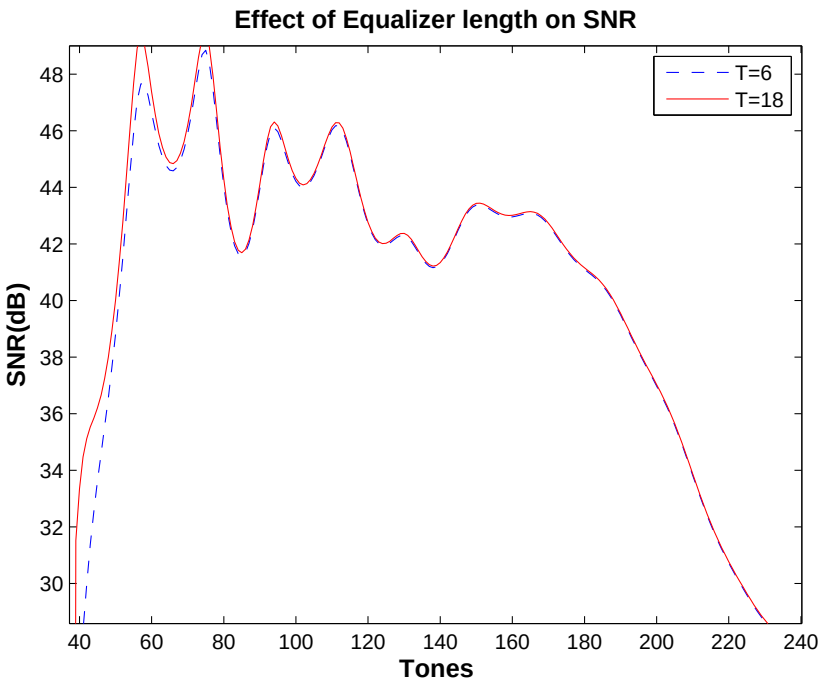


Figure 4.2: Comparison of signal to noise ratio (SNR) per tone for different MMSE-PTEQ equalizer lengths for a typical ADSL scenario

For a given equalizer tap budget, we can write this as an optimization problem as follows

$$\begin{array}{ll} \max\limits_{\mathbf{C}} & \sum_{k\in\mathcal{K}} R_k \\ \text{subject to} & \sum_{k\in\mathcal{K}} \sum_{j=1}^{T} C_{kj} < C_{\text{budget}} \end{array} \tag{4.8}$$

where,

$$R_k = \Delta_f \log_2\left(1 + \frac{\text{SNR}_k}{\Gamma}\right)$$

where $\mathcal{K}$ is the set containing the indices of the used tones, R_k is the bit-rate on tone k, Δ_f is the sampling frequency, Γ is SNR gap, $C_{kj} \in \{0, 1\}$. C_{kj} is 1 if the j-th equalizer tap for tone k is selected and 0 otherwise, C_{budget} is the predefined maximum total number of equalizer taps, $\mathbf{c}_k = [C_{k1} \cdots C_{kT}]$ is a vector that represents the position of the used equalizer taps on the k-th tone, $\mathbf{C}$ is a

matrix which has $\mathbf{c}_k^T$ as its k-th row. SNR_k is the SNR obtained for tone k, as a function of its equalizer with sparsity pattern $\mathbf{c}_k$, and designed based on (4.6).

The constraint in (4.8) is coupled over tones and furthermore it also makes the problem combinatorial. One possibility to solve (4.8) is to perform an exhaustive search for all the tones over all possible sparsity patterns of the PTEQ filters. This method has a prohibitively high complexity of $\mathcal{O}(2^{MT})$, where M is the cardinality of $\mathcal{K}$. In order to simplify (4.8), it can be posed as an unconstrained optimization problem using a dual problem formulation as

$$\min_{\lambda}\left\{\max_{\mathbf{C}}(\mathcal{L})\right\} \quad \text{where } \mathcal{L}=\sum_{k\in\mathcal{K}} R_k+\lambda(C_{\text{budget}}-\sum_{k\in\mathcal{K}}\sum_{j=1}^{T} C_{kj}) \tag{4.9}$$

where λ is known as the Lagrange multiplier and $\mathcal{L}$ is the Lagrangian.

It is seen that for a given value of λ, the maximization in (4.9) decouples over tones and can be written as

$$\max_{\mathbf{c}_k}(\mathcal{L}_k) \quad \text{where } \mathcal{L}_k = R_k-\lambda\sum_{j=1}^{T} C_{kj} \tag{4.10}$$

where $\mathcal{L}_k$ is the per-tone Lagrangian, and $\lambda\sum_{j=1}^{T} C_{kj}$ represents the penalty for increasing the number of non-zero equalizer taps for tone k. This per-tone optimization problem (for given λ) can be readily solved by exhaustively searching over all possible sparsity patterns $\mathbf{c}_k$. The value of λ can be updated until $\sum_{k\in\mathcal{K}}\sum_{j=1}^{T} C_{kj}$ matches C_{budget}. The dual problem is still combinatorial and has a complexity of $\mathcal{O}(M2^T)$. In section 4.4, we will present algorithms to further reduce the computational complexity.

4.3.2 Joint equalizer filter tap and transmit power allocation

In the previous section, the MMSE-PTEQ tap allocation problem in the case of a constant power loading was presented. The frequency selective nature of the DSL channel also calls for a different transmit power allocation over different tones to achieve a maximum overall bit-rate. Therefore, for given resource constraints (total number of non-zero equalizer taps and total power), an efficient algorithm to allocate the resources over all the tones is needed. The resource allocation problem

can be posed as an optimization problem as follows

$$\boxed{\begin{aligned} \max_{\mathbf{C},\mathbf{s}} \quad & \sum_{k\in\mathcal{K}} R_k \\ \text{subject to} \quad & \sum_{k\in\mathcal{K}}\sum_{j=1}^{T} C_{kj} \leq C_{\text{budget}} \\ & \sum_{k\in\mathcal{K}} s_k \leq S_{budget} \\ & 0 \leq s_k \leq s_k^{mask}, \end{aligned}} \tag{4.11}$$

where $s_k \in \mathcal{S}$ is the power on tone k, $\mathcal{S}$ is the set containing all possible discrete power levels, S_{budget} is the total power constraint, s_k^{mask} is the maximum power allowed on the tone k and other quantities are as defined in section 4.3.1. The primal optimization problem given by (4.11) is coupled over tones and is again a combinatorial problem. It has computational complexity of $\mathcal{O}(\tilde{L}^M 2^{MT})$, where $\tilde{L}$ is the cardinality of the set $\mathcal{S}$ and gives the number of total discrete power levels. This is intractable even for a moderate number of tones, discrete power levels and equalizer taps. In the previous section, it was shown that for a fixed power (4.8) decouples over tones if formulated as a dual problem, thus reducing the computational complexity. The dual problem formulation of (4.11) can be written as

$$\min_{\lambda,\gamma}\left\{\max_{\mathbf{C},\mathbf{s}} \quad \{\mathcal{L}\}\right\} \qquad \text{where } \mathcal{L} = \sum_{k\in\mathcal{K}} R_k + \lambda\left(C_{\text{budget}} - \sum_{k\in\mathcal{K}}\sum_{j=1}^{T} C_{kj}\right) + \gamma\left(S_{budget} - \sum_{k\in\mathcal{K}} s_k\right), \tag{4.12}$$

where λ and γ are known as the Lagrange multipliers and $\mathcal{L}$ is the Lagrangian. It is seen that for given value of λ and γ the maximization in (4.12) decouples over tones and can be written as

$$\max_{\mathbf{c}_k, s_k} (\tilde{\mathcal{L}}_k) \quad \text{where } \tilde{\mathcal{L}}_k = R_k - \lambda\sum_{j=1}^{T} C_{kj} - \gamma s_k, \tag{4.13}$$

where $\mathcal{L}_k$ is the per-tone Lagrangian. Even though (4.13) is decoupled over tones, we still have to perform an exhaustive search over all possible discrete values of s_k and all the possible $\mathbf{c}_k$'s. The search over all $\mathbf{c}_k$'s is still a combinatorial problem

and incurs exponential complexity in T. From (4.6), it can also be seen that to compute a $\mathbf{v}_k$ we need a full $\mathbf{R}_x$. Therefore, $\mathbf{v}_k$ is a function of the power allocated to all the other tones which is then assumed to be constant. After computation of the optimal $\mathbf{v}_k$ and its corresponding transmit power, the process is repeated for the next tone $k+1$. For given λ and γ, the computational complexity is $\mathcal{O}(ML2^T)$, which is still large for large T. It can be seen that if we can somehow restrict the sparsity pattern of the equalizers, then the combinatorial search is avoided and the exponential complexity reduces to linear complexity in T. In section 4.4, we will present algorithms to further reduce this complexity.

4.4 Resource allocation for a fixed power loading

4.4.1 Contiguous filter tap selection based resource allocation

Here we present an approach that is based on (4.10) to further reduce the computational complexity.

The computational complexity of the (4.10) is $\mathcal{O}(M2^T)$. The computational complexity can be reduced by restricting the sparsity patterns of the PTEQ filters such that only contiguous filter taps can be non-zero. This is referred as the *contiguous filter tap selection* (CTS) approach. Thus the combinatorial search over all the sparsity patterns is reduced to a linear search in the filter order. This can be written as

$$\max_{\mathbf{c}_k}(\mathcal{L}_k) \quad \text{where } \mathcal{L}_k = R_k - \lambda L_k \tag{4.14}$$

with

$$\mathbf{c}_k = [\underbrace{1 \cdots 1}_{L_k+1} | \underbrace{0 \cdots 0}_{T-L_k+1}] \tag{4.15}$$

where L_k is the filter order on tone k. This reduces the total number of combinations from 2^T to T and also makes the overall computational complexity $\mathcal{O}(MT)$, i.e., linear in the number of tones and the number of taps. The values of the Lagrange multipliers can then be updated until the tap budget constraint is met.

In (4.14), increasing the λ increases the penalty for increasing the equalizer length. Hence the value of λ is quite important in obtaining the optimal solution. There are many ways to update the value of λ such as the bisection method, the gradient descent method etc. [29] [154]. In [154], the update of λ is based on the difference between the total available system resources and the used system resources for the

current value of λ. For our problem this can be written as,

$$\lambda \Leftarrow [\lambda - \mu(C_{\text{budget}} - \sum_{k \in \mathcal{K}} L_k)]^+ \tag{4.16}$$

where μ is a scaling factor, whose value can be changed in order to obtain a faster convergence to the solution. For simplicity, in our simulations μ is taken as a fixed arbitrary value close to zero.

In the presented algorithm, **Alg.** 4.1, a search over the equalizer lengths for a particular tone and for a fixed λ is terminated when the maximum number of taps that can be allocated is reached.

Algorithm 4.1 Contiguous filter taps selection based PTEQ tap allocation for a fixed power loading

initialize λ, μ
repeat
  for tones $k \in \mathcal{K}$ **do**
    for filter order $j = 0 \cdots T$ **do**
      $\mathbf{c}_k = [\underbrace{1 \cdots 1}_{j+1} | \underbrace{0 \cdots 0}_{T-j}]$
      compute $\mathbf{v}_k$ using(equation (4.6)-(4.7))
      compute bit-rate on tone k with j-th order PTEQ filter, $R_{k,j}$
      $L_k \underset{\text{argmax}}{\Leftarrow} R_{k,j} - \lambda.j$
    end for
  end for
  $C_{total} = \sum_k L_k$
  $\lambda = [\lambda - \mu(C_{\text{budget}} - C_{total})]^+$
until $C_{total} \neq C_{budget}$

4.4.2 Sparse approximation based resource allocation

Computing sparse PTEQ filters

From the previous section, it is clear that if we can somehow control the possible sparsity patterns of the PTEQ filters the computational complexity of the per-tone optimization problem will be reduced significantly. In section 4.4.1, the sparsity pattern was restricted to combinations where only contiguous filter taps can be non-zero thus reducing the computational complexity from a combinatorial search to a linear search in the PTEQ filter orders. However restricting the sparsity pattern may not be the best approach, since the best sparsity pattern may not be in the restricted search space. In this section, we will use a sparse approximation

based approach to design a sparse MMSE-PTEQ filter. In order to find a better way to control the sparsity pattern, let us write the problem of designing an MMSE-PTEQ filter (4.6) as a sparse approximation problem [152, 153, 49]

$$\underset{\mathbf{v}_k}{\text{minimize}} \quad \|\mathbf{A}_k\mathbf{v}_k^* - \mathbf{b}_k\|_2^2 + \tau \|\mathbf{v}_k\|_0 , \tag{4.17}$$

where $\|.\|_0$ is an ℓ_0 quasi-norm of the vector in argument counting the number of non-zero elements of the vector, τ controls the trade off between the sparsity and the quadratic term. Problem (4.17) is however known to be NP hard in general [152]. To simplify (4.17) the non-convex ℓ_0 quasi-norm is often replaced by the convex ℓ_1 norm [152, 153, 49]. This can be written as

$$\boxed{\underset{\tilde{\mathbf{v}}_k}{\text{minimize}} \quad \|\mathbf{A}_k\tilde{\mathbf{v}}_k^* - \mathbf{b}_k\|_2^2 + \bar{\tau} \|\tilde{\mathbf{v}}_k\|_1 ,} \tag{4.18}$$

where $\tilde{\mathbf{v}}_k$ is an approximation of $\mathbf{v}_k$. $\bar{\tau}$ controls the trade off between the sparsity and the quadratic term. (4.18) is a convex problem and can be solved using any generic solver in polynomial time [24]. If the underlying system admits a sparse solution, it has been shown that solving (4.18) is equivalent to solving (4.17) [153, 49]. In our case, the underlying system does not necessarily admit a sparse solution, therefore we can not obtain a sparse MMSE-PTEQ filter by just solving (4.18). One way to obtain a sparse MMSE-PTEQ filter is to adopt a two step procedure. Firstly, we use the (4.18), for a given $\bar{\tau}$, to obtain a nearly-sparse MMSE-PTEQ and then force the coefficients below a certain threshold level ρ to zero to obtain the sparsity pattern $\mathbf{c}_k$. Secondly, we use the sparsity pattern $\mathbf{c}_k$ to compute a sparse MMSE-PTEQ filter using a modified (4.6) as follows

$$\min_{\mathbf{v}_k} \quad \|\mathbf{A}_k\mathbf{v}_k^* - \mathbf{b}_k\|_2^2$$

subject to

$$v_{kj} = 0 \quad \text{if} \quad C_{kj} = 0 \qquad \text{for} \quad j = 1 \cdots T \tag{4.19}$$

It is clear that the choice of the trade off parameter $\bar{\tau}$ and the threshold ρ is important for the algorithm to work properly. An efficient update rule for $\bar{\tau}$ is based on the difference between the total available system resources and the used system resources for the current value of $\bar{\tau}$. This can be written as

$$\bar{\tau} \Leftarrow \left[\bar{\tau} - \mu(C_{\text{budget}} - \sum_{k\in\mathcal{K}} \|\mathbf{v}_k\|_0)\right]^+ \tag{4.20}$$

where μ is a positive scaling factor, and [a]+ is max(0,a). For simplicity, in our simulations μ is taken as a fixed arbitrary positive value close to zero.

The threshold level ρ can be fixed to a constant level and the coefficients smaller than the threshold value ρ can be set to zero. But we can also update the threshold level to speed up the convergence. It is obvious that if the threshold level is set to a higher value, the probability of a sparser equalizer becomes higher. The update formula for the threshold level can be written as

$$\rho \Leftarrow \left[\rho - \sigma(C_{\text{budget}} - \sum_{k\in\mathcal{K}} \|\mathbf{v}_k\|_0)\right]^+, \tag{4.21}$$

where σ is an arbitrarily small positive scaling factor.

For given $\bar{\tau}$ and ρ, the number of non-zero PTEQ filter taps and their position is given by the sparsity pattern $\mathbf{c}_k$ computed by solving (4.18) and applying the threshold ρ. Therefore, there is no need to compute any other objective functions. After computing the sparsity pattern $\mathbf{c}_k$ for all the tones we need to check the total number of non-zero PTEQ filter taps and update the Lagrange multipliers and the threshold parameter accordingly. The sparse PTEQ filter for tone k can be computed by using (4.19).

In (4.21), the threshold is same for PTEQ filters on all the tones. However, the PTEQ filters have different MMSEs. The PTEQ which has lower MMSE can have higher threshold than the PTEQ filter with higher MMSE. The performance of the PTEQ filter tap allocation algorithm can be further improved by using the weighted version of ρ for each tone. The correction in the threshold value for each tone is first weighted by the MMSE of the PTEQ filter and can be written as

$$\rho_k \Leftarrow \left[\rho_k - \sigma_k(C_{\text{budget}} - \sum_{k\in\mathcal{K}} \|\mathbf{v}_k\|_0)\right]^+, \tag{4.22}$$

where

$$\sigma_k = \sigma\|\mathbf{A}_k\mathbf{v}^* - \mathbf{b}_k\|_2^2 \tag{4.23}$$

Even though the equalizer coefficients need to be computed twice, for a large T the overall computational complexity is similar to the complexity of the CTS based approach of section 4.4.2.

An algorithm to allocate the non-zero equalizer taps for given resource constraints in the case of a constant power loading is given in **Alg.** 4.2.

Algorithm 4.2 Sparse approximation based MMSE-PTEQ tap allocation for a fixed power loading

Initialize parameters $\bar{\tau}$ and thresholds ρ_k for $k \in \mathcal{K}$
Initialize step sizes μ and σ
repeat
  for tone $k \in \mathcal{K}$ **do**
    Compute nearly-sparse MMSE-PTEQ $\tilde{\mathbf{v}}_k$ using

$$\tilde{\mathbf{v}_k} = \underset{\mathbf{v}_k}{\operatorname{argmin}} \quad \|\mathbf{A}_k \mathbf{v}_k^* - \mathbf{b}_k\|_2^2 + \beta \|\mathbf{v}_k\|_1$$

    Apply threshold ρ_k on $\tilde{\mathbf{v}}$ to compute sparsity pattern $\mathbf{c}_k$
    Compute sparse MMSE-PTEQ $\mathbf{v}_k$ using

$$\mathbf{v}_k = \underset{\mathbf{v}_k}{\operatorname{argmin}} \|\mathbf{A}_k \mathbf{v}_k^* - \mathbf{b}_k\|_2^2$$
$$\text{subject to} \quad v_{kj} = 0 \quad \text{if} \quad c_{kj} = 0 \qquad \text{for} \quad j = 1 \cdots T$$

    $\sigma_k = \sigma \|\mathbf{A}_k \mathbf{v}_k^* - \mathbf{b}_k\|_2^2$
  end for
  Compute $C_{total} = \sum_{k \in \mathcal{K}} \|\mathbf{v}_k\|_0$
  Update $\bar{\tau} = [\bar{\tau} - \mu(C_{\text{budget}} - C_{total})]^+$
  for $k \in \mathcal{K}$ **do**
    Update $\rho_k = [\rho_k - \sigma_k(C_{\text{budget}} - C_{total})]^+$
  end for
until $(C_{budget} - C_{total} \leq \text{tolerance})$

4.5 Joint equalizer filter tap and transmit power allocation

4.5.1 Contiguous filter tap selection based resource allocation

Here, we present an approach that is based on the dual problem formulation presented in (4.13). We can restrict the sparsity pattern of the MMSE-PTEQ as suggested for CTS in the previous section. Therefore we can rewrite

$$\max_{\mathbf{c}_k, s_k} (\tilde{\mathcal{L}}_k) \quad \text{where } \tilde{\mathcal{L}}_k = R_k - \lambda L_k - \gamma s_k, \tag{4.24}$$

with

$$\mathbf{c}_k = [\underbrace{1 \cdots 1}_{L_k+1} | \underbrace{0 \cdots 0}_{T-L_k+1}] \tag{4.25}$$

where L_k is the MMSE-PTEQ filter order. This per-tone optimization problem can be solved (for fixed Lagrange multipliers) by exhaustively searching over all values of L_k and s_k. The values of the Lagrange multipliers can then be updated until all the constraints are met. An algorithm description is given in **Alg.** 4.3. The complexity of the proposed algorithm is $O(M * \tilde{L} * T)$.

Algorithm 4.3 Contiguous filter tap selection based joint MMSE-PTEQ tap and transmit power allocation

Initialize vector containing transmitted power $\mathbf{s}$, s_k^{opt}, $L_k^{opt} = T$
Initialize Lagrange multipliers λ and γ
Initialize step sizes θ and η
repeat
  for tone $k \in \mathcal{K}$ **do**
    Initialize $\mathcal{L}_k^{opt} = 0$
    for power level $s_k \in \mathcal{S}$ **do**
      for filter order $j = 0 \cdots T-1$ **do**
        Compute $\mathbf{v}_k$ of order j using $\mathbf{s}$
        Compute $\mathcal{L}_k \Leftarrow R_k - \lambda j - \gamma s_k$
        if $\mathcal{L}_k \geq \mathcal{L}_k^{opt}$ **then**
          $\mathcal{L}_k^{opt} \Leftarrow \mathcal{L}_k$
          $L_k^{opt} \Leftarrow j$
          $s_k^{opt} \Leftarrow s_k$
        end if
      end for
    end for
  end for
  Compute $C = \sum_{k \in \mathcal{K}} L_k^{opt}$
  Compute $S = \sum_{k \in \mathcal{K}} s_k^{opt}$
  Update $\lambda = [\lambda - \theta(C_{budget} - C)]^+$
  Update $\gamma = [\gamma - \eta(S_{budget} - S)]^+$
until ($S_{budget} - S \leq$ tolerance & $C_{budget} - C \leq$ tolerance)

4.5.2 Sparse approximation based resource allocation

In this section, we describe the full convex relaxation based resource allocation. With $\|\mathbf{v}_k\|_0 = \sum_{j=1}^{T} C_{kj}$, we can also write (4.10) as

$$\max_{\mathbf{c}_k} \quad R_k - \lambda \|\mathbf{v}_k\|_0 - \gamma s_k, \tag{4.26}$$

Now for each discrete power level, we can compute a sparse $\mathbf{v}_k$ using the method described in section 4.5.1. This results in solving (4.18) once for each power level and compute the sparsity pattern $\mathbf{c}_k$ and then compute the sparse PTEQ using (4.19). Even though the equalizer coefficients need to be computed twice, for a large T it has similar computational complexity to the CTS based approach of section 4.5.1, which requires solving (4.6)-(4.7) T times for each power level. The computational complexity can be further reduced by solving (4.18) only once for the initial power level and then using the same sparsity pattern for all the other power levels.

Furthermore the Lagrange multiplier γ, which enforces the total power constraint also has to be updated. The Lagrange multiplier only depends on the difference between the current total power and the total power budget and hence can be written as

$$\gamma \Leftarrow \left[\gamma - \eta(S_{\text{budget}} - \sum_{k\in\mathcal{K}} s_k)\right]^+, \tag{4.27}$$

where η is an arbitrarily small positive step size. Similarly, to enforce the total tap budget constraint in the outer loop we can use similar formulation and can be written as

$$\lambda \Leftarrow \left[\lambda - \theta(C_{\text{budget}} - \sum_{k\in\mathcal{K}} \|\mathbf{v}_k\|_0)\right]^+, \tag{4.28}$$

where θ is an arbitrarily small positive step size.

An algorithm to allocate the resources, i.e. number of equalizer taps and the transmit power, for given resource constraints is given in **Alg.** 4.4.

4.6 Simulation results

The channel under consideration here is a 400m twisted pair cable in a bundle of 8 with an interference channel of 400m. We use the same setting as in [106] in order to compare the results. In these simulations, the synchronization delay δ has not been considered. The bit error rate has been fixed to 10^{-7}, the coding

Algorithm 4.4 Sparse approximation based joint MMSE-PTEQ tap and transmit power allocation

Initialize vector containing transmitted power $\mathbf{s}$, s_k^{opt}
Initialize Lagrange multipliers β, λ and γ
Initialize step sizes μ, σ and η and threshold ρ_k $k \in \mathcal{K}$
repeat
  for tone $k \in \mathcal{K}$ **do**
    Compute $\tilde{\mathbf{v}}_k$ using (4.18) and $\mathbf{s}$
    Find the sparsity pattern $\mathbf{c}_k$ by applying the threshold to $\tilde{\mathbf{v}}_k$
    Initialize $\mathcal{L}_k^{opt} = 0$
    for power level $s_k \in \mathcal{S}$ **do**
      Compute sparse $\mathbf{v}_k$ using (4.6) and the sparsity pattern $\mathbf{c}_k$
      Compute the objective function $\mathcal{L}_k$ using
      $\max_{\mathbf{s}_k} \quad R_k - \lambda \left\|\mathbf{v}_k\right\|_0 - \gamma s_k$
      if $\mathcal{L}_k \geq \mathcal{L}_k^{opt}$ **then**
        $s_k^{opt} \Leftarrow s_k$
        $\mathcal{L}_k^{opt} \Leftarrow \mathcal{L}_k$
      end if
    end for
    Replace transmitted power tone k in $\mathbf{s}$ with s_k^{opt}
    $\mathbf{v}_k^{opt} \Leftarrow \mathbf{v}_k$
    $\sigma_k = \sigma \left\|\mathbf{A}_k \mathbf{v}_k^{opt*} - \mathbf{b}_k\right\|_2^2$
  end for
  Update $\gamma = \left[\gamma - \eta(S_{budget} - \sum_{k\in\mathcal{K}} s_k)\right]^+$
  Update $\lambda = \left[\lambda - \theta(C_{budget} - \sum_{k\in\mathcal{K}} \left\|\mathbf{v}_k\right\|_0)\right]^+$
  for $k \in \mathcal{K}$ **do**
    Update $\rho_k = \left[\rho_k - \sigma_k(C_{\text{budget}} - \sum_{k\in\mathcal{K}} \left\|\mathbf{v}_k\right\|_0)\right]^+$
  end for
until ($s_{budget} - \sum_k s_k \leq$ tolerance & $C_{budget} - \sum_k \left\|\mathbf{v}_k\right\|_0 \leq$ tolerance)

gain and the noise margin are 3 dB and 6 dB respectively. The signal and noise PSD levels are -60dB and -140 dB respectively and the total power budget is 11.5 dBm [10]. Three consecutive symbols are considered to account for the ISI. The channel is assumed to be known perfectly at the receiver. We fix the tones used for transmission as suggested in [33], i.e., 375 predefined tones, to be consistent with the previous chapter. For the variable length per-tone equalizer the maximum number of equalizer taps per tone is 20.

4.6.1 Resource allocation for a fixed power loading

In the first scenario, the transmit power loading is assumed to be fixed and only the MMSE-PTEQ filter tap allocation is performed. **Figure 4.3** compares the bit-rates for the CTS based approach, sparse approximation based approach and fixed length MMSE-PTEQ for a given per-tone equalizer tap budget. To compute the sparsity pattern using (4.18), we can use any available numerical solver e.g. CVX [67, 66]. From **Figure 4.3**, it can be clearly seen that both the CTS and the sparse approximation based approach reduce the number of the non-zero PTEQ filter taps by around 40%. It can also be seen that for a given bit-rate the sparse approximation based equalizer tap allocation approach performs better than the CTS based equalizer tap allocation. Therefore, we can conclude that for similar computational complexity we can always obtain better performance using a sparse approximation based equalizer tap allocation. In **Figure 4.4**, allocation of the non-zero PTEQ filter taps is shown. It can be seen that the tones on the band edges require more non-zero PTEQ filter taps than the tones in the middle of the band.

4.6.2 Joint equalizer filter tap and transmit power allocation

In the second scenario, we also perform transmit power loading. The total power constraint is 11dBm. In our case we have 375 used tones and -60 dBm maximum PSD. Therefore, the total power constraint is not active. It can be seen from **Figure 4.5** that transmit power loading improves the MMSE-PTEQ tap distribution. From **Figure 4.6**, it can be seen that the tap distribution over tones is similar to the distribution in **Figure 4.3**. The main concentration of non-zero PTEQ filter taps is around the band edges. But the additional power loading enables us to use a smaller number of non-zero filter taps for some of the tones in the middle of the bands, hence reducing the overall number of non-zero PTEQ filter taps.

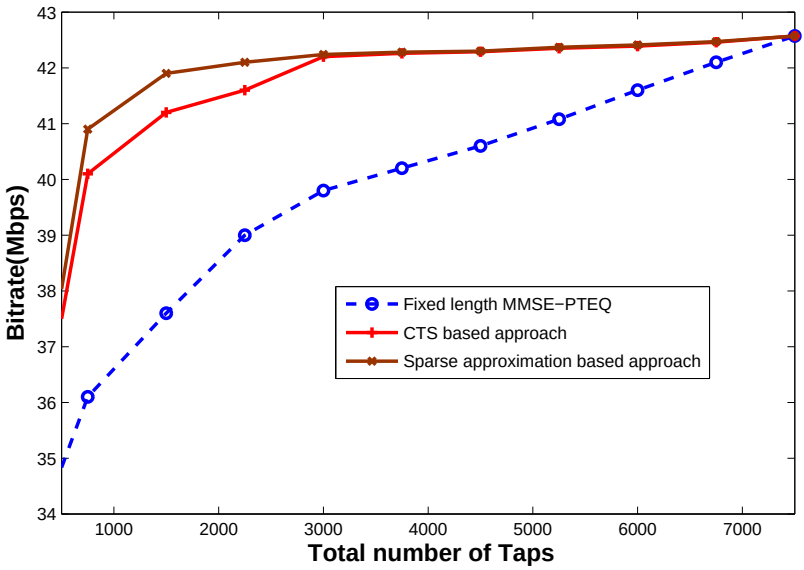


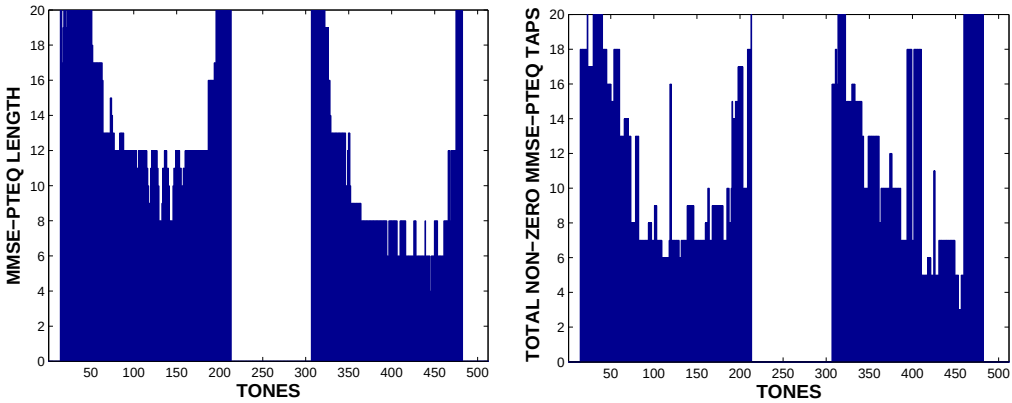
Figure 4.3: Comparison of bit-rate versus total number of non-zero MMSE-PTEQ taps for contiguous filter tap selection based approach, sparse approximation based approach and fixed length MMSE-PTEQ approach

4.7 Conclusion

In this chapter, it has been shown that the use of the MMSE-PTEQ increases the achievable bit-rate of the DMT system. Furthermore, it has also been shown that using a constant length non-sparse MMSE-PTEQ filter on every tone unnecessarily increases the run-time complexity of the DMT system. Therefore, using variably sparse MMSE-PTEQ filters tone reduces the run-time complexity without affecting the performance significantly.

To this end, we have proposed efficient resource allocation algorithms to distribute the available resources (total transmit power budget and total MMSE-PTEQ filter tap budget) over tones in a DMT receiver with per-tone equalization. We have shown that a dual problem formulation leads to an unconstrained optimization problem that is decoupled over tones but due to the combinatorial nature of the filter tap allocation the resulting optimization problem is still intractable.

We have proposed two approaches to further simplify the problem. First, by restricting the sparsity pattern of the MMSE-PTEQ such that only contiguous



(a) (b)

Figure 4.4: Optimum distribution of number of MMSE-PTEQ taps over tones using (a) the contiguous filter tap selection based approach (b) the sparse approximation based approach

MMSE-PTEQ taps are allowed to be non-zero, the combinatorial search in the sparsity pattern is reduced to a linear search in the filter order. Second, sparse approximation techniques have been used to design the sparse MMSE-PTEQ filters directly. Using convex relaxation of the sparsity constraints, the sparse filter design problem can be written as a convex problem and solved efficiently. Furthermore, the techniques have also been extended to jointly allocate MMSE-PTEQ filter taps and the transmit power.

A VDSL simulation demonstrated that under a fixed power loading, the number of MMSE-PTEQ filter taps can be reduced to approximately 40% compared to the fixed length non-sparse case without sacrificing performance. Furthermore, we have also shown that the sparse approximation based MMSE-PTEQ filter tap allocation approach performs better than the contiguous tap selection based approach. It has also been shown that when combined with transmit power loading, these approaches can further reduce the number of per-tone pulse shaping filter taps needed to achieve the same bit-rate performance.

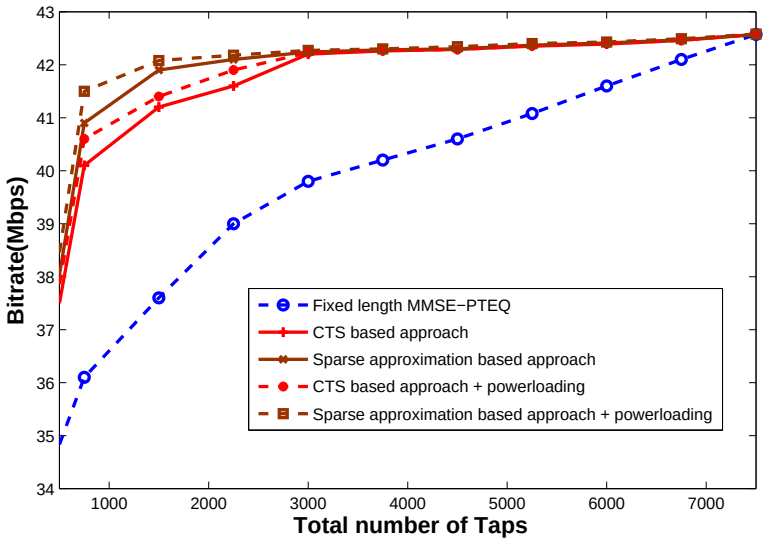
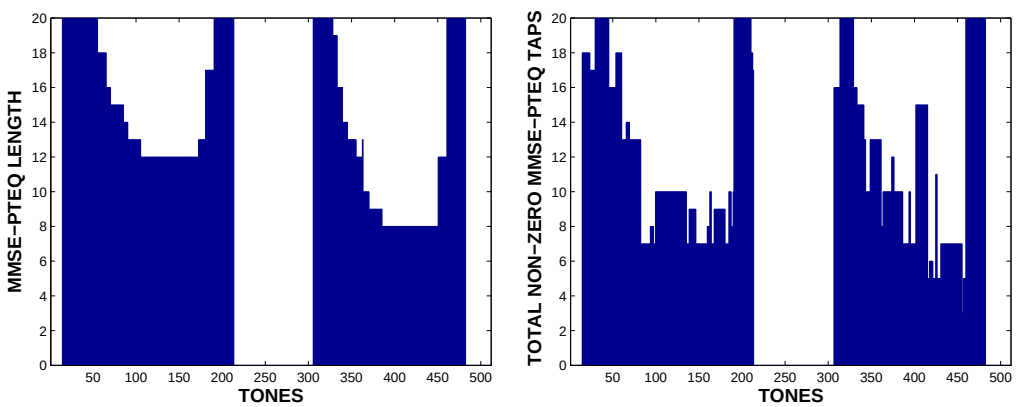


Figure 4.5: Comparison of bit-rate versus total number of non-zero MMSE-PTEQ taps for contiguous filter tap selection based approach, sparse approximation based approach and fixed length MMSE-PTEQ approach with and without transmit power loading



(a) (b)

Figure 4.6: Optimum distribution of number of MMSE-PTEQ taps under transmit power loading over tones using (a) the contiguous filter tap selection based approach(b) the sparse approximation based approach

Chapter 5

Joint resource allocation in DMT transceivers

5.1 Introduction

In chapter 3, a DMT transmitter with per-tone pulse shaping filters was considered. Under the assumption of a long enough cyclic prefix and perfect receiver, efficient resource allocation algorithms to optimally allocate pulse shaping filter taps and transmit power were presented. Then in chapter 4, a DMT receiver with per-tone equalization was considered. It was shown that dispersive channels such as the DSL channel have a very long CIR, and so to ensure there is no ISI and ICI, a very long CP is needed. Therefore, a channel shortening equalizer is needed to ensure the CP can be kept short. A per-tone equalizer combines channel shortening with the frequency domain equalization on each tone by using a multitap frequency domain equalization. It was shown in chapter 4 that not every tone needs to be equalized by an equalizer of the same order. The tones at the band edges typically need longer filters than the tones at the middle of the band. It was also shown that the number of non-zero filter taps can be further reduced by using optimal transmit power allocation along with the PTEQ tap allocation. In chapter 4, however, the effect of a pulse shaping filter at the transmitter side was not considered. Furthermore, the effect of a PSD mask constraint was also neglected.

In this chapter, we will consider both the DMT transmitter with per-tone pulse shaping and the DMT receiver with per-tone equalization. We will refer to this structure as a DMT transceiver for the sake of brevity. The non-zero PTEQ and per-tone pulse shaping filter taps and transmit power can be allocated more efficiently if the effect of the pulse shaping filter and PSD mask constraint is also

taken into account. The complexity of solving the optimization problem to jointly allocate resources in a DMT transceiver can be very high. The constraints are coupled over tones and the optimization problem is non-convex.

The Lagrange multiplier method is often used to convert a constrained optimization problem into a dual unconstrained problem. This method was used in chapter 3 and chapter 4 to reduce the complexity of solving the optimization problem. It was shown that the problem decouples over tones, hence reducing the computational complexity. In this chapter, we will also use the Lagrange multiplier method to simplify the optimization problem. We will investigate the contiguous filter tap selection algorithm, presented in chapter 3 and chapter 4, to further reduce the computational complexity. Additionally, the sparse approximation based resource allocation, presented in chapter 3 and chapter 4, will also be investigated.

This chapter is organized as follows:

In **section 5.2**, a combined system model of the DMT transceiver employing per-tone pulse shaping filters and PTEQ filters is presented.

In **section 5.3**, the resource allocation problem in a DMT transceiver is formulated under a PSD mask constraint, and transmitter and receiver filter tap budgets with and without transmit power loading.

In **section 5.4**, resource allocation algorithms to allocate the run-time complexity, i.e., non-zero pulse shaping filter taps and non-zero PTEQ taps, under a fixed power loading are then presented. The algorithms are based on a restricted filter sparsity pattern and a sparse approximation based filter design.

In **section 5.5**, resource allocation algorithms to jointly allocate the run-time complexity and per-tone transmit power are presented. The technique based on contiguous filter tap selection and sparse filter design will then be applied to reduce the computational complexity of the resource allocation algorithm.

In **section 5.6**, some simulation results will be presented. Finally conclusions are drawn in section **5.7**.

5.2 System model

The following notation is adopted in the description of the DMT transceiver system. K is the IDFT-size and k denotes the tone index. C_{max} is the maximum pulse shaping filter order, ν is the cyclic prefix length. $\mathbf{x}_i^t$ is the output of the transmitter in the time domain, i.e. a vector of length $\underline{\mathrm{K}} = K + C_{max} + \nu$, corresponding to one transmitted symbol at time i. T is the maximum PTEQ filter order.

$$\begin{bmatrix} y^t_{i.k+\nu-T+C_{max}+2} \\ \ddots \\ y^t_{(i+1).k} \end{bmatrix} = \left[\begin{array}{c|ccc|c} \mathbf{0} & \mathbf{h} & 0 & \dots & \\ & \ddots & \ddots & \ddots & \mathbf{0} \\ & 0 & \dots & \mathbf{h} & \end{array}\right] \begin{bmatrix} \mathbf{x}^t_{i-1} \\ \mathbf{x}^t_i \\ \mathbf{x}^t_{i+1} \end{bmatrix} + \begin{bmatrix} n^t_{i.k+\nu-T+C_{max}+2} \\ \vdots \\ n^t_{(i+1).k} \end{bmatrix}, \tag{5.1}$$

where from (3.6) we can see

$$\mathbf{x}^t_i = \underbrace{\begin{bmatrix} \mathbf{0} & \mathbf{I}_\nu \\ \mathbf{I}_K & \\ \mathbf{0}_{C_{max}\times K} & \end{bmatrix} \mathcal{I}_K \mathbf{D}}_{\mathbf{\Phi}} \mathbf{x}_k + \underbrace{\sum_{k\in\mathcal{K}} \begin{bmatrix} -\alpha^{k(\nu+1)}\bar{\mathbf{v}}_k \\ \mathbf{0}_{(K+\nu-C_{max})\times 1} \\ \alpha^k \bar{\mathbf{v}}_k \end{bmatrix} x_{ik}}_{\mathbf{a}_i}.$$

$$= \mathbf{\Phi}\mathbf{x}_k + \mathbf{a}_i \tag{5.2}$$

Here, all the quantities are as described in chapter 3. The per-tone transmit pulse shaping filters can be designed as suggested in chapter 3. (5.1) can then be written as

$$\overbrace{\begin{bmatrix} y_{i.k+\nu-T+C_{max}+2} \\ \ddots \\ y_{(i+1).k} \end{bmatrix}}^{\mathbf{y}} = \overbrace{\left[\begin{array}{c|ccc|c} \mathbf{0} & \mathbf{h} & 0 & \dots & \\ & \ddots & \ddots & \ddots & \mathbf{0} \\ & 0 & \dots & \mathbf{h} & \end{array}\right] \begin{bmatrix} \mathbf{\Phi} & \mathbf{0} & \mathbf{0} \\ \mathbf{0} & \mathbf{\Phi} & \mathbf{0} \\ \mathbf{0} & \mathbf{0} & \mathbf{\Phi} \end{bmatrix}}^{\mathbf{H}} \overbrace{\begin{bmatrix} \mathbf{x}_{i-1} \\ \mathbf{x}_i \\ \mathbf{x}_{i+1} \end{bmatrix}}^{\mathbf{x}}$$

$$+ \underbrace{\left[\begin{array}{c|ccc|c} \mathbf{0} & \mathbf{h} & 0 & \dots & \\ & \ddots & \ddots & \ddots & \mathbf{0} \\ & 0 & \dots & \mathbf{h} & \end{array}\right] \begin{bmatrix} \mathbf{a}_{i-1} \\ \mathbf{a}_i \\ \mathbf{a}_{i+1} \end{bmatrix} + \begin{bmatrix} n_{i.k+\nu-T+C_{max}+2} \\ \vdots \\ n_{(i+1).k} \end{bmatrix}}_{\mathbf{z}}$$

$$\mathbf{y} = \mathbf{H}\mathbf{x} + \mathbf{z}, \tag{5.3}$$

From chapter 4, we know that the PTEQ, $\mathbf{v}_k$ for tone k, can be obtained by minimizing the cost function as follows

$$\min_{\mathbf{v}_k} \quad J(\mathbf{v}_k) = \min_{\mathbf{v}_k} \quad \mathcal{E}\left\{|\mathbf{v}_k\mathbf{F}_k\mathbf{y} - x_{ik}|^2\right\}, \tag{5.4}$$

where

$$\mathbf{F}_k = \left[\begin{array}{c|c|c} \mathbf{I}_{T-1} & \mathbf{0} & -\mathbf{I}_{T-1} \\ \hline \mathbf{0} & \mathcal{F}_K(k,:) & \end{array}\right] \tag{5.5}$$

After a few trivial steps, it can be written as

$$\begin{aligned} \min_{\mathbf{v}_k} \quad J(\mathbf{v}_k) =& \min_{\mathbf{v}_k} \quad \left\| \underbrace{\left[\begin{array}{c} \mathbf{S}^{1/2}\mathbf{H}^H\mathbf{F}_k^H \\ \mathbf{R}_z^{1/2}\mathbf{F}_k^H \end{array}\right]}_{\mathbf{A}_k} \mathbf{v}_k^* - \underbrace{\left[\begin{array}{c} \mathbf{S}^{1/2}\mathbf{e}_k^H \\ \mathbf{0} \end{array}\right]}_{\mathbf{b}_k} \right\|_2^2 \\ &= \min_{\mathbf{v}_k} \|\mathbf{A}_k\mathbf{v}_k^* - \mathbf{b}_k\|_2^2 , \end{aligned} \tag{5.6}$$

where $\mathcal{E}\{.\}$ is the expectation operation, $\mathbf{S} = \mathcal{E}\{\mathbf{x}^t\mathbf{x}^{tH}\}$ and $\mathbf{R}_z = \mathcal{E}\{\mathbf{z}\mathbf{z}^H\}$ and $\mathbf{e}_k^H$ is a column vector with 1 at the kth position and 0s elsewhere.

5.3 Problem formulation

In chapter 3 and chapter 4, the motivation for using a variably sparse per-tone pulse shaping filter and PTEQ filter was presented. Chapter 3 and chapter 4 formulated and solved the resource allocation problems independently of each other. At the DMT transmitter, the receiver was considered perfect and the cyclic prefix was assumed to be long enough to remove ISI, while at the DMT receiver, the effect of a per-tone pulse shaping filter at the transmitter and the PSD mask constraint was ignored for the sake of simplicity. In this section, we will formulate the joint resource allocation for both the DMT transmitter and the receiver. Firstly, in section 5.3.1, we will formulate the resource allocation (joint transmit-receive non-zero filter tap allocation) problem under fixed power loading. Secondly, this optimization problem formulation will be extended to include optimal transmit power allocation along with the non-zero filter tap allocation in section 5.3.2.

5.3.1 Resource allocation for a fixed power loading

For given total tap budgets C^{tr}_{budget} and C^{r}_{budget} for the transmitter and the receiver, we can write the filter tap allocation problem as

$$\begin{aligned} \max_{\mathbf{C}^{tr},\mathbf{C}^{r}} \quad & \sum_{k\in\mathcal{K}} R_k \\ \text{Subject to} \quad & \sum_{k\in\mathcal{K}}\sum_{j=0}^{C_{max}} C^{tr}_{kj} \le C^{tr}_{budget} \\ & \sum_{k\in\mathcal{K}}\sum_{j=0}^{T} C^{r}_{kj} \le C^{r}_{budget} \\ & \mathbf{t}_{spec} \le \mathbf{t}_{mask}, \end{aligned} \tag{5.7}$$

where $\mathcal{K}$ is the set containing the indices of the used tones, $C^{t}_{kj} \in \{0,1\}$ is 1 if the j-th per-tone pulse shaping filter tap is selected for tone k and 0 otherwise. Similarly, $C^{r}_{kj} \in \{0,1\}$ is 1 if the j-th PTEQ filter tap is selected on tone k and 0 otherwise. C^{tr}_{budget} and C^{r}_{budget} are the pulse shaping filter and PTEQ filter tap budget respectively. $\mathbf{c}^{tr}_{k} = \left[C^{tr}_{k1}\cdots C_{kC^{tr}_{max}}\right]$ is the vector which represents the position of the used per-tone pulse shaping filter taps on the k-th tone and is referred to as the sparsity pattern of the resulting per-tone pulse shaping filter, $\mathbf{C}^{t}$ is a matrix which has $\mathbf{c}^{t}_{k}$ as its row, $\mathbf{c}^{r}_{k}$ and $\mathbf{C}^{r}$ can be similarly defined. $\mathbf{t}_{mask}$ is the vector containing M sample points of the PSD mask at different frequencies and $\mathbf{t}_{spec}$ is the vector containing the similarly sampled PSD of the transmitter output. R_k is the achieved bit-rate for tone k which is given as

$$R_k = \Delta_f \log_2(1 + \frac{SNR_k}{\Gamma}), \tag{5.8}$$

where Δ_f is the sampling frequency, Γ is the SNR gap, SNR_k is the SNR obtained for tone k, as a function of its equalizer with sparsity pattern $\mathbf{c}^{r}_{k}$, based on (5.4) and can be computed as in [2]. For the sake of convenience, let us rewrite it again as follows

$$\text{SNR}_k = \frac{S_k}{\text{Int}_k + \text{Noise}_k}, \tag{5.9}$$

where

$$S_k = \left|(\mathbf{S}^{1/2}\mathbf{H}^{H}\mathbf{F}^{H}_{k})_{(K+k,:)}\mathbf{v}^{*}_{k}\right|^2 \tag{5.10}$$

$$\text{Int}_k + \text{noise}_k = \left\|\mathbf{S}^{1/2}\mathbf{H}^{H}\mathbf{F}^{H}_{k}\mathbf{v}^{*}_{k}\right\|^2 + \left\|\mathbf{R}^{1/2}_{z}\mathbf{F}^{H}_{k}\mathbf{v}^{*}_{k}\right\|^2 - S_k. \tag{5.11}$$

The constraints in (5.7) are coupled over tones and furthermore make the problem combinatorial. One possibility to solve (4.8) is to perform an exhaustive search for all the tones over all possible sparsity patterns of the pulse shaping filter and PTEQ filter. This method has a prohibitively high complexity. In order to simplify (5.7), it can be posed as an unconstrained optimization problem using a dual formulation as

$$\min_{\lambda_t,\lambda_r,\gamma}\left\{\max_{\mathbf{C}^{tr},\mathbf{C}^{r}} \quad \Psi\right\},$$

where

$$\Psi = \sum_{k\in\mathcal{K}} R_k + \lambda_t\left(C_{budget}^{tr} - \sum_{k\in\mathcal{K}}\sum_{j=0}^{C_{max}} C_{kj}^{tr}\right) + \lambda_r\left(C_{budget}^{r} - \sum_{k\in\mathcal{K}}\sum_{j=0}^{T} {C_{kj}}^{r})\right)$$

$$+ \sum_{m=1}^{\bar{M}} \gamma_m\left(t_{mask,m} - t_{spec,m}\right)$$

$$\lambda_t, \lambda_r, \gamma_m \geq 0. \tag{5.12}$$

Here λ_r, λ_t and γ_m are Lagrange multipliers.γ is a vector containing all γ_m's. From (3.11), we know that

$$\begin{aligned} t_{spec,m} &= \sum_{k\in\mathcal{K}} s_k |F_k(e^{j\omega_m})W_k(e^{j\omega_m})|^2 \\ &= \sum_{k\in\mathcal{K}} s_k |F_k(e^{j\omega_m})\hat{\mathbf{e}}^H(e^{j\omega_m})\mathbf{w}_k|^2, \end{aligned} \tag{5.13}$$

where all the quantities are as described in chapter 3. Then the dual problem (5.12) can be written as

$$\min_{\lambda_t,\lambda_r,\gamma_m}\left\{\max_{\mathbf{C}^{tr},\mathbf{C}^{r}} \quad \Psi\right\},$$

where

$$\Psi = \sum_{k\in\mathcal{K}} R_k - \lambda_t \sum_{k\in\mathcal{K}}\sum_{j=0}^{C_{max}} {C_{kj}}^{tr} - \lambda_r \sum_{k\in\mathcal{K}}\sum_{j=0}^{T} {C_{kj}}^{r}$$

$$- \left(\sum_{m=1}^{\bar{M}} \gamma_m \sum_{k\in\mathcal{K}} s_k |F_k(e^{j\omega_m})\hat{\mathbf{e}}^H(e^{j\omega_m})\mathbf{w}_k|^2\right)$$

$$\lambda_r, \lambda_t, \gamma_m \geq 0. \tag{5.14}$$

The use of pulse shaping filters in the tranmitter side modifies the effective CIR, therefore influencing all SNRs on all the tones at the receiver side. Therefore, the (5.14) is coupled over tones. However, the effect of the increase in the effective CIR can be reduced significantly by using long enough PTEQ filters. Therefore for fixed λ_t, λ_r and γ (5.14) can be assumed to be decoupled over tones. This maximization in (5.14) can then be written as

For $k \in \mathcal{K}$

$$\max_{\mathbf{c}_k^{tr}, \mathbf{c}_k^{r}} \quad \psi_k,$$

where

$$\psi_k = R_k - \lambda \sum_{j=0}^{C_{max}} {C_{kj}}^{tr} - \lambda \sum_{j=0}^{T} {C_{kj}}^{r} - \sum_{m=1}^{\bar{M}} \gamma_m s_k |F_k(e^{j\omega_m}) \hat{\mathbf{e}}^H(e^{j\omega_m}) \mathbf{w}_k|^2 \quad (5.15)$$

5.3.2 Joint filter tap and transmit power allocation

For a given total pulse shaping filter tap budget C_{budget}^{tr}, total PTEQ filter tap budget C_{budget}^{r} and total transmit power budget S_{budget}, we can write the resource allocation problem as

$$\begin{aligned} \underset{\mathbf{C}^{tr}, \mathbf{C}^{r}, \mathbf{S}}{\text{maximum}} \quad & \sum_{k \in \mathcal{K}} R_k \\ \text{subject to} \quad & \mathbf{t}_{spec} \leq \mathbf{t}_{mask} \\ & \sum_{k \in \mathcal{K}} \sum_{j=0}^{C_{max}} C_{kj}^{tr} \leq C_{budget}^{tr} \\ & \sum_{k \in \mathcal{K}} \sum_{j=0}^{T} C_{kj}^{r} \leq C_{budget}^{r} \\ & \sum_{k \in \mathcal{K}} s_k \leq S_{budget} \\ & 0 \leq s_k \leq s_k^{mask}, \end{aligned} \quad (5.16)$$

where R_k is the bit-rate on tone k and can be described as the function of the PTEQ and the per-tone transmit power as in (5.8), S_{budget} is the total transmit

power budget, $\mathbf{s}$ is the vector containing the transmit power on all the tones, $s_k \in \mathcal{S}$ is the power allocated to tone k, $\mathcal{S}$ is the set containing all the allowed discrete power levels, s_k^{mask} is the maximum transmit power allowed on tone k. All the remaining quantities are as defined in section 5.3.1. The primal optimization problem (5.16) is coupled over tones and is a combinatorial problem. It has computational complexity of $\mathcal{O}(\tilde{L}^M 2^{M(C_{max}+1)(T+1)})$, where $\tilde{L}$ is the cardinality of the set $\mathcal{S}$ and M is the cardinality of set $\mathcal{K}$ and gives the total number of used tones. This is intractable even for moderate numbers of M, $\tilde{L}$, C_{max} and T. In chapter 3 and chapter 4, it was shown that the problem can be simplified if it is formulated as a dual optimization problem, hence reducing the computational complexity. The dual optimization problem can be written as

$$\min_{\gamma,\alpha,\lambda_t,\lambda_r} \left\{ \max_{\mathbf{C}^{tr},\mathbf{C}^r,\mathbf{S}} (\hat{\Psi}) \right\}$$

where,

$$\hat{\Psi} = \sum_{k\in\mathcal{K}} R_k + \lambda_t \left(C_{budget}^{tr} - \sum_{k\in\mathcal{K}} \sum_{j=0}^{C_{max}} C_{kj}^{tr} \right) + \lambda_r \left(C_{budget}^{r} \sum_{k\in\mathcal{K}} - \sum_{j=0}^{C_{max}} C_{kj}^{r} \right) +$$

$$\alpha \left(S_{budget} - \sum_{k\in\mathcal{K}} s_k \right) + \sum_{m=1}^{\bar{M}} \gamma_m \left(t_{mask,m} - t_{spec,m} \right)$$

$$\alpha, \gamma_m, \lambda_t, \lambda_r > 0 \tag{5.17}$$

The dual optimization problem can then be written as

$$\min_{\gamma,\alpha,\lambda_t,\lambda_r} \left\{ \max_{\mathbf{C}^{tr},\mathbf{C}^r,\mathbf{S}} (\hat{\Psi}) \right\}$$

where,

$$\hat{\Psi} = \sum_{k\in\mathcal{K}} R_k - \lambda_t \sum_{k\in\mathcal{K}} \sum_{j=0}^{C_{max}} C_{kj}^{tr} - \lambda_r \sum_{k\in\mathcal{K}} \sum_{j=0}^{T} C_{kj}^{r} - \alpha \sum_{k\in\mathcal{K}} s_k$$

$$- \sum_{m=1}^{\bar{M}} \gamma_m \sum_{k\in\mathcal{K}} s_k |F_k(e^{j\omega_m}) \hat{\mathbf{e}}^H(e^{j\omega_m}) \mathbf{w}_k|^2$$

$$\alpha, \gamma_m, \lambda_t, \lambda_r > 0 \tag{5.18}$$

The computation of the PTEQ for tone k needs the information about the transmit power in all the other tones as seen in (5.4). Therefore, (5.18) cannot be decoupled over tones. In section 5.5, we will present a simple technique to effectively decouple the problem over tones and hence reduce the computational complexity. Furthermore, (5.18) is combinatorial in $\mathbf{c}_k^r$ and $\mathbf{c}_k^{tr}$. In section 5.5, we will present techniques to reduce the combinatorial complexity based on contiguous filter tap selection or sparse approximation based filter design.

5.4 Resource allocation for a fixed power loading

Here, we present an approach that is based on restating the constrained optimization problem as an unconstrained dual problem as shown in (5.15). The computational complexity of (5.15) is combinatorial in $\mathbf{c}_k^t$ and $\mathbf{c}_k^r$, i.e., $\mathcal{O}(M2^{(C_{max}+1)(T+1)})$. This complexity can be reduced if we can fix the sparsity pattern of the per-tone filters. In the following section, we present two different approaches to fix the sparsity pattern in order to reduce the computational complexity.

5.4.1 Contiguous filter tap selection based resource allocation

One way to fix the sparsity pattern of the filters is to restrict the sparsity pattern of the filters such that only contiguous filter taps can be non-zero. This is referred to as CTS. This reduces the combinatorial search into a linear search over the filter orders. Equation (5.15) can then be written as

For $k \in \mathcal{K}$

$$\max_{\mathbf{c}_k^t, \mathbf{c}_k^r} \quad \psi_k,$$

where

$$\psi_k = R_k - \lambda_t L_k^t - \lambda_r L_k^r - \sum_{m=1}^{\bar{M}} \gamma_m s_k |F_k(e^{j\omega_m}) \hat{\mathbf{e}}^H(e^{j\omega_m}) \mathbf{w}_k|^2 \tag{5.19}$$

(5.20)

with

$$\mathbf{c}_k^t = [\underbrace{1\cdots1}_{L_k^t+1}| \quad \underbrace{0\cdots0}_{C_{max}-L_k^t+1} \quad]$$

$$\mathbf{c}_k^r = [\underbrace{1\cdots1}_{L_k^r+1}| \ \underbrace{0\cdots0}_{T-L_k^r+1}]$$

where L_k^t and L_k^r are the filter order of the pulse shaping filter and the PTEQ filter for the kth tone respectively.

This per-tone optimization problem can be solved (for fixed Lagrange multipliers) by exhaustively searching over all combinations of L_k^t and L_k^r. For fixed Lagrange multipliers, the computational complexity then becomes $\mathcal{O}(M(C_{max}+1)(T+1))$. The complexity can be further reduced by fixing the PTEQ filter order while optimizing the pulse shaping filter order. Then with the optimized pulse shaping filter order, the PTEQ filter order is optimized, thus avoiding an exhaustive search over all combinations of L_k^{tr} and L_k^r. The computational complexity then becomes $\mathcal{O}(M(C_{max}+T+2))$. The values of the Lagrange multipliers can then be updated until all the PSD constraints are met. The Lagrange multipliers, γ_m are updated based on the difference between the PSD mask and the output PSD, i.e.

$$\gamma_m \Leftarrow [\gamma_m - \mu_m(t_{mask,m} - t_{spec,m})]^+ \tag{5.21}$$

where μ_m is the step size for the update which is always positive. The μ_m can be varied in order to drop the energy at a frequency point quickly if the output spectrum at that frequency exceeds the PSD mask and to cautiously increase it if the output spectrum is under the PSD mask. A typical initialization value for $\gamma = \{\gamma_m\}$ is $\mathbf{0}$ and then $\mu = \{\mu_m\}$ can be initialized with a value generally much larger than 1 as we need to establish a very high value for γ in order to make the $\sum_m \gamma_m s_k |F_k(e^{j\omega_m})\mathbf{e}^H(e^{j\omega_m})\mathbf{w}_k|^2$ comparable to the value of L_k^{tr} and L_k^r.

The Lagrange multipliers λ_t and λ_r can be updated as

$$\lambda_t \Leftarrow [\lambda_t - \mu_t(C_{budget}^{tr} - \sum_{k\in\mathbf{K}} L_k^{tr})]^+ \tag{5.22}$$

$$\lambda_r \Leftarrow [\lambda_r - \mu_r(C_{budget}^{r} - \sum_{k\in\mathbf{K}} L_k^{r})]^+, \tag{5.23}$$

where μ_t and μ_r are positive step sizes. The algorithm stops when the number of taps stops updating. An algorithm description is given in **Alg. 5.1**.

Algorithm 5.1 Contiguous filter tap selection based filter tap allocation for a fixed power loading

Initialize λ_t, λ_r, γ
Initialize $L^r_{k,opt} = 0$, $L^{tr}_{k,opt} = 0$, $\psi^{tr}_{k,opt}$, $\psi^r_{k,opt}$
repeat
  for tone $k \in \mathcal{K}$ **do**
    Compute $\mathbf{v}_k$ of order $L^r_{k,opt}$
    for Pulse shaping filter order $L^{tr}_k = 0 \cdots C_{max}$ **do**
      compute $\mathbf{w}_k$ of order L^{tr}_k
      $\psi^{tr}_k = R_k - \lambda_t L^t_k - \sum_{m=1}^{\bar{M}} \gamma_m s_k |F_k(e^{j\omega_m})\hat{\mathbf{e}}^H(e^{j\omega_m})\mathbf{w}_k|^2$
      if $\psi^{tr}_k > \psi^{tr}_{k,opt}$ **then**
        $\psi^{tr}_{k,opt} = \psi^{tr}_k$
        $\mathbf{w}_{k,opt} = \mathbf{w}_k$
        $L^{tr}_{k,opt} = L^{tr}_k$
      end if
    end for
    for PTEQ filter order $L^r_k = 0 \cdots T$ **do**
      Compute $\mathbf{v}_k$ of order L^r_k
      $L^r_{k,opt} \Leftarrow \underset{L^r_k}{\text{argmax}} R_k - \lambda_r L^r_k$
      if $\psi^r_k > \psi^r_{k,opt}$ **then**
        $\psi^r_{k,opt} = \psi^r_k$
        $\mathbf{v}_{k,opt} = \mathbf{v}_k$
        $L^r_{k,opt} = L^r_k$
      end if
    end for
  end for
  compute $\mathbf{t}_{spec}$
  for $m = 1 \cdots \bar{M}$ **do**
    $\gamma_m = [\gamma_m - \mu_m (t_{mask,m} - t_{spec,m})]^+$
  end for
  $\lambda_t = \left[\lambda_t - \mu_t \left(C_{budget} - \sum_{k\in\mathcal{K}}(L^{tr}_{k,opt})\right)\right]^+$
  $\lambda_r = \left[\lambda_r - \mu_r \left(C_{budget} - \sum_{k\in\mathcal{K}}(L^r_{k,opt})\right)\right]^+$
until (no change in total filter taps)

5.4.2 Sparse approximation based resource allocation

Computing sparse per-tone pulse shaping filters

In the previous section, it was shown that if we can fix the sparsity pattern of the per-tone pulse shaping filters and the PTEQ filters, the computational complexity of the optimization problem will reduce significantly. In chapter 3 and chapter 4, it was shown that in order to fix the sparsity pattern, a sparse per-tone pulse shaping filter and a sparse MMSE-PTEQ filter can be directly computed. For the sake of convenience, let us rewrite the formula to compute sparse per-tone pulse shaping filter and sparse MMSE-PTEQ filter as follows

$$\boxed{\min_{\tilde{\mathbf{w}}_k} \quad \tilde{\mathbf{w}}_k^H \mathbf{Q}_k \tilde{\mathbf{w}}_k + \bar{\tau} \left\| \tilde{\mathbf{w}}_k \right\|_1 \quad \text{subject to} \quad \tilde{W}_k(e^{j\omega_k}) = 1,} \tag{5.24}$$

$$\boxed{\underset{\tilde{\mathbf{v}}_k}{\text{minimize}} \quad \left\| \mathbf{A}_k \tilde{\mathbf{v}}_k^* - \mathbf{b}_k \right\|_2^2 + \beta \left\| \tilde{\mathbf{v}}_k \right\|_1 ,} \tag{5.25}$$

Sparse approximation based tap allocation under fixed power loading

Let us rewrite ψ_i the per-tone dual optimization problem under the fixed power loading (5.15)

$$\underset{\mathbf{c}_i}{\text{minimize}} \quad \hat{\psi}_i(\Lambda)$$

$$\psi_i = R_i - \lambda \sum_{j=0}^{C_{max}} {C_{ij}}^t - \lambda \sum_{p=0}^{T} {C_{ip}}^r - \gamma \sum_{m=1}^{\bar{M}} s_i |F_i(e^{j\omega_m}) \hat{\mathbf{e}}^H(e^{j\omega_m}) \mathbf{w}_i|^2, \tag{5.26}$$

We compute the sparsity pattern $\mathbf{c}_k^{tr}$ and $\mathbf{c}_k^r$ directly by using (5.24) and (5.25) and then applying the thresholds as given in (3.28) and (4.22). After the sparsity patterns are fixed, i.e., it is implied that filter with the given sparsity pattern is the best sparse filter for given Lagrange multipliers, therefore filters computed with sparsity pattern is the only one filter available. Hence the objective function given in The problem reduces to iteratively computing $\mathbf{w}_k$ and $\mathbf{v}_k$ for different $k \in \mathcal{K}$ and then checking if the PSD mask constraint and the total pulse shaping filter tap constraint and total MMSE-PTEQ tap constraint are met. An algorithm description to iteratively optimize the total number of filter taps needed to fulfill the PSD mask constraint is given in **Alg. 5.2**. The complexity of the proposed algorithm is then $O(M * \kappa)$ per Lagrange multiplier update, where κ is the cost associated with computing the nearly-sparse filter and then a sparse filter. For

large C_{max} and T, the computational complexity of sparse approximation based per-tone pulse shaping filter tap and the PTEQ tap allocation under fixed power is similar to the per-tone exhaustive search on a restricted search space as presented in section 5.4.1.

Algorithm 5.2 Sparse approximation based filter tap allocation for a fixed power loading

1: Initialize $\bar{\mu}_t$, $\bar{\mu}_r$, γ, $\tilde{\beta}$, $\bar{\tau}$
2: **repeat**
3: **for** tone $k \in \mathcal{K}$ **do**
4: Compute nearly sparse $\tilde{\mathbf{w}}_k$ by solving
$\min_{\tilde{\mathbf{w}}_k} \quad \tilde{\mathbf{w}}_k^H \mathbf{Q}_k \tilde{\mathbf{w}}_k + \bar{\tau} \left\| \tilde{\mathbf{w}}_k \right\|_1 \quad \text{subject to} \quad \tilde{W}_k(e^{j\omega_i}) = 1$
5: Apply threshold and obtain the sparsity pattern $\mathbf{c}_k^{tr}$
6: Compute sparse $\mathbf{w}_k$ using
$\min_{\mathbf{w}_k} \quad \mathbf{w}_k^H \mathbf{Q}_k \mathbf{w}_k \quad \text{subject to} \quad W_k(e^{j\omega_i}) = 1$
with
$w_k^j = 0$ for $C_{kj}^{tr} = 0$ for all $j = 0 \cdots C_{max}$
7: Compute nearly sparse $\mathbf{v}_k$ by solving
$\min_{\tilde{\mathbf{v}}_k} \quad \left\| \mathbf{A}_k \tilde{\mathbf{v}}_k^* - \mathbf{b}_k \right\|_2^2 + \tilde{\beta} \left\| \tilde{\mathbf{v}}_k \right\|_1$
8: Apply threshold and obtain sparsity pattern $\mathbf{c}_k^r$
9: Recompute sparse $\mathbf{v}_k$ using
$\min_{\mathbf{v}_k} \quad \left\| \mathbf{A}_k \mathbf{v}_k^* - \mathbf{b}_k \right\|_2^2$
with
$v_k^j = 0$ for $C_{kj}^t = 0$ for all $j = 0 \cdots T$
10: **end for**
11: Compute $\mathbf{t}_{spec}$
12: **for** $m = 1 \cdots \bar{M}$ **do**
13: $\gamma_m = [\gamma_m - \mu_m (t_{mask,m} - t_{spec,m})]^+$
14: **end for**
15: $\lambda_t = \left[\lambda_t - \bar{\mu}_t \left(C_{budget} - \sum_{k \in \mathcal{K}} (L_{k,opt}^t) \right) \right]^+$
16: $\lambda_r = \left[\lambda_r - \bar{\mu}_r \left(C_{budget} - \sum_{k \in \mathcal{K}} L_{k,opt}^r \right) \right]^+$
17: **until** (no change in total filter taps)

5.5 Joint filter tap and transmit power allocation

In the previous section it was shown how to optimally allocate pulse shaping filter taps if the number of used tones and their transmit powers are known, for a system with PSD constraints. However, the number of used tones can be increased if a

lower transmit power at the band edges is used. Therefore, by also allocating the appropriate amount of transmit power for each tone, the total achievable data rate can be maximized for a given total transmit power budget and given total filter tap budgets. This then requires a procedure to distribute the available resources (total power and total filter tap budget) optimally over the tones such that the data rate is maximized and the PSD mask constraint is still met. Here, we present an approach that is again based on a dual problem formulation. The unconstrained dual optimization problem can be restated from (5.18).

5.5.1 Contiguous filter tap selection based resource allocation

Equation 5.18 can be rewritten as

$$\min_{\gamma,\alpha,\lambda_t,\lambda_r} \left\{ \max_{L_k^{tr},L_k^r,\mathbf{S}} (\hat{\Psi}) \right\}$$

where,

$$\hat{\Psi} = \sum_{k\in\mathcal{K}} R_k - \lambda_t \sum_{k\in\mathcal{K}} L_k^t - \lambda_r \sum_{k\in\mathcal{K}} L_k^r - \alpha \sum_{k\in\mathcal{K}} s_k - \sum_{m=1}^{\bar{M}} \gamma_m \sum_{k\in\mathcal{K}} s_k |F_k(e^{j\omega_m})\hat{\mathbf{e}}^H(e^{j\omega_m})\mathbf{w}_k|^2$$

$$\gamma_m, \alpha, \lambda_t, \lambda_r > 0 \tag{5.27}$$

(5.27) is still coupled over tones since the computation of the MMSE-PTEQ on tone k requires the transmit powers on all the tones to be known. To simplify the problem, we can iteratively update each user's power, as suggested in chapter 4, i.e., perform transmit power allocation and the filter tap allocation in tone k by fixing the transmit power on all the other tones. Then the process is repeated for tone $k+1$ with a recently allocated transmit power on tone k. This iterative update decouples (5.27) over tones and hence the optimization problem can now be written as,

$$\max_{L_k^{tr},L_k^r,s_k} (\hat{\psi}_k)$$

where,

$$\hat{\psi}_k = R_k - \lambda_t L_k^{tr} - \lambda_r L_k^r - \alpha s_k - \sum_{m=1}^{\bar{M}} \gamma_m s_k |F_k(e^{j\omega_m})\hat{\mathbf{e}}^H(e^{j\omega_m})\mathbf{w}_k|^2 \tag{5.28}$$

where γ is a vector containing all γ_m's. This per-tone optimization problem can be solved (for fixed Lagrange multipliers) by exhaustively searching over all possible

values of s_k and all filter orders L_k^{tr} and L_k^r. The values of the Lagrange multipliers can then be updated until all the constraints are met. An algorithm description is given below.

The Lagrange multipliers ($\gamma, \alpha, \lambda_t$ and λ_r) are updated based on the difference between the obtained values for the corresponding resources and their target values, i.e.

$$\begin{aligned}
\gamma_j &\Leftarrow [\gamma_j - \mu_m(t_{mask,m} - t_{spec,m})]^+ \\
\lambda_t &\Leftarrow [\lambda_t - \hat{\mu}_t(C_{budget}^t - \sum_{k\in\mathcal{K}} L_k^t)]^+ \\
\lambda_r &\Leftarrow [\lambda_r - \hat{\mu}_r(C_{budget}^r - \sum_{k\in\mathcal{K}} L_k^r)]^+ \\
\alpha &\Leftarrow [\alpha - \bar{\mu}(S_{budget} - \sum_{k\in\mathcal{K}} s_k)]^+
\end{aligned} \tag{5.29}$$

where μ_m, $\hat{\mu}_t$, $\hat{\mu}_r$, and $\bar{\mu}$ are the step sizes for the updates which are always positive.

5.5.2 Sparse approximation based resource allocation

We can rewrite the per-tone optimization problem for the joint filter tap allocation and power loading given in (5.18) as

$$\begin{aligned}
\hat{\Psi} = \quad & \textstyle\sum_{k\in\mathcal{K}} R_k - \lambda_t \sum_{k\in\mathcal{K}} \|\mathbf{w}_k\|_0 - \lambda_t \sum_{k\in\mathcal{K}} \|\mathbf{v}_k\|_0 - \alpha \sum_{k\in\mathcal{K}} s_k \\
& - \textstyle\sum_{m=1}^{\bar{M}} \gamma_m \sum_{k\in\mathcal{K}} s_k |F_k(e^{j\omega_m})\hat{\mathbf{e}}^H(e^{j\omega_m})\mathbf{w}_k|^2
\end{aligned} \tag{5.30}$$

By fixing the sparsity pattern using the sparse approximation technique the total computational complexity of the sparse approximation based approach is $\mathcal{O}(M\tilde{L} + \kappa)$ per Lagrange multiplier iteration in contrast to $\mathcal{O}(M\tilde{L}(C_{max} + T + 2))$ per Lagrange multiplier iteration in the CTS based approach discussed in the previous section. For large C_{max} and T, this is a significant reduction in computational complexity. The values of the Lagrange multipliers can then be updated until all the constraints are met. An algorithm description is given in **Alg. 5.2**. The Lagrange multipliers $\lambda_m$and α can be updated using (5.29)

5.6 Simulation results

The channel under consideration here is a 400m twisted pair cable in a bundle of 8 with an interference channel of 400m. In the first scenario, the tones used for

Algorithm 5.3 Contiguous filter tap selection based joint filter tap and transmit power allocation

Initialize $L^r_{k,opt}$, $L^{tr}_{k,opt}$, $\psi^{tr}_{k,opt}$, ψ_k, opt^r, $\mathbf{s}$,α
repeat
  for tone $k \in \mathcal{K}$ **do**
    for $s_k = 0 \cdots S^{mask}$ **do**
      Compute $\mathbf{v}_k$ of order $L^r_{k,opt}$
      for Pulse shaping filter order $L^{tr}_k = 0 \cdots C_{max}$ **do**
        compute $\mathbf{w}_k$ of order L^{tr}_k
        $\psi^{tr}_k = R_k - \lambda_t L^{tr}_k - \alpha \sum_{k\in\mathcal{K}} - \sum_{m=1}^{\bar{M}} \gamma_m s_k |F_k(e^{j\omega_m})\hat{\mathbf{e}}^H(e^{j\omega_m})\mathbf{w}_k|^2$
        if $\psi^{tr}_k > \psi^{tr}_{k,opt}$ **then**
          $\psi^{tr}_{k,opt} = \psi^{tr}_k$
          $\mathbf{w}_{k,opt} = \mathbf{w}_k$
          $L^t_{k,opt} = L^t_k$
          $s^{opt}_k = s_k$
        end if
      end for
      for PTEQ filter order $L^r_k = 0 \cdots T$ **do**
        compute $\mathbf{v}_k$ of order L^r_k
        $L^r_{k,opt} \Leftarrow \underset{L^r_k}{\text{argmax}} R_k - \lambda_r L^r_k - \alpha \sum_{k\in\mathcal{K}}$
        if $\psi^r_k > \psi^r_{k,opt}$ **then**
          $\psi^r_{k,opt} = \psi^r_k$
          $\mathbf{v}_{k,opt} = \mathbf{v}_k$
          $L^r_{k,opt} = L^r_k$
        end if
      end for
    end for
  end for
  compute $\mathbf{t}_{spec}$
  for $m = 1 \cdots \bar{M}$ **do**
    $\gamma_m = [\gamma_m - \mu_m (t_{mask,m} - t_{spec,m})]^+$
  end for
  $\lambda_t = \left[\lambda - \bar{\mu}\left(C_{budget} - \sum_{k\in\mathcal{K}}(L^{tr}_{k,opt})\right)\right]^+$
  $\lambda_r = \left[\lambda_r - \bar{\mu}\left(C_{budget} - \sum_{k\in\mathcal{K}}(L^r_{k,opt})\right)\right]^+$
until (no change in total filter taps)

Algorithm 5.4 Sparse approximation based joint filter tap and transmit power allocation

Initialize $\bar{\mu}_t$, $\bar{\mu}_r$, γ, $\tilde{\beta}$, $\bar{\tau}$,
repeat
  for tone $k \in \mathcal{K}$ **do**
    for $s_k = 0 \cdots S^{mask}$ **do**
      Compute nearly sparse $\tilde{\mathbf{w}}_k$ by solving
      $\min_{\tilde{\mathbf{w}}_k} \quad \tilde{\mathbf{w}}_k^H \mathbf{Q}_k \tilde{\mathbf{w}}_k + \bar{\tau} \left\| \tilde{\mathbf{w}}_k \right\|_1 \quad \text{subject to} \quad \tilde{W}_k(e^{j\omega_i}) = 1$
      apply threshold and obtain the sparsity pattern $\mathbf{c}_k^{tr}$
      Compute sparse $\mathbf{w}_k$ using
      $\min_{\mathbf{w}_k} \quad \mathbf{w}_k^H \mathbf{Q}_k \mathbf{w}_k \quad \text{subject to} \quad W_k(e^{j\omega_i}) = 1$
      with
      $w_k^j = 0$ for $C_{kj}^{tr} = 0$ for all $j = 0 \cdots C_{max}$
      $\psi_k^{tr} = R_k - \lambda_t L_k^{tr} - \alpha \sum_{k \in \mathcal{K}} - \sum_{m=1}^{\bar{M}} \gamma_m s_k |F_k(e^{j\omega_m}) \hat{\mathbf{e}}^H(e^{j\omega_m}) \mathbf{w}_k|^2$
      Compute nearly sparse $\tilde{\mathbf{v}}_k$ by solving
      $\min_{\tilde{\mathbf{v}}_k} \quad \left\| \mathbf{A}_k \tilde{\mathbf{v}}_k^* - \mathbf{b}_k \right\|_2^2 + \tilde{\beta} \left\| \tilde{\mathbf{v}}_k \right\|_1$
      apply threshold and obtain sparsity pattern $\mathbf{c}_k^r$
      recompute sparse $\mathbf{v}_k$ using
      $\min_{\mathbf{v}_k} \quad \left\| \mathbf{A}_k \mathbf{v}_k^* - \mathbf{b}_k \right\|_2^2$
      with
      $v_k^j = 0$ for $C_{kj}^r = 0$ for all $j = 0 \cdots T$
    end for
  end for
  compute $\mathbf{t}_{spec}$
  for $m = 1 \cdots \bar{M}$ **do**
    $\gamma_m = [\gamma_m - \mu_m (t_{mask,m} - t_{spec,m})]^+$
  end for
  $\lambda_t = \left[\lambda_t - \bar{\mu}_t \left(C_{budget} - \sum_{k \in \mathcal{K}} (L_{k,opt}^{tr}) \right) \right]^+$
  $\lambda_r = \left[\lambda_r - \bar{\mu}_r \left(C_{budget} - \sum_{k \in \mathcal{K}} L_{k,opt}^{r} \right) \right]^+$
until (no change in total filter taps)

Total filter taps	CTS based approach	SA based approach
5000	9	9
1000	15	13

Table 5.1: Number of outer iterations taken to converge to the solution for a fixed transmit power loading

transmission are fixed as suggested in [33], i.e., 375 predefined tones, in order to compare with the results in chapter 3.

5.6.1 Resource allocation for a fixed power loading

In **Figure 5.1**, the distribution of the non-zero pulse shaping filter and PTEQ filter taps is shown. It can be seen that the allocation of the number of taps in the transmitter, i.e., in the pulse shaping filters, is nearly the same as in the scenario when we had only transmitter optimization under the assumption that the receiver is perfect as described in chapter 3. This is due to the fact that for a fixed number of tones with fixed power loading, the PSD constraint only depends on the pulse shaping filter. Therefore, parameters at the receiver do not affect it. However the PTEQ filter tap distribution is affected in order to accommodate the effect of the per-tone pulse shaping at the transmitter. Similar observations can be made in Figure 5.2 for sparse approximation based tap allocation in this scenario. The transmit PSD for this scenario is the same as for the scenario when the transmit per-tone pulse shaping filter was optimized without taking the effect of the receiver into account. This is illustrated in **Figure 5.3** showing the transmit PSD in this scenario. It can also be seen that the sparse approximation based approach outperforms the CTS based approach. From **Table 5.1**, it can be seen that the sparse approximation based approach converges faster than the CTS approach.

5.6.2 Joint filter tap and transmit power allocation

In the second scenario, now we make all the 428 tones available for the data transmission. The total available power is 11.5 dBm [10]. The tap distribution over tones for both the CTS based approach and the sparse approximation based approach is coupled in both the transmit pulse shaping filter tap budget as well as the PTEQ filter tap budget. Therefore, the tap distribution in both the per-tone pulse shaping based transmitter and the PTEQ based receiver vary from the independent optimization problems presented in chapter 3 and chapter 4. This enables joint optimization to perform better than the independent optimization for given constraints. **Tables 5.3** and **5.4** present the achievable bit-rates for

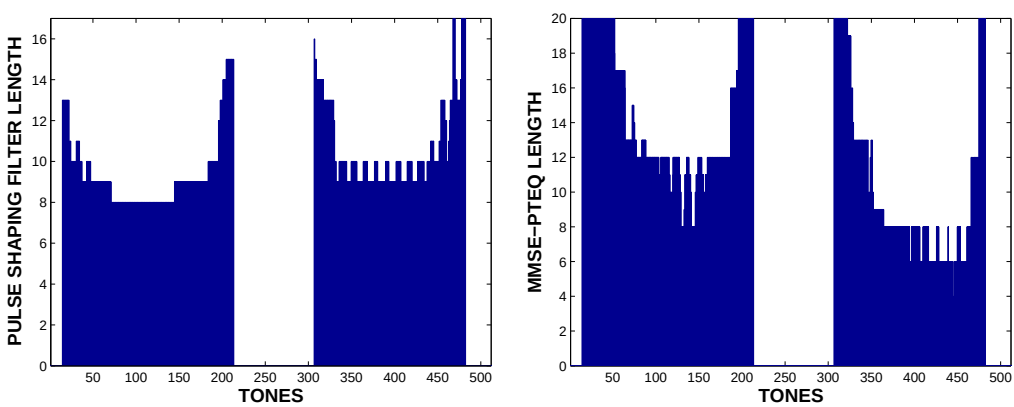
Total filter taps	CTS based approach	SA based approach
5000	25	21
1000	30	28

Table 5.2: Number of outer iterations taken to converge to the solution for a joint filter tap and transmit power allocation

C^{r}_{budget} \ C^{tr}_{budget}	1000	3000	5000
1000	22.99	24.12	25.8
2000	23.028	34.01	35.6
3000	23.06	39.73	40.1
4000	23.09	41.61	42.08
5000	23.091	42.81	42.9

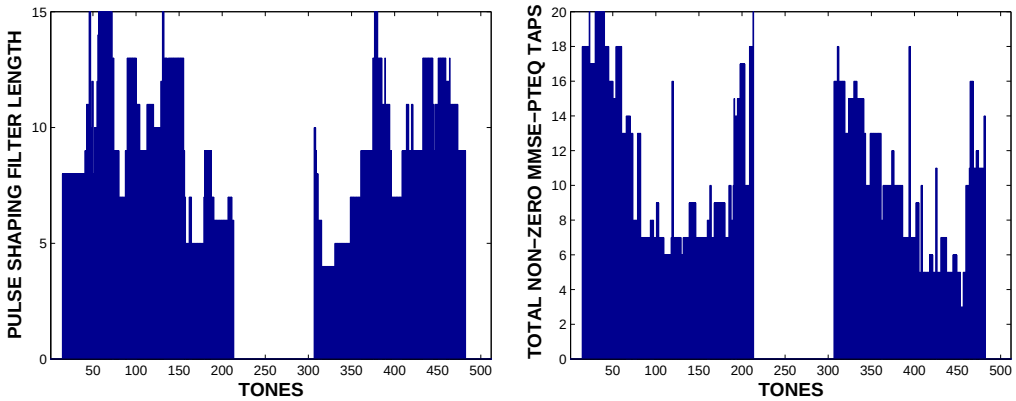
Table 5.3: Achievable bit-rate in Mbps for various combinations of C^{r}_{budget} and C^{tr}_{budget} using the CTS based approach and transmit power allocation

different combinations of transmit pulse shaping filter budget and PTEQ tap budget for joint filter tap and transmit power allocation using the CTS based approach and the sparse approximation based approach. It can be seen that the sparse approximation approach outperforms the CTS based approach. From **Table 5.2**, it can be seen that the sparse approximation based approach converges to the solution faster than the CTS.



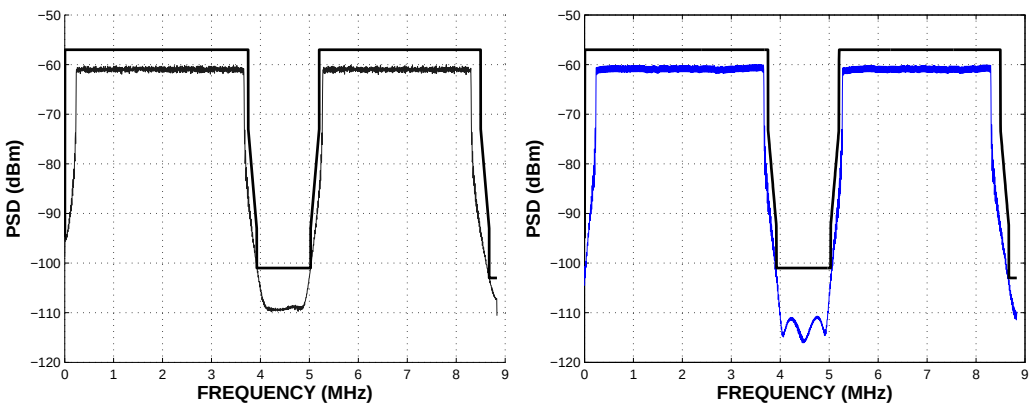
(a) (b)

Figure 5.1: For a fixed transmit power loading, optimum distribution of (a) pulse shaping filter taps (b) PTEQ taps, using the CTS approach



(a) (b)

Figure 5.2: For a fixed transmit power loading optimum distribution of (a) pulse shaping filter taps (b) MMSE-PTEQ taps, using sparse approximation based approach

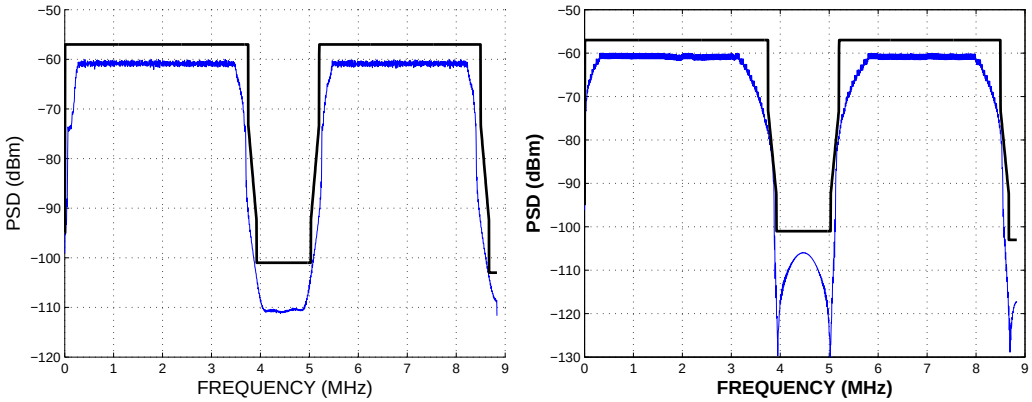


(a) (b)

Figure 5.3: For a fixed transmit power loading, transmit PSD for (a) the CTS based approach (b) the sparse approximation based approach

5.7 Conclusion

In this chapter, a per-tone pulse shaping and PTEQ based DMT transceiver has been considered. The presence of a per-tone pulse shaping filter affects the tap allocation in the PTEQ based receiver also under a constant transmit power



(a) (b)

Figure 5.4: Transmit PSD in the case of joint filter tap and transmit power allocation for the tap budget of 5000 taps each in the transmitter and the receiver using (a) the CTS based approach, (b) the sparse approximation based approach

C^{r}_{budget} \ C^{tr}_{budget}	1000	3000	5000
1000	24.85	26.7	27.6
2000	24.91	35.88	36.4
3000	24.96	41.03	42.1
4000	25	43.67	44.6
5000	25.01	44.81	45.133

Table 5.4: Achievable bit-rate in Mbps for various combinations of C^{r}_{budget} and C^{tr}_{budget} using the sparse approximation based approach and transmit power allocation

loading. It has been shown that, with the additional assumpton that the PTEQ is sufficiently long, the joint filter tap optimization problem in the DMT transceiver can be decoupled over tones by formulating it as a dual problem along with an iterative MMSE-PTEQ computation scheme. It can be seen that the achievable bit-rate for the same number of taps is lower in the presence of per-tone pulse shaping filter. This is due to the fact that the pulse shaping filter acts as a dispersive channel and hence effectively lengthens the effective CIR. In our case, we do not increase the overall symbol length, but decrease the effective cyclic prefix to accommodate the extra symbol, therefore better per-tone equalizers are needed to mitigate the effects. Similarly in the case of joint filter taps and transmit power allocation in the DMT transceiver, effects such as the filtering effect at the edge of the bands at the receiver are also taken into account while performing transmit

power allocation at the transmitter. This improves the performance of the system for the same number of non-zero filter taps.

Part II

MULTI-USER RESOURCE ALLOCATION

Chapter 6

Resource allocation in multi-user crosstalk cancellation

6.1 Introduction

To meet the demand for higher data rates, recent DSL systems use higher frequencies, e.g. up to 30 MHz [143]. At these frequencies, it has been shown that out-of-domain (alien) and in-domain crosstalk between different DSL lines in the same bundle become the dominant source of interference, limiting the performance of the DSL systems.

Crosstalk cancellation is one way to mitigate the effect of crosstalk. Several crosstalk cancellation techniques have been proposed in e.g. [145, 28, 61, 176, 25]. Different techniques may require different levels of transmitter and receiver coordination. In the case of upstream VDSL, only receiver coordination is possible, therefore a successive interference cancellation scheme performs optimally [61, 176]. However, the upstream VDSL channel matrix has a column-wise diagonally dominant (CWDD) structure which is due to the fact that the power transmitted on a direct channel is always much larger than the power transmitted on any crosstalk channel by the same transmitter. In [25], under the assumption that the background noise is AWGN, it was shown that the CWDD structure allows a simple linear zero-forcing (ZF) crosstalk canceler to perform near optimally. However, in [27], it was shown that even for a simple linear crosstalk canceler such as a linear ZF crosstalk canceler, the run-time complexity increases with the

square of the number of lines. For a practical number of lines and number of tones, this becomes computationally infeasible. For example, in a binder of 8 VDSL lines with 4096 tones and transmitting at a block rate of 4000 blocks per second, the run-time complexity of linear ZF crosstalk cancellation is larger than 1 billion multiplications per second.

It was shown in [27] that the majority of the crosstalk originates from a small set of crosstalkers on a limited number of tones. Therefore, only a fraction of the original crosstalk cancellation is actually required to cancel most of the crosstalk. To reduce the run-time complexity of the crosstalk cancellation, in [27], a technique to cancel only the strong interferers was introduced. This technique is known as partial crosstalk cancellation.

However, in the case of spatially correlated background noise, e.g., when alien crosstalk is present, a prewhitening operation is needed to whiten the noise [21]. This operation destroys the CWDD structure of the channel matrix. The linear ZF canceler is then found to perform very poorly. In this scenario, an alternative structure that exploits the information provided by the noise correlation matrix should be used. For this purpose, MMSE-based cancelers, both linear and nonlinear, are the natural choices. The linear MMSE canceler is a simple structure and yet significantly outperforms the linear ZF canceler in the presence of spatially correlated noise. However, it is still a suboptimal canceler. The non-linear MMSE-GDFE is shown to perform optimally under spatially correlated background noise [143]. It is however more complex than the linear MMSE canceler.

The MMSE based cancelers also suffer from the run-time complexity issue. To reduce the run-time complexity of the MMSE based cancelers, partial crosstalk cancellation can again be used. One of the advantages of using a linear ZF canceler is that there exists a very simple strategy to perform partial crosstalk cancellation. However, for MMSE-based cancelers there is no obvious strategy that can be followed to realize partial cancellation. Earlier approaches [180, 12] adopt some per-line/per canceler exhaustive search method, which is computationally complex. The complexity of the partial crosstalk cancellation selection schemes also increases significantly, if it is combined with optimal spectrum balancing (OSB). In this chapter, we propose algorithms to reduce the complexity of the partial crosstalk cancellation scheme in MMSE based crosstalk cancelers with and without spectrum balancing.

This chapter is organized as follows: In **section 6.2**, the multi-user DSL system with spatially correlated background noise (alien crosstalk) is introduced.

In **section 6.3**, various crosstalk cancelers are presented and their performance in the presence of spatially correlated noise is compared. We show that the MMSE-based cancelers, i.e., the linear MMSE canceler and the non-linear MMSE-GDFE, perform significantly better than the linear ZF canceler in this scenario.

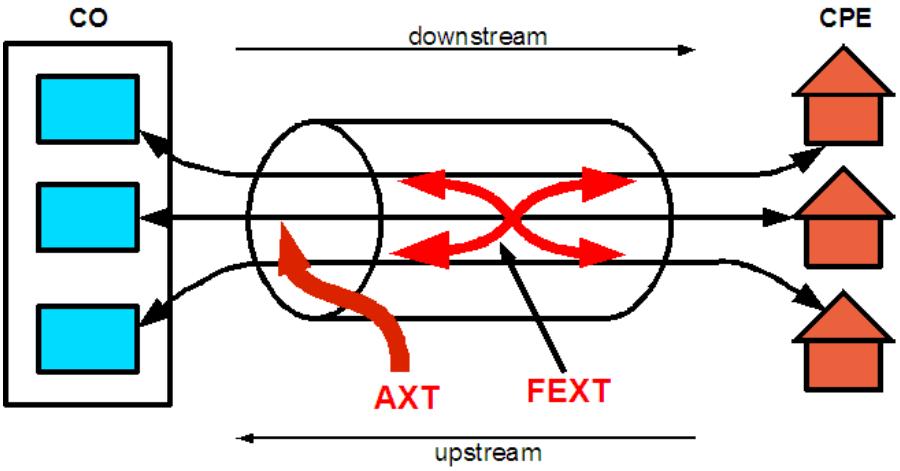


Figure 6.1: A typical VDSL scenario with co-located receivers at the CO (central office) and non co-located transmitters at the CPE (customer-premises equipment) side

In section **6.4**, we first present a scheme to compute the crosstalk canceler coefficients once the lines to be canceled have been selected.

In **section 6.5**, the partial crosstalk cancellation selection is formulated as an optimization problem in the case of a fixed power loading, i.e., no spectrum balancing, and in the case of the joint partial crosstalk cancellation and spectrum balancing.

In **section 6.6**, efficient algorithms for partial crosstalk cancellation selection for linear MMSE-based crosstalk cancelers based on selection metrics and sparse canceler design are proposed for scenarios both with and without spectrum balancing.

In **section 6.7**, the algorithms developed for the linear MMSE based partial crosstalk cancellation selection are then extended to perform partial crosstalk in the nonlinear MMSE crosstalk cancelers.

In **section 6.8**, simulation results are presented. Finally, in **section 6.9** conclusions are drawn.

6.2 System model

In this chapter, we consider DMT-based upstream VDSL transmission, where the receivers are co-located as shown in **Fig.** 6.1. The system is first described by

$$\underbrace{\begin{bmatrix} y_k^1 \\ \vdots \\ y_k^N \end{bmatrix}}_{\mathbf{y}_k} = \underbrace{\begin{bmatrix} h_k^{1,1} & \cdots & h_k^{1,N} \\ \vdots & \ddots & \cdots \\ h_k^{N,1} & \cdots & h_k^{N,N} \end{bmatrix}}_{\mathbf{H}_k} \underbrace{\begin{bmatrix} x_k^1 \\ \vdots \\ x_k^N \end{bmatrix}}_{\mathbf{x}_k} + \underbrace{\begin{bmatrix} n_k^1 \\ \vdots \\ n_k^N \end{bmatrix}}_{\mathbf{n}_k}, \tag{6.1}$$

where k is the tone index ($k = 1 \cdots K$), x_k^n and y_k^n are the transmitted and received symbols in line n on tone k and n_k^n is the additive spatially white Gaussian background noise (AWGN) experienced by line n on tone k, such that $\mathcal{E}\{\mathbf{n}_k \mathbf{n}_k^H\} = \sigma_k^2 \mathbf{I}_N$, where $\{.\}^H$ denotes the Hermitian transpose operation and $\mathcal{E}\{.\}$ denotes the expected value operation. Finally, $h_k^{n,n}$ is the direct channel for line n on tone k and $h_k^{n,m}$ is the crosstalk channel from line m into line n. Let $\mathcal{E}\{\mathbf{x}_k \mathbf{x}_k^H\} = \mathbf{S}_k$. Since the transmitters are not coordinated, $\mathbf{S}_k$ is a diagonal matrix. Here, the channel matrix $\mathbf{H}_k$ is CWDD [25].

In the presence of alien crosstalk, the above model is generalized as

$$\begin{bmatrix} y_k^1 \\ \vdots \\ y_k^N \end{bmatrix} = \begin{bmatrix} h_k^{1,1} & \cdots & h_k^{1,N} \\ \vdots & \ddots & \cdots \\ h_k^{N,1} & \cdots & h_k^{N,N} \end{bmatrix} \begin{bmatrix} x_k^1 \\ \vdots \\ x_k^N \end{bmatrix} + \underbrace{\begin{bmatrix} h_k^{1,axt1} & \cdots & h_k^{1,axtm} \\ \vdots & \ddots & \cdots \\ h_k^{N,axt1} & \cdots & h_k^{N,axtm} \end{bmatrix} \begin{bmatrix} x_k^{axt1} \\ \vdots \\ x_k^{axtm} \end{bmatrix}}_{\text{Alien Crosstalk } (\mathbf{a}_k)} + \begin{bmatrix} n_k^1 \\ \vdots \\ n_k^N \end{bmatrix}. \tag{6.2}$$

In (6.2), $\mathbf{a}_k$ is the vector containing the sum of all the alien crosstalk contributions. Hence, (6.2) can be succinctly written as

$$\begin{aligned} \mathbf{y}_k &= \mathbf{H}_k \mathbf{x}_k + \underbrace{\mathbf{a}_k + \mathbf{n}_k}_{\mathbf{z}_k} \\ &= \mathbf{H}_k \mathbf{x}_k + \mathbf{z}_k \end{aligned} \tag{6.3}$$

Even though the individual alien crosstalk channels are not known at the receiver, it is assumed that the total noise correlation matrix $\mathbf{R}_{k,z} = E\{\mathbf{z}_k\mathbf{z}_k^H\}$ is known or can be estimated. Generally, the alien crosstalk is spatially correlated therefore the correlation matrix $\mathbf{R}_{k,z}$ is not a diagonal matrix.

6.3 MMSE-based crosstalk cancellation

The upstream VDSL scenario with receiver coordination and no transmitter coordination corresponds to the multiple access channel (MAC) in information theory. The capacity of the MAC in the AWGN case can be written as [21]

$$b = \sum_{k\in\mathcal{K}} \log_2 |\mathbf{I}_N + \sigma_k^{-2}\mathbf{H}_k\mathbf{S}_k\mathbf{H}_k^H| \tag{6.4}$$

In [25], it was shown that due to the CWDD structure of the channel matrix $\mathbf{H}_k$, a simple linear ZF canceler can be used to obtain near-optimal capacity approaching performance.

In the case of alien crosstalk, the background noise is spatially correlated. The capacity formula then includes a prewhitening operation and can be written as [21]

$$\tilde{b} = \sum_{k\in\mathcal{K}} \log_2 |\mathbf{I}_N + \underbrace{(\mathbf{R}_{kz}^{-1/2}\mathbf{H}_k)}_{\tilde{\mathbf{H}}_k}\mathbf{S}_k(\mathbf{R}_{kz}^{-1/2}\mathbf{H}_k)^H|, \tag{6.5}$$

where $\tilde{\mathbf{H}}_k$ is the equivalent channel matrix after prewhitening. This equivalent channel matrix is no longer CWDD and hence a linear ZF canceler no longer provides near-optimal performance. Therefore we consider MMSE-based cancelers which take the noise correlation matrix into account explicitly.

6.3.1 Linear MMSE canceler

The linear MMSE canceler output can be written as in chapter 2

$$\hat{\mathbf{x}}_k = decision\left(\mathbf{W}_k\mathbf{y}_k\right), \tag{6.6}$$

where

$$\mathbf{W}_k = \mathbf{S}_k\mathbf{H}_k^H(\mathbf{H}_k\mathbf{S}_k\mathbf{H}_k^H + \mathbf{R}_{kz})^{-1} \tag{6.7}$$

is the $N \times N$ linear MMSE canceler matrix. Unlike the linear ZF canceler, the linear MMSE canceler takes the noise correlation matrix into account. This enables the linear MMSE canceler to cancel the alien crosstalk much more efficiently than the linear ZF canceler. In a high SNR AWGN scenario, the linear MMSE canceler approaches the linear ZF canceler.

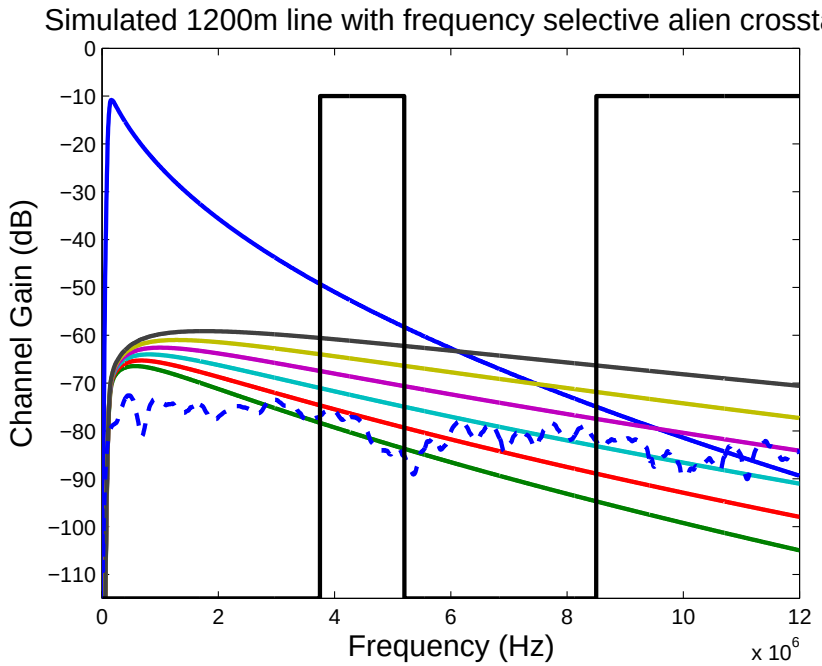


Figure 6.2: Channel characteristics for a 1200m line with 6 in-domain crosstalkers ranging from 600m to 1100m and an alien-crosstalker (dashed line). The solid black rectangular line represents the transmit band for upstream VDSL.

6.3.2 Nonlinear MMSE canceler

The linear MMSE canceler in general performs suboptimally. A non-linear MMSE canceler such as the MMSE-GDFE [143, 61, 176, 165] and the MMSE-VBLAST [173] achieves optimal performance by feeding back the already detected symbols to remove the corresponding interference. We will refer to the non-linear MMSE cancelers as MMSE-GDFE but will use the VBLAST formulation of section 2.10.3.

6.3.3 Performance comparison

Fig. 6.2 plots a direct channel characteristic for a 1200m line and also shows the in-domain crosstalk from 6 other lines ranging from 600m to 1100m with increments of 100m, as simulated using the analytical channel model given in [52]. The dashed line gives an example of a typical alien crosstalk characteristic.

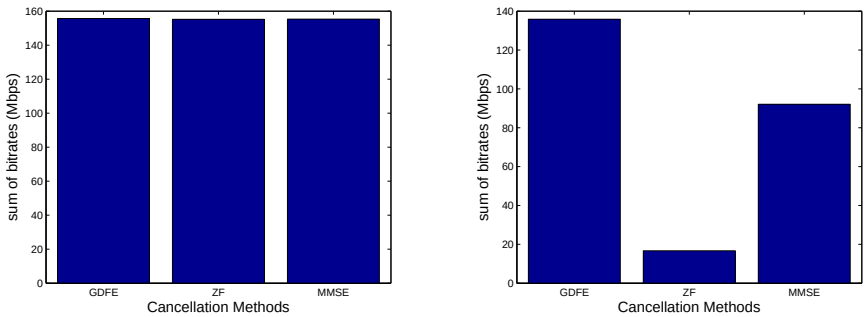


Figure 6.3: Comparison of the total bit-rate achieved with the linear ZF canceler and MMSE-based cancelers when alien crosstalk is (a) not present (b) present.

In the absence of alien crosstalk, it can be seen from **Fig.** 6.3(a) that the performance (i.e. total bit-rate summed over 7 lines) of the linear ZF canceler, the linear MMSE canceler and the MMSE-GDFE are similar. As can be seen from **Fig.** 6.3(b), as soon as alien crosstalk is introduced the performance decreases for the linear cancelers. The performance of the linear ZF canceler is extremely poor whereas the linear MMSE canceler still provides relatively good performance. The best performance is given by the MMSE-GDFE. This is our motivation for using the MMSE-based cancelers. Even though the performance of the linear MMSE canceler is lower compared to the MMSE-GDFE, it has a lower complexity and hence represents an attractive intermediate solution. Even for the linear MMSE canceler, however, the complexity of full crosstalk cancellation is still $\mathcal{O}(KN^2)$ [27], hence for a large number of lines the crosstalk cancellation becomes computationally heavy. This provides the motivation for developing partial crosstalk cancellation algorithms.

6.4 MMSE-based resource allocation

In [27], a simple partial crosstalk cancellation scheme for the linear ZF canceler was presented, which exploits the spatial and frequency selectivity of the crosstalk. Only strong crosstalkers are canceled which reduces the run-time complexity significantly without any dramatic performance degradation. For the MMSE-based cancelers, however, there is no obvious strategy that can be followed to realize partial cancellation. Before delving into different schemes to select the crosstalkers to be canceled, we first establish how the partial crosstalk canceler

coefficients can be computed once the lines have been selected that are used for the cancellation.

6.4.1 Computation of linear MMSE partial crosstalk canceler coefficients

Let us assume that there are N lines, therefore there are $N-1$ in-domain crosstalkers to be canceled for each individual line. Let $p_{k,n}$ be the number of observed lines, i.e., used by the crosstalk canceler, to detect the signal in line n on tone k, where $p_{k,n} = N-1$ corresponds to full crosstalk cancellation and $p_{k,n} = 0$ corresponds to no crosstalk cancellation i.e. single-user detection (SUD). Let $\mathcal{M}_n^k$ be the set of indices of all the observed lines including the index of line n, i.e.,

$$\mathcal{M}_k^n \triangleq \{m_{k,n}(1) \cdots m_{k,n}(p_{k,n}+1)\}. \tag{6.8}$$

Similarly, let $\underline{\mathcal{M}_k^n}$ be the set of indices of the unobserved lines, i.e., lines that are not used to detect the signal in line n on tone k, i.e.,

$$\underline{\mathcal{M}_k^n} \triangleq \mathcal{N} \backslash \mathcal{M}_k^n, \tag{6.9}$$

where $\mathcal{N}$ is a set containing all indices $1 \cdots N$. Let $\overline{\mathbf{H}}_k^n$ be the channel matrix containing the channels corresponding to the observed lines, i.e.,

$$\overline{\mathbf{H}}_k^n \triangleq \left[[\mathbf{H}_k]_{rows \mathcal{M}_k^n, cols \mathcal{M}_k^n} \right], \tag{6.10}$$

and $\underline{\mathbf{H}}_k^n$ be the matrix containing all the crosstalk channels from the unobserved lines into the observed lines, i.e.,

$$\underline{\mathbf{H}}_k^n \triangleq \left[[\mathbf{H}_k]_{rows \mathcal{M}_k^n, cols \underline{\mathcal{M}_k^n}} \right]. \tag{6.11}$$

Similarly $\overline{\mathbf{R}}_k^n$ is defined as the noise correlation matrix of the observed lines, i.e.,

$$\overline{\mathbf{R}}_k^n \triangleq \mathbf{R}_{kz}^n + \underline{\mathbf{H}}_k^n \underline{\mathbf{S}}_k^n \underline{\mathbf{H}}_k^{nH} \tag{6.12}$$

where $\underline{\mathbf{S}}_k^n$ is the diagonal matrix containing powers transmitted on the unobserved lines and $\mathbf{R}_{kz}^n$ is the background noise correlation matrix for the observed lines. Now the linear MMSE partial crosstalk cancellation for line n on tone k can be written as

$$\hat{x}_k^n = decision \left(\overline{\mathbf{w}}_k^n \left[\mathbf{y}_k \right]_{rows \mathcal{M}_k^n} \right), \tag{6.13}$$

where the partial cancellation coefficient vector $\overline{\mathbf{w}}_k^n$ can be calculated using (6.7) and (6.12) as

$$\overline{\mathbf{w}}_k^n \triangleq \overline{\mathbf{e}}_q^H \left(\mathbf{S}_k^n \overline{\mathbf{H}}_k^{nH} \left(\overline{\mathbf{H}}_k^n \mathbf{S}_k^n \overline{\mathbf{H}}_k^{nH} + \overline{\mathbf{R}}_k^n \right)^{-1} \right), \tag{6.14}$$

where $\overline{\mathbf{e}}_q \triangleq \left[\mathbf{I}_{p_{k,n}+1} \right]_{col\, q}$ represents the q-th column of the identity matrix of size $p_{k,n}+1$. Here, q is the position of line n in the set $\mathcal{M}_k^n$ and $\mathbf{S}_k^n$ is the diagonal matrix containing the powers transmitted on the observed lines.

6.4.2 Computation of MMSE-GDFE partial crosstalk canceler coefficients

Let $\mathcal{W}_k^n$ be the set of indices of all the observed lines by the feedforward section to detect the signal in line n on tone k, including line n, and let $\underline{\mathcal{W}}_k^n$ be the set of indices of the unobserved lines not used by the feedforward section. Similarly, let $\mathcal{B}_k^n$ be the set of indices of all the observed lines used by the feedback section to detect the signal in line n on tone k and let $\underline{\mathcal{B}}_k^n$ be the set of indices of the unobserved lines not used by the feedback section. The channel matrix corresponding to the observed lines in the feedforward section can be written as

$$\overline{\mathbf{H}}_{k,ff}^n \triangleq \left[[\mathbf{H}_k]_{rows\mathcal{W}_k^n, cols\mathcal{W}_k^n \setminus \mathcal{B}_k^n} \right], \tag{6.15}$$

where $\mathcal{W}_k^n \setminus \mathcal{B}_k^n$ is the set of indices of the observed lines except those that are in $\mathcal{B}_k^n$. The crosstalk channel matrix corresponding to the unobserved lines can then be written as

$$\underline{\mathbf{H}}_{k,ff}^n \triangleq \left[[\mathbf{H}_k]_{rows\mathcal{W}_k^n, cols\underline{\mathcal{W}}_k^n \setminus \mathcal{B}_k^n} \right], \tag{6.16}$$

where $\underline{\mathcal{W}}_k^n \setminus \mathcal{B}_k^n$ is the set of indices of the unobserved lines except those are in $\mathcal{B}_k^n$. Similarly $\overline{\mathbf{R}}_{k,ff}^n$ is defined as the noise correlation matrix of the observed lines, i.e.,

$$\overline{\mathbf{R}}_{k,ff}^n \triangleq \mathbf{R}_{kz,ff}^n + \underline{\mathbf{H}}_{k,ff}^n \underline{\mathbf{S}}_{k,ff}^n \underline{\mathbf{H}}_{k,ff}^{nH} \tag{6.17}$$

where $\underline{\mathbf{S}}_{k,ff}^n$ is the diagonal matrix containing powers transmitted on the unobserved lines except those in $\mathcal{B}_k^n$ and $\mathbf{R}_{kz,ff}^n$ is a background noise correlation matrix for the observed lines. The MMSE feedforward filter coefficient can then be computed as

$$\mathbf{w}_{ff,k}^n = \mathbf{e}_q^H \left(\mathbf{S}_{k,ff}^n \overline{\mathbf{H}}_{k,ff}^{nH} (\overline{\mathbf{H}}_{k,ff}^n \mathbf{S}_{k,ff}^n \overline{\mathbf{H}}_{k,ff}^{nH} + \overline{\mathbf{R}}_{k,ff}^n)^{-1} \right), \tag{6.18}$$

where $\mathbf{e}_q$ is the $q-th$ column of the identity matrix whose size is defined by the cardinality of $\mathcal{W}_k^n$. Here q is the position of the line n in the set $\mathcal{W}_k^n$ and $\mathbf{S}_{k,ff}^n$ is the diagonal matrix containing the power of the observed lines used by the feedforward section except those in $\mathcal{B}_k^n$. With

$$\overline{\mathbf{h}}_{k,fb}^n \triangleq \left[[\mathbf{H}_k]_{row\, \mathcal{W}_k^n, cols\mathcal{B}_k^n} \right], \tag{6.19}$$

the feedback coefficient vector in line n on tone k can be written as

$$\mathbf{w}_{fb,k}^n = \mathbf{w}_{ff,k}^n \overline{\mathbf{h}}_{k,fb}^n. \tag{6.20}$$

Now the output of the nonlinear MMSE partial crosstalk canceler can be written as

$$\hat{x}_k^n = decision \left(\mathbf{w}_{ff,k}^n \mathbf{y}_{ff,k}^n - \mathbf{w}_{fb,k}^n \mathbf{x}_{fb,k}^n \right), \tag{6.21}$$

where $\mathbf{x}_{fb,k}^n$ is a vector containing the detected symbols from all the observed lines used by the feedback section and $\mathbf{y}_{ff,k}^n$ is a vector containing the received symbols from all the observed lines used by feedforward section.

6.5 Problem formulation

6.5.1 Partial crosstalk cancellation tap allocation for a fixed power loading

The partial crosstalk cancellation problem amounts to maximizing the total bit-rate summed over all lines when using only C_{budget} cancellation taps, i.e., non-zero elements in the canceler matrices. This comes down to the following maximization problem,

$$\max_{\mathbf{c}} \sum_{k\in\mathcal{K}} \sum_{n=1}^{N} \tilde{b}_k^n$$

$$\text{s.t} \sum_{k\in\mathcal{K}} \sum_{n=1}^{N} \sum_{\substack{m=1 \\ m\neq n}}^{\tilde{N}} c_k^{n,m} \leq C_{budget}, \tag{6.22}$$

where $\mathbf{c} = [\mathbf{c}_1, \mathbf{c}_2, ..., \mathbf{c}_K]$, $[\mathbf{c}_k]_{n,m} = c_k^{n,m} \in \{0, 1\}$.

- For the linear MMSE, $\tilde{N} = N$ therefore $\mathbf{c}_k$ is an $N \times N$ matrix containing the cancellation tap configurations $c_k^{n,m}$ on tone k. Here $c_k^{n,m} = 1$ indicates that a cancellation tap has been assigned to position (n, m), i.e., that line m is used for the detection of line n the tone k ($m \in \mathcal{M}_k^n$). Similarly, $c_k^{n,m} = 0$ indicates a cancellation tap has not been assigned to position (n, m) ($m \in \underline{\mathcal{M}}_k^n$). Finally, $\tilde{b}_k^n$ is the bit-rate of line n on tone k given as

$$\tilde{b}_k^n \triangleq \log_2 \left(1 + \frac{1}{\Gamma} \frac{\left|\overline{\mathbf{h}}_k^n\right|^2 s_k^n}{\hat{n}} \right), \tag{6.23}$$

  where Γ is the SNR gap, $\overline{\mathbf{h}}_k^n = \overline{\mathbf{w}}_k^n \overline{\mathbf{H}}_k^n$, $\overline{\mathbf{h}}_k^n(q)$ represents the q-th element of vector $\overline{\mathbf{h}}_k^n$, $\hat{n} = \sum_{i\neq q} \left|\overline{\mathbf{h}}_k^n(i)\right|^2 s_k^i + Tr(\overline{\mathbf{w}}_k^n \overline{\mathbf{R}}_k^n \overline{\mathbf{w}}_k^{nH})$, $Tr(\mathbf{X})$ takes the trace of the matrix $\mathbf{X}$ and s_k^q represents the q-th element of $\mathbf{s}_k$.

- For the MMSE-GDFE, the maximum feedback filter length is equal to N therefore the $\tilde{N} = 2N$. Hence $\mathbf{c}_k$ is a $N \times 2N$ matrix, where the N added

columns account for the tap allocation in the feedback section. Due to the triangular structure of the feedback section the maximum number of non-zero elements in $\mathbf{c}_k$ is $N^2 + \frac{N(N-1)}{2}$. If $m \leq N$ then $c_k^{n,m} = 1$ indicates that a cancellation tap has been assigned to the feedforward section in position (n, m) $(m \in \mathcal{W}_k^n)$ and when $m > N$ it indicates that a cancellation tap has been assigned to the feedback section in position $(n, m-N)$ $(m \in \mathcal{B}_k^n)$. The bit-rate of line n on tone k is given by

$$\tilde{b}_k^n \triangleq \log_2 \left(1 + \frac{1}{\Gamma} \frac{\left| \overline{\mathbf{h}}_k^n \right|^2 s_k^n}{\tilde{n}} \right), \tag{6.24}$$

where $\tilde{n} = \sum_{i \neq q} \left| \overline{\mathbf{h}}_k^n(i) \right|^2 s_k^n(i) + Tr(\overline{\mathbf{w}}_{f,k}^n \overline{\mathbf{R}}_k^n \overline{\mathbf{w}}_{f,k}^{nH}) - Tr(\mathbf{w}_{fb,k}^n \underline{\mathrm{S}}_{k,bb}^n \mathbf{w}_{fb,k}^{nH})$, $\underline{\mathrm{S}}_{k,bb}^n$ is the diagonal matrix containing powers transmitted on the observed fedback lines, $\overline{\mathbf{h}}_k^n = \overline{\mathbf{w}}_{f,k}^n \overline{\mathbf{H}}_k^n$, $\overline{\mathbf{h}}_k^n(i)$ represents the i-th element of vector $\overline{\mathbf{h}}_k^n$ and s_k^i represents the i-th diagonal element of $\underline{\mathrm{S}}_{k,ff}^n$.

The global optimum for (6.22) can be found by exhaustively searching over all possible cancellation tap configurations. However, the constraint is coupled over tones, which results in an exponential complexity in the number of tones. The overall complexity is then $\mathcal{O}(2^{KN(N-1)})$ for the linear MMSE canceler and $\mathcal{O}(2^{K\frac{3}{2}N(N-1)})$ for the MMSE-GDFE, which is generally intractable. This complexity can be made linear in K by using a dual decomposition approach. To achieve this, the constraint in the optimization problem is moved into the objective with the help of a Lagrange multiplier λ. This can then be written as

$$\min_{\lambda} \left(\max_{\mathbf{c}} \left(\sum_{k=1}^{K} \sum_{n=1}^{N} \tilde{b}_k^n + \lambda (C_{budget} - \sum_{k=1}^{K} \sum_{n=1}^{N} \sum_{\substack{m=1 \\ m \neq n}}^{\tilde{N}} c_k^{n,m}) \right) \right)$$

$$\text{subject to } \lambda \geq 0 \qquad n = 1 \cdots N \tag{6.25}$$

In [177], for multicarrier systems with a sufficiently large number of tones, the duality gap was shown to be zero for this type of optimization problems. For a given λ, the maximization problem in (6.25) is decoupled over tones hence it can be solved for each tone separately. The per-tone optimization can then be written

as

$$\text{For } k = 1 \cdots K$$

$$\max_{\mathbf{c}_k} \sum_{n=1}^{N} \tilde{b}_k^n - \sum_{n=1}^{N} \sum_{\substack{m=1 \\ m \neq n}}^{\tilde{N}} \lambda c_k^{n,m}.$$

(6.26)

The maximization of (6.26) can be performed by an exhaustive search over all possible $\mathbf{c}_k$'s. Additionally, the constraint can be enforced by tuning λ. An algorithm to efficiently tune the Lagrange multiplier is given in [78]. An exhaustive search of the partial crosstalk canceler configuration still has a complexity of $\eta K \mathcal{O}(2^{N(N-1)})$ for the linear MMSE canceler and $\eta K \mathcal{O}(2^{\frac{3}{2}N(N-1)})$ for the MMSE-GDFE, where η is the number of iterations required for the tuning of λ. However, this complexity can be further reduced based on two properties, namely line independence and line selection [78]:

Line independence

For each line, a crosstalk cancellation configuration has to be decided on. However, from (6.23) and (6.24), it can be seen that when it is decided to observe line m for the detection of line n, this obviously only affects the performance of line n. Hence, (6.26) can be further decoupled over lines, leading to

$$\text{For } k = 1 \cdots K$$

$$\text{For } n = 1 \cdots N$$

$$\max_{\mathbf{c}_k(n,:)} \tilde{b}_k^n - \sum_{\substack{m=1 \\ m \neq n}}^{\tilde{N}} \lambda c_k^{n,m}.$$

(6.27)

This reduces the complexity from $\eta K \mathcal{O}(2^{N(N-1)})$ to $\eta K N \mathcal{O}(2^{(N-1)})$ for the linear MMSE canceler and from $\eta K \mathcal{O}(2^{\frac{3}{2}N(N-1)})$ to $\eta K N \mathcal{O}(2^{\frac{3}{2}(N-1)})$ for the MMSE-GDFE.

Line selection

For the linear MMSE canceler, for each line n it has to be decided whether or not $N-1$ other lines are observed. Hence, there are 2^{N-1} possible crosstalk cancellation configurations for each line. Similarly, for the MMSE-GDFE there are $2^{(N-1+l)}$ possible crosstalk cancellation configurations for each line, where l is the number of previously decoded lines, i.e., $l = 1 \cdots (N-1)$. If $\bar{q}$ cancellation taps are available then these should be allocated such that the effectively canceled interference is maximized. For a line n if we can define a metric, $\mathcal{I}^{n,k}$ such that the $N-1$ cancellation taps for the linear MMSE canceler or $(N-1+l)$ cancellation taps for the MMSE-GDFE can be ordered, then $\bar{q}$ lines can be selected that have the largest values for this metric. In this fashion the number of possible crosstalk configurations reduces from 2^{N-1} to $N-1$ for the linear MMSE canceler and from $2^{(N-1+l)}$ to $(N-1+l)$ for the MMSE-GDFE, and so the overall complexity becomes $\eta\mathcal{O}(KN(N-1))$ for the linear MMSE canceler and $\eta\mathcal{O}(K\frac{3}{2}N(N-1))$ for the MMSE-GDFE. Hence the optimization problem can be written as

$$\begin{aligned} &\text{For } k = 1 \cdots K \\ &\text{For } n = 1 \cdots N \\ &\max_{\mathbf{c}_k(n,:)} \tilde{b}_k^n(\bar{q}) - \lambda \bar{q} \end{aligned} \tag{6.28}$$

where $\tilde{b}_n^k(\bar{q})$ is the bit-rate when $\bar{q}$ lines are observed and selected based on the selection metric $\mathcal{I}_k^n$.

6.5.2 Joint partial crosstalk cancellation and spectrum balancing

The partial crosstalk cancellation problem amounts to maximizing the total bit-rate summed over all lines when using only C_{budget} cancellation taps, i.e., non-zero elements in the canceler matrices and a total transmit power budget S_{budget}^n for

line n. This comes down to the following maximization problem,

$$\max_{\mathbf{c},\mathbf{s}} \sum_{k=1}^{K}\sum_{n=1}^{N} \tilde{b}_k^n$$

$$\text{subject to } \sum_{k=1}^{K}\sum_{n=1}^{N}\sum_{\substack{m=1\\ n\neq m}}^{\tilde{N}} c_k^{n,m} \leq C_{budget}$$

$$\sum_{k=1}^{K} s_k^n \leq S_{budget}^n$$

$$0 \leq s_k^n \leq s_k^{n,mask}, \tag{6.29}$$

where $\mathbf{c} = [\mathbf{c}_1, \mathbf{c}_2, ..., \mathbf{c}_K]$, $[\mathbf{c}_k]_{n,m} = c_k^{n,m} \in \{0,1\}$, S_{budget}^n is the total power of line n and $s_k^{n,max}$ is the maximum allowed transmit power by line n on tone k. Let $\mathcal{S}$ be the set containing possible power levels with cardinality $\tilde{L}$.

The joint resource allocation problem (6.29) is a non-convex constrained optimization problem. Finding the global optimum for (6.29) requires an exhaustive search over all possible solutions. The problem is coupled over tones and users, which results in exponential complexity in the number of tones and number of users. Therefore, the computational complexity is $\mathcal{O}(\tilde{L}2^{N-1})^{KN}$ for the linear MMSE canceler and $\mathcal{O}(\tilde{L}2^{N-1})^{K\frac{3}{2}N}$ for the MMSE-GDFE, which is generally intractable. This complexity can be made linear in the number of tones by using a dual decomposition approach. To achieve this, the constraint in the optimization problem is moved into the objective with the help of Lagrange multipliers. This can then be written as

$$\min_{\lambda,\gamma}\left(\max_{\mathbf{c},\mathbf{s}}\left(\sum_{k=1}^{K}\sum_{n=1}^{N}\tilde{b}_k^n + \lambda\left(C_{budget} - \sum_{k=1}^{K}\sum_{n=1}^{N}\sum_{\substack{m=1\\ m\neq n}}^{\tilde{N}} c_k^{n,m}\right) + \sum_{n=1}^{N}\gamma_n\left(S_{budget}^n - \sum_{k=1}^{K} s_k^n\right)\right)\right)$$

$$\text{subject to } \lambda, \gamma_n \geq 0 \tag{6.30}$$

For multicarrier systems with a sufficiently large number of tones, the duality gap was shown to be zero [177]. For a given λ, the maximization problem in (6.30) is decoupled over tones hence it can be solved for each tone separately. The per-tone

optimization can then be written as

$$\text{For } k = 1 \cdots K$$

$$\max_{\mathbf{c}_k, \mathbf{s}_k} \sum_{n=1}^{N} \tilde{b}_k^n - \sum_{n=1}^{N} \sum_{\substack{m=1 \\ m \neq n}}^{\tilde{N}} \lambda c_k^{n,m} - \sum_{n=1}^{N} \gamma_n s_k^n \tag{6.31}$$

The maximization of (6.31) can be performed by an exhaustive search over all possible combinations of $\mathbf{c}_k$'s and $\mathbf{s}_k$'s. Additionally, the constraint can be enforced by tuning λ and γ_n. An algorithm to efficiently tune the Lagrange multiplier is given in [78]. An exhaustive search of all partial crosstalk canceler configurations still has a complexity of $K\mathcal{O}((\tilde{L}2^{(}N-1))^N)$ for the linear MMSE canceler and $K\mathcal{O}((\tilde{L}2^{(N-1)})^{\frac{2}{2}N})$ for the MMSE-GDFE for each update of the Lagrange multipliers λ and γ_n. This is still intractable for practical values of $\tilde{L}$ and N. In section 6.6.2, we will present various techniques to reduce the complexity.

6.6 Resource allocation in linear MMSE based crosstalk cancellation

6.6.1 Partial crosstalk cancellation tap allocation for a fixed power loading

In [27], it was shown that for a linear ZF canceler the interferers can be ordered based on their crosstalk power as selection metric, i.e.,

$$\mathcal{I}_{k,zf}^n = \left\{ |h_k^{n,m}|^2 s_k^m \right\}. \tag{6.32}$$

The interferers are then ordered in descending order with respect to the selection metric. Then a simple exhaustive search over all the ordered interferers was performed to allocate the crosstalk cancellation taps based on the defined cost function.

For the ZF canceler, the metric, $\mathcal{I}_{k,zf}^n$, could be easily defined based only on the crosstalk power [27]. However, in the presence of spatially correlated background noise, the metric cannot be defined so easily for the MMSE-based cancelers. In the next section, we address the issue of defining a suitable metric for the linear MMSE canceler.

Algorithm 6.1 Linear ZF based partial crosstalk cancellation tap allocation for a fixed power loading

Initialize $\tilde{b}_k^n(\bar{q})$, λ, $\mathcal{L}_{k,opt}^n = 0$
while $C \neq C_{budget}$ **do**
  for tone $k = 1 \cdots K$ **do**
    for line $n = 1 \cdots N$ **do**
      Compute metric $\mathcal{I}_{k,zf}^n$
      Order the interferers based on $\mathcal{I}_{k,zf}^n$
      for number of crosstalkers to be cancelled $\bar{q} = 1 \cdots N-1$ **do**
        compute $\mathbf{w}_{k,ZF}^n$ for $\bar{q}$ lines with indices from $\mathcal{M}_k^n(q)$
        $\mathcal{L}_k^n = \tilde{b}_k^n(\bar{q}) - \lambda\bar{q}$
        if $\mathcal{L}_k^n > \mathcal{L}_{k,opt}^n$ **then**
          $\mathcal{L}_{k,opt}^n = \mathcal{L}_k^n$
          $\mathbf{w}_{k,ZF,opt}^n = \mathbf{w}_{k,ZF}^n$
          $\bar{q}_{k,opt}^n = \bar{q}$
        end if
      end for
    end for
  end for
  compute $C = \sum_k \sum_n \bar{q}_{k,opt}^n$
  update $\lambda = [\lambda - \mu(C_{budget} - C)]^+$
end while

Selection metric for linear MMSE partial crosstalk cancelers

For the linear MMSE canceler, a first option is to use the metric used in the case of the ZF canceler, which is based only on the in-domain crosstalk power so that the information about the spatially correlated background noise is ignored. So the strategy is to cancel the strongest in-domain crosstalker first. This first metric can be written as

$$\mathcal{I}_{k,1}^n = \left\{ |h_k^{n,m}|^2 s_k^m \right\}, \tag{6.33}$$

The interferers are then ordered in descending order with respect to the selection metric $\mathcal{I}_{k,1}^n$. Then the indices are stored in $\mathcal{M}_k^n$. This is a good strategy when the alien crosstalk is white/nearly white or very small. However, if the background noise is spatially correlated and strong then this metric may not provide good results. In such a scenario, instead of the in-domain crosstalk information, the spatial correlation of the background noise can be used as a selection metric. This second metric can thus be defined as

$$\mathcal{I}_{k,2}^n = \{ r_k^{n,m} \}, \tag{6.34}$$

where $r_k^{i,j}$ is the entry in the ith row and the jth column in the noise correlation matrix $\mathbf{R}_k$ on tone k. The interferers are ordered in descending order with respect to the slection metric $\mathcal{I}_{k,2}^n$ and the indices are stored in $\mathcal{M}_k^n$. If the alien crosstalk is much stronger than the in-domain crosstalk then this metric provides a good cancellation order. In the scenario, where both the in-domain crosstalk and the alien crosstalk are large, a metric can be defined that combines the available information about the in-domain crosstalk power and the background noise correlation. For line n, the total information provided by the background noise correlation can be written empirically as follows

$$n_{k,emp}^{n,m} \triangleq \underbrace{r_k^{n,n}\tilde{r}_k^{n,m}}_{I} \underbrace{\left(\frac{r_k^{m,m}}{|h_k^{m,m}|^2 s_k^m}\right)}_{II}, \tag{6.35}$$

where $\tilde{r}_k^{n,m}$ is the entry in the nth row and the mth column in the noise correlation matrix $\mathbf{R}_k$ after normalization such that the $\tilde{r}_k^{n,m}$ provides the value relative to $r_k^{n,n}$. Part I of (6.35) yields the amount of alien crosstalk that can be canceled if line m is selected. Part II accounts for the fact that the effective alien crosstalk that can be canceled also depends on the SINR of line m. The third metric is then defined as

$$\mathcal{I}_3^{n,k} = \left\{ n_{k,emp}^{n,m} + |h_k^{n,m}|^2 s_k^m \right\}, \tag{6.36}$$

The interferers are ordered in descending order with respect to the slection metric $\mathcal{I}_{k,3}^n$ and the indices are stored in $\mathcal{M}_k^n$. The performance achieved with $\mathcal{I}_{k,3}^n$ is found to be close to the performance achieved with the optimum tap selection scheme, i.e., obtained with an exhaustive search (see section 6.8).

Selection metric based partial crosstalk cancellation tap selection

Here, we present the technique to perform the partial crosstalk cancellation tapselection using the selection metric.

$$\text{For } k = 1 \cdots K$$

$$\text{For } n = 1 \cdots N$$

$$\max_{\bar{q}} \tilde{b}_k^n(\bar{q}) - \lambda \bar{q} \tag{6.37}$$

The complexity of choosing $\bar{q}$ after the selection order of the cancellation tap is fixed by the selection metric reduces from a combinatorial complexity to a linear complexity.

In (6.37), increasing the λ increases the penalty for increasing the number of canceler taps. Hence, the value of λ is quite important in obtaining the optimal solution. There are many ways to update the value of λ such as the bisection method, the gradient descent method etc. [29] [154]. In [154], the update of λ is based on the difference between the total available system resources and the used system resources for the current value of λ. For our problem this can be written as,

$$\lambda \Leftarrow [\lambda - \mu(C_{\text{budget}} - \sum_{k\in\mathcal{K}}\sum_{n=1}^{N}\sum_{\substack{m=1\\m\neq n}}^{N} c_k^{n,m})]^+ \tag{6.38}$$

where μ is a scaling factor, whose value can be changed in order to obtain a faster convergence to the solution. For simplicity, in our simulations μ is taken as a fixed positive value close to zero.

An algorithm description is provided as Alg. 6.2. In the presented algorithm, a search over the canceler taps for a particular tone and for a fixed λ is terminated when either the maximum number of taps that can be allocated is reached or when the cost function for a particular number of canceler taps is lower than that for the previous number of canceler taps.

Algorithm 6.2 Selection metric based linear MMSE partial crosstalk cancellation tap allocation for a fixed power loading

initialize $\tilde{b}_k^n(\bar{q})$, λ^0, $\mathcal{L}_{k,opt}^n = 0$, $\mathbf{w}_{k,MMSE,opt}^n$
while $C \neq C_{budget}$ **do**
  for tone $k = 1 \cdots K$ **do**
    for line $n = 1 \cdots N$ **do**
      compute metric $\mathcal{I}_{k,3}^n$
      order the interferers based on $\mathcal{I}_{k,3}^n$
      for number of crosstalkers to be cancelled $\bar{q} = 1 \cdots N-1$ **do**
        compute $\mathbf{w}_{k,MMSE}^n$ for $\bar{q}$ interferers with indices in $\mathcal{M}_k^n(q)$
        $\mathcal{L}_k^n = \tilde{b}_k^n(\bar{q}) - \lambda^t \bar{q}$
        if $\mathcal{L}_k^n > \mathcal{L}_{k,opt}^n$ **then**
          $\mathcal{L}_{k,opt}^n = \mathcal{L}_k^n$
          $\mathbf{w}_{k,MMSE,opt}^n = \mathbf{w}_{k,MMSE}^n$
          $\bar{q}_{k,opt}^n = \bar{q}$
        end if
      end for
    end for
  end for
  compute $C = \sum_k \sum_n \bar{q}_{k,opt}^n$
  update $\lambda = [\lambda - \mu(C_{budget} - C)]^+$
end while

Sparse approximation based partial cancellation

From the previous section, it is clear that if the order of the crosstalk cancellation taps can be fixed, then the computational complexity of the partial crosstalk cancellation can be reduced avoiding the exhaustive search for each line n. In order to avoid the exhaustive search, the non-zero crosstalk canceler coefficients can also be determined by using a sparse approximation based linear MMSE crosstalk canceler design. In the following section, we will present a sparse linear MMSE crosstalk canceler design procedure.

Sparse linear MMSE crosstalk canceler design

Let us rewrite the linear MMSE design criterion for line n as follows

$$\mathbf{w}_{k,MMSE}^{n} = \underset{\mathbf{w}_k^n}{\operatorname{argmin}} \quad \mathcal{E}\left\{|\mathbf{w}_k^n(\mathbf{H}_k\mathbf{x}_k + \mathbf{z}_k) - x_k^n|^2\right\} \tag{6.39}$$

We can rewrite (6.39) as follows

$$\mathbf{w}_{k,MMSE}^{n} = \underset{\mathbf{w}_k^n}{\operatorname{argmin}} \quad \left\| \underbrace{\begin{bmatrix} \mathbf{S}_k^{1/2}\mathbf{H}_k^H \\ \mathbf{R}_{z,k}^{1/2} \end{bmatrix}}_{\mathbf{A}_k} \mathbf{w}_k^{nH} - \underbrace{\begin{bmatrix} \mathbf{S}_k^{1/2} e_n \\ \mathbf{0} \end{bmatrix}}_{\mathbf{b}_k} \right\|_2^2$$

$$\mathbf{w}_{k,MMSE}^{n} = \underset{\mathbf{w}_k^k}{\operatorname{argmin}} \quad \left\|\mathbf{A}_k\mathbf{w}_k^{nH} - \mathbf{b}_k\right\|_2^2 \tag{6.40}$$

In order to find a better way to control the sparsity pattern, let us write the problem of designing a linear MMSE crosstalk canceler in (6.40) as a sparse approximation problem [152, 153, 49] as

$$\boxed{\tilde{\mathbf{w}}_{k,MMSE}^{n} = \underset{\tilde{\mathbf{w}}_k^n}{\operatorname{argmin}} \quad \left\|\mathbf{A}_k\tilde{\mathbf{w}}_k^{nH} - \mathbf{b}_k\right\|_2^2 + \gamma\left\|\tilde{\mathbf{w}}_k^n\right\|_0} \tag{6.41}$$

where $\|.\|_0$ is a ℓ_0 quasi-norm of the vector in the argument counting the number of non-zero elements of the vector. γ controls the trade off between the sparsity and the quadratic term. Problem (6.41) is however known to be NP hard in general [152].

To simplify (6.41), the non-convex ℓ_0 quasi-norm is replaced by the convex ℓ_1 norm [152, 153, 49]. This can be written as

$$\boxed{\bar{\mathbf{w}}_{k,MMSE}^{n} = \underset{\bar{\mathbf{w}}_{k}^{n}}{\operatorname{argmin}} \quad \left\|\mathbf{A}_k \bar{\mathbf{w}}_{k}^{nH} - \mathbf{b}\right\|_2^2 + \tilde{\gamma}\left\|\bar{\mathbf{w}}_{k}^{n}\right\|_1}, \tag{6.42}$$

where $\tilde{\gamma}$ controls the trade off between the sparsity and the quadratic term. (6.42) is a convex problem and can be solved using any generic solver in polynomial time [24]. If the underlying system admits a sparse solution, it has been shown that solving (6.42) is equivalent to solving (6.41) [153, 49]. In our case, the underlying system does not necessarily admit a sparse solution, therefore we can not obtain a sparse linear MMSE crosstalk canceler by just solving (6.42). One way to obtain a sparse linear MMSE crosstalk canceler is to adopt a two step procedure. Firstly, we use (6.42), for a given $\tilde{\gamma}$, to obtain a nearly-sparse linear MMSE crosstalk canceler and then force the coefficients below a certain threshold level ζ to zero and obtain the sparsity pattern $\mathbf{c}_k^n$ and hence $\mathcal{M}_k^n$. Secondly, we use the sparsity pattern obtained after applying the threshold and we compute the linear MMSE crosstalk canceler using (6.14).

It is clear that the choice of the trade off parameter $\tilde{\gamma}$ and the threshold level ζ is important for the algorithm to work properly. An efficient update rule for $\tilde{\gamma}$ is based on the difference between the total available system resources and the used system resources for the current value of $\tilde{\gamma}$. This can be written as

$$\tilde{\gamma} \Leftarrow \left[\tilde{\gamma} - \mu(C_{\text{budget}} - \sum_{k\in\mathcal{K}}\sum_{n}\left\|\mathbf{w}_{k,MMSE}^{n}\right\|_0)\right]^{+} \tag{6.43}$$

where μ is a positive scaling factor, and [a]+ is max(0,a). For simplicity, in our simulations μ is taken as a fixed value close to zero.

The threshold level ζ can be fixed to a constant level and the coefficients smaller than the threshold value can be set to zero. However, we can also update the threshold level to speed up the convergence. It is obvious that if the threshold level is set to a higher value, the probability of a sparser equalizer becomes higher. The update formula for the threshold level can be written as

$$\zeta \Leftarrow \left[\zeta - \sigma(C_{\text{budget}} - \sum_{k\in\mathcal{K}}\sum_{n}\left\|\bar{\mathbf{w}}_{k,MMSE}^{n}\right\|_0)\right]^{+}, \tag{6.44}$$

where σ is an small positive scaling factor. In (6.44), the threshold ζ is same for the cancellation filters for all the lines and tone. But cancellation filters different lines and tones obtain different MMSEs. Therefore, the cancellation tap allocation

algorithm can be improved if the threshold ζ is weighted by the MSE of the cancelers. This can be given as

$$\zeta_k^n \Leftarrow \left[\zeta_k^n - \sigma_k^n(C_{\text{budget}} - \sum_{k\in\mathcal{K}}\sum_n \left\|\bar{\mathbf{w}}_{k,MMSE}^n\right\|_0)\right]^+, \tag{6.45}$$

where

$$\sigma_k^n = \sigma \left\|\mathbf{A}_k \mathbf{w}_{k,MMSE}^{nH} - \mathbf{b}_k\right\|_2^2 \tag{6.46}$$

Sparse approximation based partial cancellation

We are now ready to describe the full sparse approximation based partial crosstalk cancellation scheme.

Since the sparsity pattern $\mathbf{c}_k^n$ directly gives the number and the position of crosstalkers to be canceled with minimum approximation error, explit computation of other objective function can be avoided. The indices of the interferers cancelled can then be stored in $\mathcal{M}_k^n$ and the linear MMSE canceler can be computed using (6.14).

Even though the crosstalk canceler has to be computed twice, for large N, it has similar complexity to the selection metric based crosstalk canceler coefficient selection algorithm presented in the section above. The algorithm to implement this is presented in **Alg. 6.3**.

6.6.2 Joint partial crosstalk cancellation tap allocation and spectrum balancing

In the previous section, the linear MMSE crosstalk canceler tap allocation in the case of a fixed power loading was presented. In order to avoid severe crosstalk, different lines can vary their transmit power on a certain tone such that the crosstalk caused by a line is reduced without significantly reducing its own performance. This is known as spectrum balancing.

Here we present an approach based on the joint crosstalk canceler tap selection and spectrum balancing problem formulation given in (6.31).As in the case of a fixed power loading scheme, the problem in (6.31) is decoupled over tones and lines. However, computation of linear MMSE crosstalk cancelers relies on the power transmitted by other lines as seen in (6.7).

$\mathbf{S}_k$ contains the power transmitted by all the lines on tone k, therefore changing the power transmitted on one line changes the crosstalk caused by that line and

Algorithm 6.3 Sparse approximation based linear MMSE partial crosstalk cancellation tap allocation for a fixed power loading

Initialize γ, ζ_k^n, σ
while $C \neq C_{budget}$ **do**
  for tone $k = 1 \cdots K$ **do**
    for line $n = 1 \cdots N$ **do**
      Compute nearly sparse $\bar{\mathbf{w}}_k^n$ with (6.42)
      Apply threshold ζ_k on $\bar{\mathbf{w}}_k^n$ to obtain $\mathbf{c}_k^n$
      Compute the sparse $\mathbf{w}_{k,MMSE}^n$ using (6.14)
      $\sigma_k^n = \sigma \left\| \mathbf{A}_k \mathbf{w}_{k,MMSE}^{nH} - \mathbf{b}_k \right\|_2^2$
    end for
  end for
  Compute $C = \sum_k \sum_n \bar{c}_n^k$
  Update $\gamma = [\gamma - \mu(C - C_{budget})]^+$
  for tone $k = 1 \cdots K$ **do**
    for line $n = 1 \cdots N$ **do**
      Update $\zeta_k^n = [\zeta_k^n - \sigma_k^n(C - C_{budget})]^+$
    end for
  end for
end while

hence the linear MMSE coefficients of all the other lines. Therefore, the solution of (6.31) requires a search over all combinations of powers for all the lines. This can be reduced by iteratively updating the power of each line fixing the power of all the other lines. Hence, the problem is decoupled over lines. This can be written as

$$\begin{aligned} &\text{For } k = 1 \cdots K \\ &\text{For } n = 1 \cdots N \\ &\text{For } s_k^n = 0 \cdots s_k^{n,max} \\ &\max_{\mathbf{c}_k^n} \quad \tilde{b}_k^n - \sum_{\substack{m=1 \\ m \neq n}}^{\tilde{N}} \lambda c_k^{n,m} - \gamma_n s_k^n. \end{aligned} \tag{6.47}$$

This problem still has a combinatorial complexity since the sparsity pattern $\mathbf{c}_k^n$ is combinatorial. In order to further reduce the complexity, we aim to restrict the search space for the canceler tap selection. In the following sections, we present techniques to further reduce the complexity of the canceler tap selection and spectrum balancing.

Selection metric based joint linear MMSE partial cancellation and spectrum balancing

The complexity of (6.47) can be further reduced if we can restrict the search space of the canceler taps. For a given transmit power for user n, this can be achieved by using the selection metric based approach described in section 6.6.1. The combinatorial search space of the crosstalk canceler tap selection then reduces to the linear search space based on the selection metric, $\mathcal{I}^n_{k,3}$. Therefore, the problem now reduces to per-tone per-line exhaustive search over all the crosstalk cancellation taps and transmit power. This can be written as follows

$$\begin{aligned}
&\text{For } k = 1 \cdots K \\
&\text{For } n = 1 \cdots N \\
&\text{For } s^n_k = 0 \cdots s^{n,max}_k \\
&\text{For } q^n_k = 1 \cdots N-1 \\
&\max_{\mathbf{c}^n_k} \quad \tilde{b}^n_k - \lambda q^n_k - \gamma_n s^n_k. \qquad (6.48)
\end{aligned}$$

where λ and γ_n are Lagrange multipliers and can be updated as

$$\lambda \Leftarrow [\lambda + \mu(C_{budget} - \sum_{k\in\mathcal{K}} \sum_{n=1}^{N} q^n_k)]^+ \qquad (6.49)$$

$$\gamma_n \Leftarrow [\gamma_n - \tilde{\mu}^n(S_{budget} - \sum_{k\in\mathcal{K}} \sum_{n=1}^{N} s^n_k)]^+ \qquad (6.50)$$

While updating the power for line n on tone k, the power on all the other lines on that tone assumed fixed.

The algorithm to implement this scheme is given in **Alg. 6.4**.

Even though the overall computational complexity is reduced to $\mathcal{O}(\tilde{L}NK)$, the exhaustive search over all the ordered canceler taps has to be performed for each power level. Furthermore, we need to compute new linear MMSE coefficients for each change in power. To reduce this complexity we can use sparse approximation based linear MMSE crosstalk canceler design as proposed in section 6.6.1. This will be described in the following section.

Algorithm 6.4 Selection metric based joint linear MMSE partial crosstalk cancelltion tap allocation and spectrum balancing

initialize $\tilde{b}_k^n(\bar{q})$, $\mathbf{s}_k$, λ, γ_n, $s_{k,opt}^n$, $\mathcal{L}_{k,opt}^n = 0$
while $C \neq C_{budget}$ **do**
  for tone $k = 1 \cdots K$ **do**
    for line $n = 1 \cdots N$ **do**
      for transmit power $s_k^n = 0 \cdots s_k^{n,max}$ **do**
        compute metric $\mathcal{I}_{k,3}^n$
        update the nth entry of vector $\mathbf{s}_k$ as $\mathbf{s}_k[n] = s_k^n$
        for the number of interferers to be cancelled $\bar{q}_k^n = 1 \cdots N-1$ **do**
          compute $\mathbf{w}_{k,MMSE}^n$ using (6.14) and updated s_k^n and $\bar{q}_k^n$
          $[\bar{q}_k^n, s_{k,opt}^n]\mathcal{L}_k^n = \tilde{b}_k^n(\bar{q}_k^n) - \lambda^t \bar{q}_k^n$
          if $\mathcal{L}_k^n > \mathcal{L}_{k,opt}^n$ **then**
            $s_{k,opt}^n = s_k^n$
            $\mathbf{w}_{k,opt}^n = \mathbf{w}_k^n$
          end if
        end for
      end for
    end for
  end for
  compute $C = \sum_{k=1}^K \sum_{n=1}^N \bar{q}_k^n$
  update $\lambda = \lambda - \mu(C_{budget} - C)$
  for $n = 1 \cdots N$ **do**
    compute $S^n = \sum_{k=1}^K \bar{s}_k^n$
    update $\gamma_n = \gamma_n + \mu(S^n - S_{budget}^n)$
  end for
end while

Sparse approximation based joint linear MMSE partial cancellation and spectrum balancing

Based on the sparse linear MMSE crosstalk canceler design in section (6.6.1), we are now ready to describe the full sparse approximation based joint partial crosstalk cancellation and spectrum balancing. From definition, we can see that $\|\mathbf{w}_k^n\|_0 = \sum_{i=1}^N C_{ik}$ therefore we can also write (6.47) as

$$\max_{\mathbf{c}_k^n} \quad b_k^n - \lambda \|\mathbf{c}_k^n\|_0 - \gamma s_k^n, \tag{6.51}$$

Now for each discrete power level, we can compute a sparse MMSE canceler using the method described above. Even though the MMSE canceler coefficients need to be computed twice, first using (6.42) to determine the sparsity pattern $\mathbf{c}_k^n$ and then (6.14) to compute the MMSE canceler coefficients, for a large N it has similar computational complexity to the contiguous tap selection based approach

of section 6.6.2, which requires solving (6.14) N times for each power level. The computational complexity can be further reduced by solving (6.42) only once for the initial power level and then using same sparsity pattern for all the other power levels. We can write (6.51) as

$$\max_{\mathbf{c}_k} \quad \tilde{b}_k^n - \gamma_n s_k^n, \tag{6.52}$$

Furthermore the Lagrange multiplier γ_n, which enforces the power constraint also has to be updated. The Lagrange multiplier only depends on the difference between the current total power and the total power budget and hence can be written as

$$\gamma_n^{t+1} = \left[\gamma_n^t - \eta(S_{budget}^n - \sum_{k\in\mathcal{K}} s_k^n)\right]^+, \tag{6.53}$$

where η is an arbitrarily small scaling factor.

An algorithm to allocate the resources, i.e. number of equalizer taps and the power, for given resource constraints is given in **Alg.** 6.5.

6.7 Resource allocation in MMSE-GDFE based crosstalk cancellation

6.7.1 Partial crosstalk cancellation with a fixed power loading

Selection metric for MMSE-GDFE partial crosstalk cancelers

In the MMSE-GDFE, in addition to a selection metric for the feedforward path we also need a selection metric for the feedback path. If the detection order is fixed, only already decoded lines can be used in the feedback. The feedforward path in the MMSE-GDFE is basically a linear MMSE canceler. Therefore the selection metric for the feedforward section can also be given by (6.36). The feedback section in the MMSE-GDFE can only cancel the in-domain interference from the already decoded lines, hence the selection metric for the feedback section can be given as (6.33). Combining these selection metrics, the final selection metric for the MMSE-GDFE can be written as

$$\mathcal{I}_4^{n,k} = \{\mathcal{I}_3^{n,k}, |h_{(n,g)}^k|^2 s_g^k\}, \quad \text{for } g = 1\cdots l \tag{6.54}$$

$$g \neq n,$$

Algorithm 6.5 Sparse approximation based joint linear MMSE partial crosstalk cancellation tap allocation and spectrum balancing

initialize $\tilde{b}_k^n(\bar{q})$, λ, $\mathcal{L}_{k,opt}^n = 0$
while $C \neq C_{budget}$ **do**
  for tone $k = 1 \cdots K$ **do**
    for line $n = 1 \cdots N$ **do**
      Compute nearly sparse $\mathbf{w}_k^n$
      Apply threshold ζ_k^n and obtain the indices of the interferers to be cancelled store in $\mathcal{M}_k^n$
      for transmit powers $s_k^n = 0 \cdots s_k^{n,max}$ **do**
        Compute sparse $\mathbf{w}_{k,MMSE}^n$ using $\mathcal{M}_k^n$
        $\mathcal{L}_n^k = \ b_k - \gamma s_k$
        if $\mathcal{L}_n^k > \mathcal{L}_{k,opt}^n$ **then**
          $\mathcal{L}_{k,opt}^n = \mathcal{L}_n^k$
          $s_{k,opt} = s_n^k$
          $\mathbf{w}_{k,opt,MMSE}^n = \mathbf{w}_{k,MMSE}^n$
          Compute $\bar{C}_n^k$
        end if
        $\sigma_k^n = \sigma \left\| \mathbf{A}_k \mathbf{w}_{k,MMSE}^{nH} - \mathbf{b}_k \right\|_2^2$
      end for
    end for
  end for
  Compute $C = \sum_k \sum_n \bar{c}_n^k$
  Update $\lambda = [\lambda - \mu(C_{budget} - C)]^+$
  for tone $k = 1 \cdots K$ **do**
    for line $n = 1 \cdots N$ **do**
      $\zeta_k^n = [\zeta_k^n - \sigma_k^n(C_{budget} - C)]^+$
    end for
  end for
end while

where g represents previously detected lines. The interferers are ordered with respect to $\mathcal{I}_{k,4}^{n}$ and stored in $\mathcal{M}_{k}^{n}$. The performance achieved with $\mathcal{I}_{4}^{n,k}$ is found to be close to the performance achieved with the optimum tap selection scheme, i.e., obtained with an exhaustive search (see section 6.8).

Selection metric based crosstalk canceler selection

The resource allocation problem in MMSE-GDFE based DMT receiver can be written as

$$\begin{aligned} &\text{For } k = 1 \cdots K \\ &\text{For } n = 1 \cdots N \\ &\max_{\bar{q}} \ \tilde{b}_{k}^{n}(\bar{q}) - \lambda \bar{q} \end{aligned} \tag{6.55}$$

The complexity of choosing $\bar{q}$ now reduces from a combinatorial complexity to a linear complexity.

The Lagrange multiplier λ can be updated using following formula

$$\lambda \Leftarrow [\lambda - \mu(C_{\text{budget}} - \sum_{k=1}^{K}\sum_{n=1}^{N} c_{k}^{n})]^{+} \tag{6.56}$$

where μ is a positive scaling factor, whose value can be changed in order to obtain a faster convergence to the solution. For simplicity, in our simulations μ is taken as a fixed arbitrary value close to zero.

Algorithm 6.6 Selection metric based MMSE-GDFE partial crosstalk cancellation tap allocation

initialize $\tilde{b}_k^n(\bar{q})$, λ, $\mathcal{L}_{k,opt}^n = 0$
while $C \neq C_{budget}$ **do**
  for tone $k = 1 \cdots K$ **do**
    for line $n = 1 \cdots N$ **do**
      compute metric $\mathcal{I}_{k,4}^n$
      order the interferers based on $\mathcal{I}_{k,4}^n$ and the combination is stored in $\mathcal{M}_k^n$
      for number of crosstalkers to be cancelled $\bar{q} = 1 \cdots N-1$ **do**
        compute $\mathbf{w}_{ff,k}^n$ and $\mathbf{w}_{fb,k}^n$ for $\bar{q}$ interferers with indices in $m(\bar{q}) \in \mathcal{M}_k^n$
        $\mathcal{L}_{k,opt}^n = \tilde{b}_k^n(\bar{q}) - \lambda\bar{q}$
        if $\mathcal{L}_k^n > \mathcal{L}_{k,opt}^n$ **then**
          $\mathcal{L}_{k,opt}^n = \mathcal{L}_k^n$
          $\mathbf{w}_{ff,k,opt}^n = \mathbf{w}_{ff,k}^n$
          $\mathbf{w}_{fb,k,opt}^n = \mathbf{w}_{fb,k}^n$
          $\bar{q}_{k,opt}^n = \bar{q}$
        end if
      end for
    end for
  end for
  compute $C = \sum_k \sum_n \bar{q}_{k,opt}^n$
  update $\lambda = [\lambda - \mu(C_{budget} - C)]^+$
end while

6.7.2 Joint partial crosstalk cancellation and spectrum balancing

Selection metric based joint partial crosstalk canceler and power allocation

The joint partial crosstalk cancellation and transmit power allocation problem in MMSE-GDFE based DMT receiver can be written as

$$\begin{aligned}
&\text{For } k = 1 \cdots K \\
&\text{For } n = 1 \cdots N \\
&\text{For } s_k^n = 0 \cdots s_k^{n,max} \\
&\text{For } q_k^n = 1 \cdots N-1 \\
&\max_{\mathbf{c}_k, \mathbf{s}_k} \quad \tilde{b}_k^n - \lambda_n q_k^n - \gamma_n s_k^n \\
&\quad \text{subject to} \quad \lambda_m \geq 0 \quad m = 1 \cdots \tilde{N} \\
&\qquad\qquad\qquad\quad \gamma_n \geq 0 \quad n = 1 \cdots N.
\end{aligned} \tag{6.57}$$

The complexity of choosing $\bar{q}$ now reduces from the combinatorial complexity to linear complexity.

And the Lagrange multiplier λ can be updated as

$$\lambda \Leftarrow [\lambda - \mu(C_{\text{budget}} - \sum_{k \in \mathcal{K}}^{K} \sum_{n=1}^{N} c_{ij})]^+ \tag{6.58}$$

where μ is a scaling factor, whose value can be changed in order to obtain a faster convergence to the solution. For simplicity, in our simulations μ is taken as a fixed arbitrary value close to zero. For further details of the algorithm we refer to [154].

6.8 Simulation results

Simulations were run for a scenario with 7 lines ranging from 600m to 1200m in 100m increments and an alien crosstalk line of 500m. The direct channels, the crosstalk channels and the alien crosstalk channel are generated using the analytical and semi-analytical model in [52]. The simulation parameters are summarized in **Table** 6.1.

The maximum number of taps that can be allocated to the linear MMSE canceler is $N \times (N-1) \times$ number of used tones. Here $N = 7$ and the number of used tones

Algorithm 6.7 Selection metric based joint MMSE-GDFE partial crosstalk cancellation tap allocation and spectrum balancing

initialize $\tilde{b}_k^n(\bar{q})$, $\mathbf{s}_k$, λ, γ_n, $s_{k,opt}^n$, $\mathbf{L}_{k,opt}^n$
while $C \neq C_{budget}$ **do**
  for tone $k = 1 \cdots K$ **do**
    for line $n = 1 \cdots N$ **do**
      for transmit power $s_k^n = 0 \cdots s_k^{n,max}$ **do**
        compute metric $\mathcal{I}_{k,4}^n$
        update the nth entry of vector $\mathbf{s}_k$ as $\mathbf{s}_k[n] = s_k^n$
        for the number of interferers to be cancelled $\bar{q}_k^n = 1 \cdots N-1$ **do**
          compute $\mathbf{w}_{ff,k}^n$ using (6.14) and updated s_k^n and $\bar{q}_k^n$
          $\mathcal{L}_k^n = \tilde{b}_k^n(\bar{q}_k^n) - \lambda \bar{q}_k^n$
          if $\mathcal{L}_k^n > \mathcal{L}_{k,opt}^n$ **then**
            $\mathcal{L}_{k,opt}^n = \mathcal{L}_k^n$
            $s_{k,opt}^n = s_k^n$
            $\mathbf{w}_{ff,k,opt}^n = \mathbf{w}_{ff,k}^n$
            $\mathbf{w}_{ff,k,opt}^n = \mathbf{w}_{ff,k}^n$
            $\bar{q}_{k,opt}^n = \bar{q}_k^n$
          end if
        end for
      end for
    end for
  end for
  compute $C = \sum_{k=1}^K \sum_{n=1}^N \bar{q}_{k,opt}^n$
  compute $S = \sum_{k=1}^K \bar{s}_k^n$
  update $\lambda = [\lambda^t - \mu(C_{budget} - C)]^+$
  update $\gamma_n = [\gamma_n^t + \mu(S - S_{budget}^n)]^+$ for all $n = 1 \cdots N$
end while

Table 6.1: Simulation Parameters

Number of DMT tones	4096
Tone width	4.3125 kHz
symbol rate	4 kHz
Coding gain	3 dB
Noise margin	6 dB
Symbol error probability	$< 10^{-7}$
Transmit PSD	Flat (-60 dBm/Hz)
FDD band plan	998
Cable type	0.5 mm

is 1147 hence the C_{budget}^{max} is 48174. With the additional lower triangular feedback section the C_{budget}^{max} in the case of MMSE-GDFE is 72261.

In the first scenario, we consider a fixed power loading linear MMSE based crosstalk cancellation scheme. In **Figure 6.4**, we compare various crosstalk canceler selection schemes based on selection metric given in (6.33), (6.34) and (6.36) and the exhaustive search over all the canceler taps. The result demonstrates that the selection metric which takes both in-domain crosstalk and the background noise information into account perform close to the performance of the exhaustive search based approach. From **Figure** 6.3 (b), it was shown that linear ZF canceler performs poorly in the presence of spatially correlated background noise, therefore the performance is not compared.

In **Figure** 6.5, we then compare the selection metric based approach to the sparse approximation based approach presented in section 6.6.1, for a fixed power loading scenario. It can be seen that the sparse approximation based approach also performs close to the exhaustive search based approach.

In the joint spectrum balancing and partial crosstalk cancellation scenario, it can be seen that the achievable bit-rate increase at both no crosstalk cancellation and full crosstalk cancellation scenario. This due to the fact that the by reducing the power transmitted in the shorter line the crosstalk longer lines is reduced. Furthermore, the lower SNR on the shorter line also help to cancel alien crosstalk in the longer loop more effectively.

In **Figure 6.6**, we compare the performance of the selection metric based approach and sparse approximation based approach combined with the spectrum balancing. This is then compared with the iterative spectrum balancing (ISB) approach with partial crosstalk cancellation. This is a suboptimal algorithm but it was shown to perform very close to optimal spectrum balancing in [155] with much reduced computational complexity. It can be seen that the the selection metric based joint partial crosstalk cancellation and spectrum balancing performs close to the ISB. Similarly we can see that sparse approximation based joint partial crosstalk cancellation and spectrum balancing also performs close to the performance of ISB and selection metric based approach but it has much lower computational complexity that the selection metric based approach.

In the next scenario, a MMSE-GDFE based crosstalk canceler was considered. In **Figure 6.7**, it can be seen that the full crosstalk cancellation using MMSE-GDFE requires higher number of canceler taps but achieves higher bit-rate. In **Figure 6.7**, we then compare the exhaustive search based partial crosstalk canceler selection with the selection metric based crosstalk canceler selection for a fixed power loading. It is seen that the selection metric based crosstalk canceler tap selection performs close to the exhaustive search based approach. In **Figure 6.8**, we compare the selection metric based method and exhaustive search based approach for joint partial crosstalk cancellation and spectrum balancing. It can be

seen that the selection metric based partial crosstalk cancellation scheme performs close to the exhaustive search based approach.

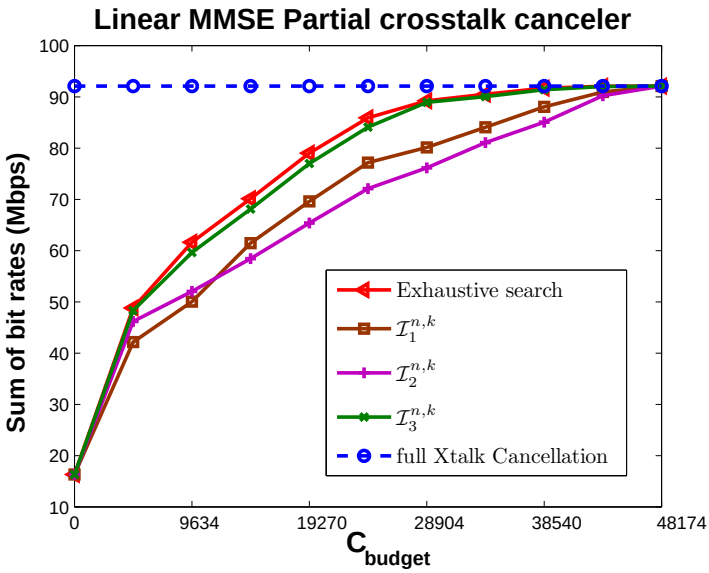


Figure 6.4: Performance comparison of the different metrics for partial cancellation using a linear MMSE canceler

6.9 Conclusion

In this chapter, we have considered crosstalk cancellation in upstream VDSL, where receivers are co-located, in the presence of spatially correlated background noise such as alien crosstalk . It is shown that the MMSE based crosstalk canceler perform significantly better than a linear ZF based canceler in this scenario. It is shown full crosstalk cancellation scheme has a run-time complexity of $\mathcal{O}(N^2)$, therefore for a large number of lines the run-time complexity might be prohibitive. Previously, it had been shown that, for a system with only AWGN background noise and linear ZF canceler, the run-time complexity might be reduced by selectively canceling only few significant crosstalker on each tone. This is known as partial crosstalk cancellation. In this chapter, this technique was extended to include MMSE-based crosstalk cancelers.

It is shown that in the case of linear MMSE crosstalk canceler and a fixed power loading, the combinatorial search over all the crosstalkers can be reduce to linear search by ordering the interferers based on some selection metric. Similarly the

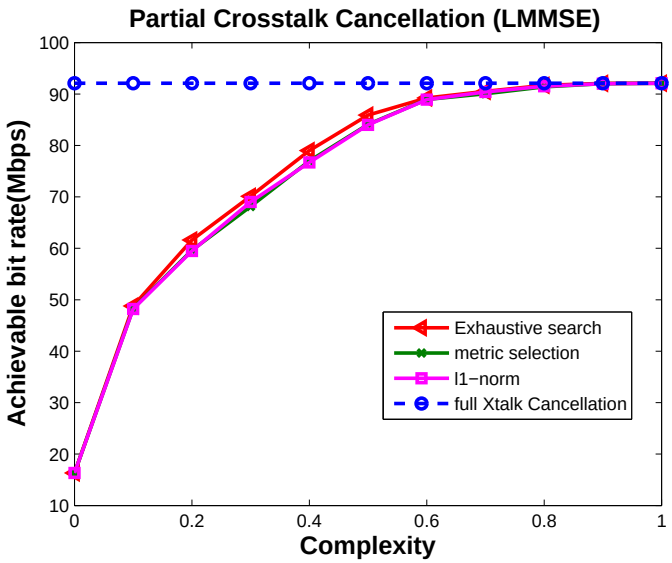


Figure 6.5: Performance comparison of the different metrics for partial cancellation using a linear MMSE canceler

crosstalk canceler selection can be simplified by directly designing sparse linear MMSE crosstalk cancelers. These methods are shown to achieve performance close to the exhaustive search based crosstalk canceler selection. Furthermore, it is shown that the achievable rate increases if spectrum balancing is performed alongside crosstalk cancellation. In order to reduce the overall complexity of the joint partial cancellation and spectrum balancing on linear MMSE based systems, the selection metric based approach was used alongside iterative spectrum balancing. It was shown that the sparse approximation based partial crosstalk cancellation further reduces the overall search complexity. These methods are shown to achieve performance close to the performance of exhaustive search based approach.

The selection metric based approach is then simply extended to accommodate MMSE-GDFE based crosstalk cancellation scheme. It is shown that the MMSE-GDFE based crosstalk cancellation achieve higher data rate but at higher run-time complexity. The selection metric based approach then used to reduce the overall complexity of partial crosstalk canceler tap selection. It was shown that selection metric based crosstalk cancellation selection approaches the performance of exhaustive search based approach. Furthermore, the approach is then extended to perform partial crosstalk cancellation with spectrum balancing. It is shown that selection metric based approach alongside ISB performs very close to exhaustive

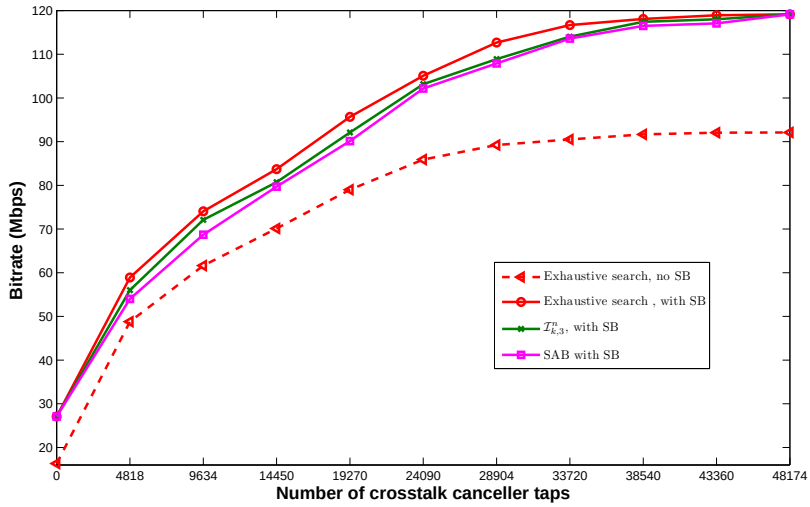


Figure 6.6: Performance comparison of the different metrics for partial cancellation using a linear MMSE canceler

search based crosstalk cancellation scheme with ISB.

It was also shown that for the same number of crosstalk cancelers MMSE-GDFE based crosstalk cancellation outperforms linear MMSE based crosstalk cancellation.

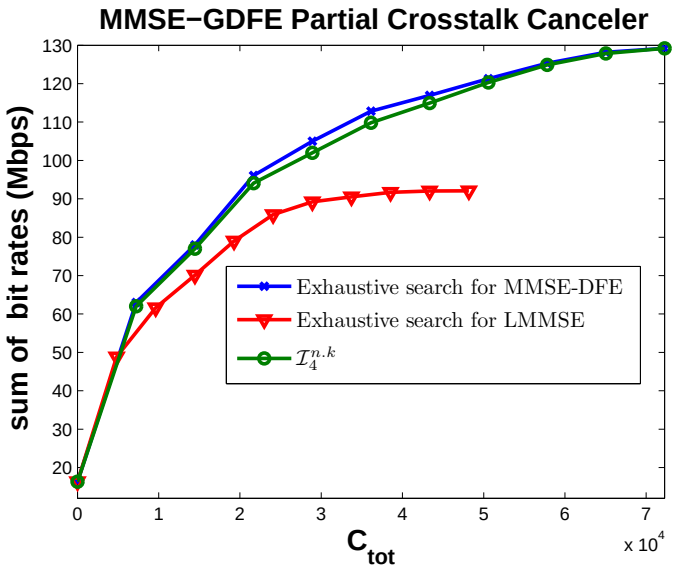


Figure 6.7: Comparison between the optimum linear MMSE partial cancellation and the MMSE-GDFE partial cancellation

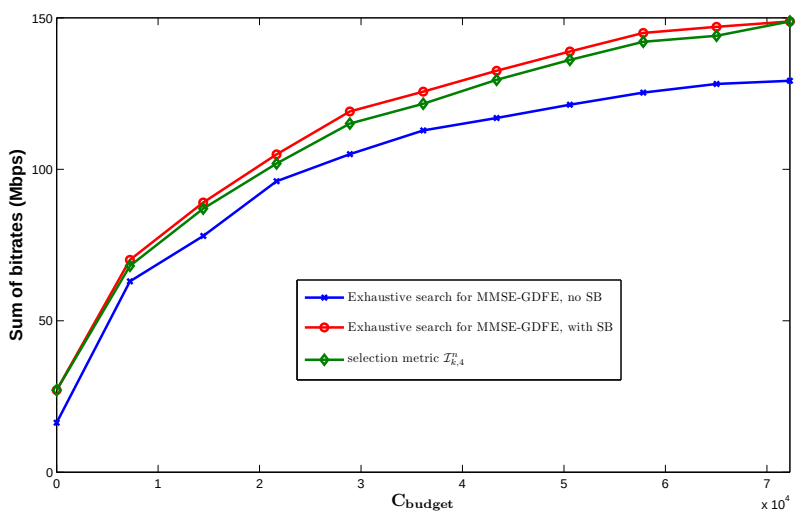


Figure 6.8: Comparison between the optimum linear MMSE partial cancellation and the MMSE-GDFE partial cancellation

Chapter 7

Conclusions and Future Work

In this chapter we will highlight the main conclusions and list some suggestions for the future works.

7.1 Conclusions

The channel impairments such as ISI, crosstalks etc., have a large impact on the achievable bit-rate of the DMT system. Furthermore, achievable bit-rate is reduced by nulling certain carriers at the band edges in order to comply with the PSD mask constraints. In order to combat these effects, several signal processing techniques have been proposed. However, the use of sophisticated signal processing techniques increases the run-time computational complexity. In some cases, the prohibitive computational complexity renders the signal processing algorithm impractical.

The DSL channel is a slowly time-varying channel. This provides us with the opportunity to optimize the signal processing algorithms used to mitigate various non-ideal effects in the DMT transceiver. This dissertation focuses on reducing the run-time computational complexity of various signal processing blocks used in the DMT transceiver by exploiting various characteristics of the DSL channel in both the single-user and the multi-user scenario. The main goals of this thesis are

- to design low complexity resource allocation algorithms with near optimal performance in the single-user DSL scenario
- to design low complexity resource allocation algorithm without compromising the performance in the multi-user DSL scenario

This dissertation was divided into two parts: **Part I** focused on various run-time computational complexity reduction techniques in the single-user DSL scenario. Specific scenario of a per-tone pulse shaping DMT transmitter and a per-tone equalization based DMT receiver has been considered. In **Part II**, we investigated the resource allocation algorithms in the multi-user DSL scenario in the presence of alien crosstalk.

In **chapter 2**, we provided introduction to various aspects of a DSL system. All the important building blocks of a DSL transceiver were explained. A brief overview of different modulation schemes considered for the DSL system was introduced and the motivation for using the multicarrier modulation was then presented. A mathematical model of a DMT based system was also introduced and the DMT based transmitter and receiver structures were then described. Various techniques to increase the capacity of the DMT system, such as bit loading and power loading were also discussed in detail. Various channel impairments present in the DSL system were then presented. In the end, techniques such as time domain equalization and per-tone based equalization to mitigate the effect of channel impairments were introduced. The effect of crosstalk in the case of multi-user DSL scenario was discussed and then a simple multi-user channel modeling technique was presented. Various techniques to optimize the transmission in this scenario were also discussed in order to either avoid the crosstalk or to cancel it. At the end, various receiver structures that are generally used to cancel the effect of crosstalk were presented.

In **chapter 3**, it was shown that the use of the per-tone pulse shaping filters reduces the number of virtual carriers on the band edges, thus increasing the achievable bit-rate of the DMT system. Furthermore, it was also shown that using a constant length non-sparse pulse shaping filter on every tone unnecessarily increases the run-time complexity of the system. This motivates the use of variably sparse pulse shaping filter on each tone. But the constrained optimization problem to optimally allocate the non-zero per-tone pulse shaping filter was shown to be coupled in tones. Furthermore, computation of a sparse per-tone pulse shaping filter was also shown to be a combinatorial problem. We showed that a dual problem formulation leads to an unconstrained optimization problem that is decoupled over tones, but the sparse filter design problem still remains a combinatorial problem. In order to reduce this combinatorial complexity of filter design, some simple techniques were presented. Firstly, the restriction on the sparsity pattern of the filter allowing only contiguous taps to be non-zero was shown to reduce the combinatorial complexity to a linear search in filter order, thereby reducing the the overall complexity of the filter tap selection problem. But the restriction in sparsity pattern of the pulse shaping filter may not be the best approach, since the best sparsity pattern may not lie in the restricted sparsity set. Secondly, it was shown that a sparse approximation based approach with convex relaxation allows design of sparse pulse shaping filter without imposing

any restriction on the sparsity pattern of the pulse shaping filter with similar complexity as the linear search over the filter order. Furthermore, these techniques were also extended to jointly allocate pulse shaping filter taps and the transmit power. It was shown that these techniques reduce the run-time complexity significantly without affecting the performance much. Furthermore, it was shown that when combined with a transmit power loading algorithm these approaches can further reduce the number of per-tone pulse shaping filter taps needed to achieve the same bit-rate performance.

In **chapter 4**, we showed that the use of the MMSE-PTEQ increases the achievable bit-rate of the DMT system. Furthermore, it was also shown that using a constant length non-sparse MMSE-PTEQ filter on every tone unnecessarily increases the run-time complexity of the DMT system. Therefore, using variably sparse MMSE-PTEQ filter on each tone reduces the run-time complexity without affecting the performance significantly. The constrained optimization problem to allocate the non-zero MMSE-PTEQ taps was shown to be coupled in tones. To this end, for a constant transmit power , we have proposed efficient resource allocation algorithms to distribute the available resources (total transmit power budget and total MMSE-PTEQ filter tap budget) over tones in a DMT receiver with per-tone equalization. We have shown that a dual problem formulation leads to an unconstrained optimization problem that is decoupled in tones but due to the combinatorial nature of the filter tap allocation the resulting optimization problem is still NP hard in general. Two approaches were proposed to further simplify the problem. The first approach restricted only contiguous MMSE-PTEQ taps to be non-zero hence the combinatorial search in the sparsity pattern is reduced to the linear search in filter order. The second approach used sparse approximation technique to design the MMSE-PTEQ filter. Using convex relaxation of the sparsity constraints, the sparse filter design problem can be written as convex problem and solved efficiently. Furthermore, the techniques were also extended to jointly allocate MMSE-PTEQ filter taps and the transmit power. A VDSL simulation demonstrated that under a fixed power loading, the number of MMSE-PTEQ filter taps can be reduced significantly compared to the fixed length non-sparse case without sacrificing much performance. Furthermore, it was also shown that the sparse approximation based MMSE-PTEQ filter tap allocation approach performs better than the contiguous tap selection based approach. When combined with a transmit power loading algorithm these approaches can further reduce the number of per-tone pulse shaping filter taps needed to achieve the same bit-rate performance.

In **chapter 5**, a per-tone pulse shaping and a per-tone equalizer based DMT transceiver is considered. It is first shown that the presence of per-tone pulse shaping filter affects the tap allocation in the per-tone equalization based receiver under a constant transmit power loading. It was shown that the joint filter tap optimization problem in the DMT transceiver could be decoupled in tone by

formulating as a dual problem along with an iterative MMSE-PTEQ computation scheme. It can be seen that the achievable rate for the same number of taps is lower in the presence of a per-tone pulse shaping filter. This is due to the fact that the pulse shaping filter act as a dispersive channel and hence lengthens the output of the transmitter. In our case, we do not increase the overall symbol length, but decrease the effective cyclic prefix to accommodate the extra symbol, therefore better per-tone equalizers are needed to mitigate the effects. Similarly in the case of the joint filter tap and transmit power allocation in the DMT transceiver, it can be seen that since the signal-to noise ratio at the output receiver is fed back to the transmitter, the effect such as filtering effect at the edge of the bands at the receiver is also taken into account while performing transmit power allocation at the transmitter side. This improves the performance of the system for the same number of non-zero filter taps.

In **chapter 6**, we have considered crosstalk cancellation in upstream VDSL, where receivers are co-located, in the presence of spatially correlated background noise such as alien crosstalk . It is shown that the MMSE based crosstalk canceler perform significantly better than a linear ZF based canceler in this scenario. It is shown full crosstalk cancellation scheme has a run-time complexity of $\mathcal{O}(N^2)$, therefore for a large number of lines the run-time complexity might be prohibitive. Previously it had been shown that for a system with only AWGN background noise and a linear ZF canceler, the run-time complexity might be reduced by selectively canceling only few significant crosstalker on each tone. This is known as partial crosstalk cancellation. In this chapter, this technique was extended to include the MMSE-based crosstalk cancelers. It is shown that in the case of the linear MMSE crosstalk canceler and constant powerloading, the combinatorial search over all the crosstalkers can be reduce to linear search by ordering the interferers based on some selection metric. Similarly the crosstalk canceler selection can be simplified by directly designing sparse linear MMSE crosstalk cancelers. These methods are shown to achieve performance close to the exhaustive search based crosstalk canceler selection. Furthermore, it is shown that the achievable rate increases if spectrum balancing is performed alongside crosstalk cancellation. In order to reduce the overall complexity of the joint partial cancellation and spectrum balancing on linear MMSE based systems, the selection metric based approach was used alongside iterative spectrum balancing. It was shown that the sparse approximation based partial crosstalk cancellation further reduces the overall search complexity. These methods are shown to achieve performance close to the performance of an exhaustive search based approach.The selection metric based approach is then simply extended to accommodate MMSE-GDFE based crosstalk cancellation scheme. It is shown that the MMSE-GDFE based crosstalk cancellation achieve higher data rate but incurs a higher run-time complexity. The selection metric based approach then used to reduce the overall complexity of partial crosstalk canceler tap selection. It was shown that selection metric based crosstalk cancellation selection approaches the performance

of exhaustive search based approach. Furthermore, the approach is then extended to perform partial crosstalk cancellation with spectrum balancing. It is shown that selection metric based approach alongside iterative spectrum balancing performs very close to exhaustive search based crosstalk cancellation scheme with iterative spectrum balancing. It was also shown that for the same number of crosstalk cancelers MMSE-GDFE based crosstalk cancellation outperforms linear MMSE based crosstalk cancellation.

7.2 Future Work

Initialization complexity reduction

In this dissertation, the main focus was to reduce the run-time complexity of the signal processing blocks. But the number of filter taps to be initialized is still quite high. Therefore, better and efficient initialization schemes are desired. In [2], initialization complexity reduction based on tone grouping is presented, but it is not really applicable to the sparse filters. Therefore, efficient filter coefficient initialization schemes for variably sparse filters needs to be investigated in depth.

Effect of channel estimation error

In this dissertation, in the case of a multi-user DSL scenario, the crosstalk channels and the noise correlation matrices are assumed to be perfectly known. But, practical estimation techniques have inherent estimation errors. The MMSE based cancelers rely on accurate estimation of crosstalk channels and the noise correlation. Therefore, it is important to investigate the effect of such errors in the performance of the DSL system. Furthermore, more reliable channel and noise correlation estimation techniques need to be investigated.

Efficient computation of MMSE canceler coefficients

In the case of a multi-user DSL, it is shown that in the vectored DSL lines, whenever the transmit power of a line changes or a line joins or leaves of vectored group, the full MMSE coefficients have to be recomputed. This adds extra computational complexity. In order to reduce this computational complexity, a simplified MMSE canceler computation scheme is needed. Since the noise covariance changes with respect to which lines are taken into account, a simple matrix inversion lemma based recursive update is not possible.

Dynamic crosslayer partial crosstalk cancellation

In this dissertation, We optimized the resources only with respect to achievable bit-rate. But it has been shown in [89] that this can be extended to include crosslayer objectives, which are more related to user experience, QoS and are more meaningful to the end users.

Stability of the DSL system

In this dissertation, the lines in vectored DSL was considered to be static, i.e., it remains in the vectored group for ever. But in practice, the lines continuously join and leave the vectored DSL system. This may create instability in the DSL system. Therefore, the impact of the dynamical entry and exit if the lines in a DSL system has to be analyzed, And the impact in the initialization as well as run-time complexity of the MMSE based cancelers has to be investigated.

Partial crosstalk precoding

In this dissertation, we have only investigated upstream VDSL scenario. The receiver was assumed to be co-located. Similar approaches may be possible in the downstream scenario, where all the transmitters are co-located. An optimum precoding structure in the presence of AWGN background noise was presented in [26]. It might be interesting to extend this idea in the presence of spatially correlated background noise.

Bibliography

[1] K. Van Acker. *Equalization and echo cancellation for DMT-based DSL modems*. PhD Thesis, Department of Electrical Engineering, Katholieke Universiteit Leuven, Belgium, Jan 2001.

[2] K. Van Acker, G. Leus, M. Moonen, O. Van de Wiel, and T. Pollet. Per tone equalization for DMT-based systems. *Communications, IEEE Transactions on*, 49:109–119, January 2001.

[3] A.N. Akansu, P. Duhamel, Lin Xueming, and M. de Courville. Orthogonal transmultiplexers in communication: a review. *Signal Processing, IEEE Transactions on*, 46(4):979 –995, April 1998.

[4] A.N. Akansu and L. Xueming. A comparative performance evaluation of dmt (ofdm) and dwmt (dsbmt) based dsl communications systems for single and multitone interference. In *Acoustics, Speech and Signal Processing, 1998. Proceedings of the 1998 IEEE International Conference on*, volume 6, pages 3269 –3272, May 1998.

[5] N. Al-Dhahir and J.M. Cioffi. Fast computation of channel-estimate based equalizers in packet data transmission. *Signal Processing, IEEE Transactions on*, 43(11):2462 –2473, November 1995.

[6] N. Al-Dhahir and J.M. Cioffi. Efficient computation of the delay-optimized finite length mmse-dfe. *Signal Processing, IEEE Transactions on*, 44(5):1288 –1292, May 1996.

[7] N. Al-Dhahir and J.M. Cioffi. Efficiently computed reduced-parameter input-aided mmse equalizers for ml detection: a unified approach. *Information Theory, IEEE Transactions on*, 42(3):903 –915, May 1996.

[8] N. Al-Dhahir and J.M. Cioffi. Optimum finite-length equalization for multicarrier transceivers. *Communications, IEEE Transactions on*, 44:56–64, 1996.

[9] N. Al-Dhahir and J.M. Cioffi. A bandwidth-optimized reduced-complexity equalized multicarrier transceiver. *Communications, IEEE Transactions on*, 45(8):948 –956, August 1997.

[10] ANSI. Interface between networks and customer installations: very-high speed digital subscriber lines (VDSL). *ANSI T1E1.4/2002-031R2*, 2002.

[11] ANSI. Spectrum management for loop transmission systems. *ANSI T1.417, Issue 2*, 2003.

[12] S. Ariyavisitakul and L.J. Greenstein. Reduced-complexity equalization techniques for broadband wireless channels. *Selected Areas in Communications, IEEE Journal on*, 15(1):5 –15, January 1997.

[13] E. Baccarelli, A. Fasano, and M. Biagi. Novel efficient bit-loading algorithms for peak-energy-limited adsl-type multicarrier systems. *Signal Processing, IEEE Transactions on*, 50(5):1237 –1247, May 2002.

[14] R. Baldemair. Suppression of narrow frequency bands in multicarrier transmission systems. *in Proc. European Signal Processing Conf. EUSIPCO 2000, Tampere, Finland*, pages 553–556, Sept. 2000.

[15] M. Barton, L. Chang, and T.R. Hsing. Performance study of high-speed asymmetric digital subscriber lines technology. *Communications, IEEE Transactions on*, 44(2):156 –157, February 1996.

[16] A.G. Bell. Improvement in telegraphy. Letters Patent No. 174,465, 7 March 1876. Application filed on 14 February 1876.

[17] J. Bingham and M. Mallory. RFI egress supression for SDMT. *ANSI Contribution T1E1.4/96-085*, 1996.

[18] J.A.C. Bingham. Multicarrier modulation for data transmission: An idea whose time has come. *Communications Magazine, IEEE*, 28:5–14, May 1990.

[19] John A. C. Bingham. *ADSL, VDSL, and multicarrier modulation.* John Wiley & Sons, Hoboken, NJ, USA, 2000.

[20] P. Biyani, A. Mahadevan, P. Duvaut, and S. Singh. Cooperative mimo for alien noise cancellation in upstream vdsl. In *Acoustics, Speech and Signal Processing, 2009. ICASSP 2009. IEEE International Conference on*, pages 2645 –2648, 2009.

[21] R.S. Blum. Mimo capacity with interference. *Selected Areas in Communications, IEEE Journal on*, 21(5):793 – 801, 2003.

[22] H. Bolcskei, P. Duhamel, and R. Hleiss. Design of pulse shaping ofdm/oqam systems for high data-rate transmission over wireless channels. In *Communications, 1999. ICC '99. 1999 IEEE International Conference on*, 1999.

[23] B. Borna and T.N. Davidson. Efficient filter bank design for filtered multitone modulation. In *Communications, 2004 IEEE International Conference on*, volume 1, pages 38 – 42, 2004.

[24] S. Boyd and L. Vandenberghe. *Convex Optimization*. Cambridge University Press, New York, NY, USA, 2004.

[25] R. Cendrillon, G. Ginis, E. Van den Bogaert, and M. Moonen. A near-optimal linear crosstalk canceler for upstream VDSL. *Signal Processing, IEEE Transactions on*, 54(8):3136 –3146, 2006.

[26] R. Cendrillon, G. Ginis, E. Van den Bogaert, and M. Moonen. A near-optimal linear crosstalk precoder for downstream VDSL. *Communications, IEEE Transactions on*, 55(5):860 –863, May 2007.

[27] R. Cendrillon, M. Moonen, G. Ginis, K. Van Acker, T. Bostoen, and P. Vandaele. Partial crosstalk cancellation for upstream vdsl. *Applied Signal Processing, EURASIP Journal on*, 2004(10):1520–1535, 2004.

[28] R. Cendrillon, M. Moonen, R. Suciu, and G. Ginis. Simplified power allocation and tx/rx structure for mimo-dsl. In *Global Telecommunications Conference, 2003. GLOBECOM '03. IEEE*, volume 4, pages 1842 – 1846 vol.4, 2003.

[29] R. Cendrillon, M. Moonen, J. Verlinden, T. Bostoen, and W. Yu. Optimal multi-user spectrum management for digital subscriber lines. In *Proc. IEEE ICC*, Paris, France, 2004.

[30] R. Cendrillon, Wei Yu, M. Moonen, J. Verlinden, and T. Bostoen. Optimal multiuser spectrum balancing for digital subscriber lines. *Communications, IEEE Transactions on*, 54(5):922 – 933, May 2006.

[31] R. Chang. Synthesis of band-limited orthogonal signals for multichannel data transmission. *Bell System Tech., Journal*, 45:1775 –1796, 1966.

[32] R. Chang and R. Gibby. A theoretical study of performance of an orthogonal multiplexing data transmission scheme. *Communication Technology, IEEE Transactions on*, 16(4):529 –540, 1968.

[33] C-Y. Chen and S-M. Phoong. Per tone shaping filters for DMT transmitters. *Acoustics, Speech, and Signal Processing, 2004. Proceedings. (ICASSP '04). IEEE International Conference on*, 4:iv–1061–4 vol.4, 17-21 May 2004.

[34] G. Cherubini, E. Eleftheriou, and S. Ölçer. Filtered multitone modulation for very high-speed digital subscriber lines. *Selected Areas in Communications, IEEE Journal on*, 20(5):1016 –1028, June 2002.

[35] G. Cherubini, E. Eleftheriou, S. Ölçer, and J.M. Cioffi. Filter bank modulation techniques for very high speed digital subscriber lines. *Communications Magazine, IEEE*, 38(5):98 –104, May 2000.

[36] J.S. Chow, J.C. Tu, and J.M. Cioffi. A discrete multitone transceiver system for hdsl applications. *Selected Areas in Communications, IEEE Journal on*, 9(6):895 –908, August 1991.

[37] P.S. Chow, J.M. Cioffi, and J.A.C. Bingham. A practical discrete multitone transceiver loading algorithm for data transmission over spectrally shaped channels. *Communications, IEEE Transactions on*, 43(234):773 –775, 1995.

[38] P.S. Chow, J.C. Tu, and J.M. Cioffi. Performance evaluation of a multichannel transceiver system for adsl and vhdsl services. *Selected Areas in Communications, IEEE Journal on*, 9(6):909 –919, August 1991.

[39] J. Cioffi, W. Yu, G. Ginis, Zheng S, F. Sjoberg, and R. Nilsson. Robust VDSL in the presence of bridged taps. Tech. Rep. NT-039, ITU-SG15, Nashville, Tennessee, November 1999.

[40] J. M. Cioffi. *Advanced digital communication, class reader, EE379C*. Stanford University, 2005.

[41] J.M. Cioffi. A multicarrier primer. *T1E1.4 contribution number 91-157*, 1991.

[42] J.M. Cioffi and M. Mohseni. Dynamic spectrum management- A methodology for providing significantly higher broadband capacity to the users. *Teletronikk*, 4, 2004.

[43] J.M. Cioffi, V. Oksman, J. J. Werner, T. Pollet, P.M.P. Spruyt, J.S. Chow, and K.S. Jacobsen. Very-high-speed digital subscriber lines. *Communications Magazine, IEEE*, 37(4):72 –79, April 1999.

[44] J.M. Cioffi, P. Silverman, and T. Starr. *Understanding Digital subscriber line technology*. Prentice Hall, first edition, 1999.

[45] J. Cook. Wideband impulsive noise survey of the access network. *BT Technol. Journal*, 11:155 –162, 1993.

[46] J.W. Cook, R.H. Kirkby, M.G. Booth, K.T. Foster, D.E.A. Clarke, and G. Young. The noise and crosstalk environment for ADSL and VDSL systems. *Communications Magazine, IEEE*, 37(5):73 –78, May 1999.

[47] G. Cuypers, K. Vanbleu, G. Ysebaert, and M. Moonen. Egress reduction by intra-symbol windowing in DMT-based transmitters. In *Acoustics, Speech, and Signal Processing, 2003. Proceedings. (ICASSP '03). 2003 IEEE International Conference on*, volume 4, pages IV – 532–5 vol.4, 2003.

[48] G. Cuypers, K. Vanbleu, G. Ysebaert, M. Moonen, and P. Vandaele. Combining raised cosine windowing and per tone equalization for RFI mitigation in dmt receivers. In *Communications, 2003. ICC '03. IEEE International Conference on*, volume 4, pages 2852 – 2856 vol.4, May 2003.

[49] D. L. Donoho, M. Elad, and V. N. Temlyakov. Stable recovery of sparse overcomplete representations in the presence of noise. 52:6–18, January 2006.

[50] M. Ergen. *Mobile Broadband: Including WiMAX and LTE*. Springer Science + Business Media LLC., Spring Street, NY, USA, 2009.

[51] ETSI. Transmission and multiplexing(TM); access transmission systems on metallic access cables; very high speed digital subscriber line(VDSL);part 2: Transceiver specification. *ETSI Std. TS 101 270-2, V.0.1.0 (2000-03)*, March 2000.

[52] ETSI. Transmission and multiplexing(TM); access transmission systems on metallic access cables; very high speed digital subscriber line(VDSL);part 1:functional requirements. *ETSI Std. TS 101 270-1, Rev. V.1.3.1*, 2003.

[53] R. Fano. A theory of impulse noise in telephone networks. *Communications, IEEE Transactions on*, 25(6):577 – 588, June 1977.

[54] B. Farhang-Boroujeny and L. Lekun. Cosine modulated multitone for very high-speed digital subscriber lines. In *Acoustics, Speech, and Signal Processing, 2005. Proceedings. (ICASSP '05). IEEE International Conference on*, volume 3, pages iii/345 – iii/348, 2005.

[55] R.F.H. Fischer and J.B. Huber. Comparison of precoding schemes for digital subscriber lines. *Communications, IEEE Transactions on*, 45(3):334 –343, March 1997.

[56] G. Foschini. Crosstalk in outside plant cable systems. *Bell System Tech. Journal*, 50:2421 –2448, 1971.

[57] J.J. Fuchs. Recovery of exact sparse representations in the presence of noise. In *Acoustics, Speech, and Signal Processing, 2004. Proceedings. (ICASSP '04). IEEE International Conference on*, volume 2, pages ii – 533–6 vol.2, May 2004.

[58] A. Gibbs and R. Addie. The covariance of near end crosstalk and its application to pcm system engineering in multipair cable. *Communications, IEEE Transactions on*, 27(2):469 – 477, February 1979.

[59] G. Ginis and J.M. Cioffi. On the relation between v-blast and the gdfe. *Communications Letters, IEEE*, 5(9):364 –366, September 2001.

[60] G. Ginis and J.M. Cioffi. Vectored-DMT: a FEXT canceling modulation scheme for coordinating users. In *Communications, 2001. ICC 2001. IEEE International Conference on*, volume 1, pages 305 –309 vol.1, June 2001.

[61] G. Ginis and J.M. Cioffi. Vectored transmission for digital subscriber line systems. *Selected Areas in Communications, IEEE Journal on*, 20(5):1085 –1104, June 2002.

[62] G. Ginis and C.-N. Peng. Alien crosstalk cancellation for multipair digital subscriber line systems. *Applied Signal Processing, EURASIP Journal on*, 2006:12, 2006.

[63] P. Golden, H. Dedieu, and K.S. Jacobsen. *Implementation and Applications of DSL Technology*. Auerbach Publication, FL, USA, 2000.

[64] P. Golden, H. Dedieu, and K.S. Jacobsen. *Fundamentals of DSL Technology*. Auerbach Publication, FL, USA, 2006.

[65] W. Goralski. xDSL loop qualification and testing. *Communications Magazine, IEEE*, 37(5):79 –83, May 1999.

[66] M. Grant and S. Boyd. Graph implementations for nonsmooth convex programs. In V. Blondel, S. Boyd, and H. Kimura, editors, *Recent Advances in Learning and Control*, Lecture Notes in Control and Information Sciences, pages 95–110. Springer-Verlag Limited, 2008. `http://stanford.edu/~boyd/graph-dcp.html`.

[67] M. Grant and S. Boyd. CVX: Matlab software for disciplined convex programming, version 1.21. `http://cvxr.com/cvx`, October 2010.

[68] F.H. Gregorio, J.L. Figueroa, and J.E. Cousseau. Impulsive noise reduction in dsl using a nonlinear TEQ. In *Circuits and Systems, 2004. ISCAS '04. Proceedings of the 2004 International Symposium on*, volume 3, pages III – 353–6 Vol.3, May 2004.

[69] H. Harashima and H. Miyakawa. Matched-transmission technique for channels with intersymbol interference. *Communications, IEEE Transactions on*, 20(4):774 – 780, August 1972.

[70] J. Heiskala and J. Terry. *OFDM Wireless LANs: A Theoritical and Practical Guide*. Sams Publishing, Indianapolis, USA, 2002.

[71] W. Henkel and T. Kessler. A wideband impulse noise survey in the German telephone network: statistical description and modeling. *AEÜ*, 48:277 –288, 1994.

[72] B. Hirosaki. An analysis of automatic equalizers for orthogonally multiplexed qam systems. *Communications, IEEE Transactions on*, 28(1):73 – 83, January 1980.

[73] B. Hirosaki, S. Hasegawa, and A. Sabato. Advanced groupband data modem using orthogonally multiplexed qam technique. *Communications, IEEE Transactions on*, 34(6):587 – 592, June 1986.

[74] H. Hrasnica, A. Haidine, and R. Lehnert. *Broadband Powerline Communications: Network Design*. John Wiley & Sons, West Sussex, England, 2004.

[75] Dai Huaiyu and H.V. Poor. Crosstalk mitigation in DMT VDSL with impulse noise. *Circuits and Systems I: Fundamental Theory and Applications, IEEE Transactions on*, 48(10):1205 –1213, October 2001.

[76] Gi-Hong Im and J.-J. Werner. Bandwidth-efficient digital transmission over unshielded twisted-pair wiring. *Selected Areas in Communications, IEEE Journal on*, 13(9):1643 –1655, December 1995.

[77] H.-H. Im and J.-J. Werner. Bandwidth-efficient digital transmission up to 155 mb/s over unshielded twisted pair wiring. In *Communications, 1993. ICC 93. Geneva. Technical Program, Conference Record, IEEE International Conference on*, volume 3, pages 1797 –1803 vol.3, May 1993.

[78] M. Moonen J. Verlinden J. Vangorp, P. Tsiaflakis and G. Ysebaert. A dual decomposition aprroach to partial crosstalk cancellation in a multiuser dmt-xdsl environment. *Applied Signal Processing, EURASIP Journal on*, 2004(10):1520–1535, 2004.

[79] ITU-T Rec J.222.1. Third-generation transmission systems for interactive cable television services IP cable modems: Physical layer specification, 2007.

[80] K.S. Jacobsen. Methods of upstream power backoff on very high speed digital subscriber lines. *Communications Magazine, IEEE*, 39(3):210 –216, March 2001.

[81] G.D. Forney Jr. and M.V. Eyuboglu. Combined equalization and coding using precoding. *Communications Magazine, IEEE*, 29(12):25 –34, December 1991.

[82] I. Kalet. The multitone channel. *Communications, IEEE Transactions on*, 37(2):119 –124, February 1989.

[83] I. Kalet and S. Shamai. On the capacity of a twisted-wire pair: Gaussian model. *Communications, IEEE Transactions on*, 38(3):379 –383, March 1990.

[84] K.J. Kerpez and A.M. Gottlieb. The error performance of digital subscriber lines in the presence of impulse noise. *Communications, IEEE Transactions on*, 43(5):1902 –1905, May 1995.

[85] K.J. Kerpez and K. Sistanizadeh. High bit rate asymmetric digital communications over telephone loops. *Communications, IEEE Transactions on*, 43(6):2038 –2049, June 1995.

[86] W. Kozek and A.F. Molisch. Nonorthogonal pulseshapes for multicarrier communications in doubly dispersive channels. *Selected Areas in Communications, IEEE Journal on*, 16(8):1579–1589, Oct 1998.

[87] E.A. Lee and D.G. Messerschnitt. *Digital Communication*. Kluwer Academic Publisher, second edition, 1994.

[88] A. Leke and J.M. Cioffi. A maximum rate loading algorithm for discrete multitone modulation systems. In *Global Telecommunications Conference, 1997. GLOBECOM '97., IEEE*, volume 3, pages 1514 –1518, November 1997.

[89] B. Li, P. Tsiaflakis, M. Moonen, J. Maes, and M. Guenach. Dynamic resource allocation based partial crosstalk cancellation in dsl networks. In *GLOBECOM 2010, 2010 IEEE Global Telecommunications Conference*, pages 1 –5, dec. 2010.

[90] Y.-P. Lin and S.-M. Phoong. Window designs for DFT-based multicarrier systems. *IEEE Trans. on Signal Processing*, 53:1015–1024, March 2005.

[91] J. Maes, M. Guenach, and M. Peeters. Statistical mimo channel model for gain quantification of dsl crosstalk mitigation techniques. In *Communications, 2009. ICC '09. IEEE International Conference on*, pages 1 –5, 2009.

[92] T. Magesacher. *Common-Mode Aided Wireline Communications*. PhD Thesis, Department of Information Technology, Lund University, Sweden, ISBN 91-7167-041-6, ISRN LUTEDX/TEIT-06/1037-SE, September 2006.

[93] T. Magesacher. Optimal intra-symbol transmit windowing for multicarrier modulation. *in Proc. Intl. Symp. on Communications, Control and Signal Processing ISCCSP 2006, Marrakech, Morocco*, March 2006.

[94] T. Magesacher, P. Ödling, and P. O. Börjesson. Optimal intersymbol transmit windowing for multicarrier modulation. *in Proc. Nordic Signal Processing Symp. NORSIG 2006*, June 2006.

[95] A. Mahadevan, J. Pons, and P. Duvaut. Performance and design of an impulse noise detector for OFDM systems with Reed-Solomon erasure-decoding. In *Global Telecommunications Conference, 2008. IEEE GLOBECOM 2008. IEEE*, 30 2008.

[96] K. W. Martin. Small side-lobe filter design for multitone data-communication applications. *Circuits and Systems II: Analog and Digital Signal Processing, IEEE Transactions on [see also Circuits and Systems II: Express Briefs, IEEE Transactions on]*, 45(8):1155–1161, Aug 1998.

[97] R.K. Martin, K. Vanbleu, Ming Ding, G. Ysebaert, M. Milosevic, B.L. Evans, M. Moonen, and C.R. Johnson. Implementation complexity and communication performance tradeoffs in discrete multitone modulation equalizers. *Signal Processing, IEEE Transactions on*, 54(8):3216 –3230, 2006.

[98] R.K. Martin, K. Vanbleu, Ming Ding, G. Ysebaert, M. Milosevic, B.L. Evans, M. Moonen, and C.R. Johnson Jr. Unification and evaluation of equalization structures and design algorithms for discrete multitone modulation systems. *Signal Processing, IEEE Transactions on*, 53(10):3880 – 3894, 2005.

[99] R.K. Martin, G. Ysebaert, and K. Vanbleu. Bit error rate minimizing channel shortening equalizers for cyclic prefixed systems. *Signal Processing, IEEE Transactions on*, 55(6):2605 –2616, 2007.

[100] D.G. Mestdagh, M.R. Isaksson, and P. Odling. Zipper VDSL: A solution for robust duplex communication over telephone lines. *Communications Magazine, IEEE*, 38(5):90 –96, May 2000.

[101] A. F. Molisch. *Wideband wireless digital communications*. Prentice Hall PTR, Upper Saddle River, NJ, USA, 2000.

[102] J. Nocedal and S. Wright. *Numerical Optimization*. Springer verlag, 2006.

[103] M. Ouzzif, D. Toumpakaris, J. Cioffi, and A. Zeddam. Comparison of QAM-VDSL and DMT-VDSL in an impulse noise environment. In *Global Telecommunications Conference, 2003. GLOBECOM '03. IEEE*, volume 4, pages 2141 – 2145 vol.4, 2003.

[104] S Braet P Spruyt, P Reusens. Performance of improved DMT transceiver for VDSL. *Tech. Report T1E1.4/96-104, ANSI*, 1996.

[105] K. Pahlavan and J.L. Holsinger. Voice-band data communication modems-a historical review: 1919-1988. *Communications Magazine, IEEE*, 26(1):16 –27, January 1988.

[106] P. K. Pandey and M. Moonen. Resource allocation in ADSL variable length per-tone equalizers. *Signal Processing, IEEE Transactions on*, 56:2161–2164, May 2008.

[107] P. K. Pandey, M. Moonen, and L. Deneire. Joint transmit power and filter tap allocation in DMT transmitters with per-tone pulse shaping. In *Proc. IEEE Global Communications Conference (GLOBECOM 08)*., New Orleans, LA, USA, November 2008.

[108] P. K. Pandey, M. Moonen, and L. Deneire. Resource allocation in DMT transmitters with per-tone pulse shaping. In *Proc. IEEE International Conference on Acoustics, Speech and Signal Processing*, Las Vegas, Nevada, USA, 2008.

[109] P. K. Pandey, M. Moonen, and L. Deneire. MMSE-based partial crosstalk cancellation for upstream VDSL. In *Proc. IEEE International Conference on Communications (ICC '10)*, Cape Town, South Africa, May 2010.

[110] P. K. Pandey, M. Moonen, and L. Deneire. Joint transmit power and filter tap allocation in DMT transceivers. *to be submitted*, 2011.

[111] P. K. Pandey, M. Moonen, and L. Deneire. Sparse approximation based partial cancellation in upstream VDSL. *to be submitted*, 2011.

[112] P. K. Pandey, M. Moonen, and L. Deneire. Sparse approximation based resource allocation in DMT receivers with per-tone equalization. *to be submitted*, 2011.

[113] P. K. Pandey, M. Moonen, and L. Deneire. MMSE-based partial crosstalk cancellation for upstream VDSL. *Submitted to Signal Processing*, June 2011.

[114] P. K. Pandey, M. Moonen, and L. Deneire. Sparse approximation based resource allocation in DMT transmitters with per-tone pulse shaping. *submitted to Signal Processing*, June 2011.

[115] White Paper. Broadband technology overview. WP6321 ed. Corning, June 2005. http://www.corning.com.

[116] White Paper. VDSL2, The ideal access technology for delivering video services (Revision 2). Aware Inc., 2006. http://www.aware.com.

[117] White Paper. Optical Access. International Engineering Consortium (IEC), 2007. http://www.iec.org.

[118] Z. Papir and A. Simmonds. Competing for throughput in the local loop. *Communications Magazine, IEEE*, 37(5):61 –66, May 1999.

[119] A. Peled and A. Ruiz. Frequency domain data transmission using reduced computational complexity algorithms. In *Acoustics, Speech, and Signal Processing, IEEE International Conference on ICASSP '80.*, volume 5, pages 964 – 967, April 1980.

[120] T. Pollet, M. Peeters, M. Moonen, and L. Vandendorpe. Equalization for dmt based broadband modems. *Communications Magazine, IEEE*, 38(5):106 –113, May 2000.

[121] J.G. Proakis. *Digital Communications*. McGraw-Hill, New York, NY, USA, third edition, 1995.

[122] R. Ramaswami, K.N. Sivarajan, and G.H. Sasaki. *Optical Networks: A practical perspective*. Morgan Kaufman Publishers, Burlington, MA, USA, third edition, 2010.

[123] Bell Communications Research. NYNEX loop performance survey: Report of results. *Loop survey report, Bellcore*, 1986.

[124] W. Rhee, J.C. Chuang, and L.J. Cimini Jr. Performance comparison of OFDM and multitone with polyphase filterbank for wireless communications. *Vehicular Technology Conference, 1998. VTC 98. 48th IEEE*, 2:768–772 vol.2, 18-21 May 1998.

[125] D. Roddy. *Satellite Communications*. The Mcgraw Hill Companies Inc., NY, USA, fourth edition, 2006.

[126] A. Ruiz, J.M. Cioffi, and S. Kasturia. Discrete multiple tone modulation with coset coding for the spectrally shaped channel. *Communications, IEEE Transactions on*, 40(6):1012 –1029, June 1992.

[127] C. Salema. *Microwave Radio Links: From Theory to Design*. John Wiley & Sons, Hoboken, NJ, USA, 2002.

[128] B. Saltzberg. Performance of an efficient parallel data transmission system. *Communication Technology, IEEE Transactions on*, 15(6):805 –811, 1967.

[129] B.R. Saltzberg. Comparison of single-carrier and multitone digital modulation for adsl applications. *Communications Magazine, IEEE*, 36(11):114 –121, November 1998.

[130] J. Salz. Optimum mean-square decision feedback equalization. *Bell System Tech. Journal*, 52(9):1341 –1373, 1973.

[131] L. Sandstrom, K. Schneider, L. Joiner, and A. Wilson. Spatial correlation of alien crosstalk in MIMO DSL systems. *Communications, IEEE Transactions on*, 57(8):2269 –2271, 2009.

[132] S. Schelstraete. Defining upstream power backoff for VDSL. *Selected Areas in Communications, IEEE Journal on*, 20(5):1064 –1074, June 2002.

[133] A. Sendonaris, V.V. Veeravalli, and B. Aazhang. Joint signaling strategies for approaching the capacity of twisted-pair channels. *Communications, IEEE Transactions on*, 46(5):673 –685, May 1998.

[134] C. Shannon. A mathematical theory of communication. *Bell System Techn. Journal*, 27(5):379–423, 623–656, July and October 1948.

[135] The Samuel Morse Historic Site. http://www.lgny.org/history/morse.html.

[136] F. Sjoberg. *A VDSL tutorial*. Research report, Institutionen för Systemteknik, Avdelningen för Signalbehandling, Lulea tekniska Universitet, Sweden, ISSN 1402-1528, ISRN LTU-FR-00/02-SE, 2000.

[137] F. Sjoberg, M. Isaksson, R. Nilsson, P. Odling, S.K. Wilson, and P.O. Borjesson. Zipper: a duplex method for VDSL based on DMT. *Communications, IEEE Transactions on*, 47(8):1245 –1252, August 1999.

[138] F. Sjoberg, R. Nilsson, P.O. Borjesson, P. Odling, B. Wiese, and J.A.C. Bingham. Digital RFI suppression in DMT-based VDSL systems. *Circuits and Systems I: Regular Papers, IEEE Transactions on*, 51(11):2300 – 2312, 2004.

[139] F. Sjoberg, R. Nilsson, M. Isaksson, P. Odling, and P.O. Borjesson. Asynchronous zipper [subscriber line duplex method]. In *Communications, 1999. ICC '99. 1999 IEEE International Conference on*, 1999.

[140] N. Sloane and A. Wyner. *Claude E. Shannon(Collected Papers)*. 1993.

[141] Kee Bong Song, Seong Taek Chung, G. Ginis, and J.M. Cioffi. Dynamic spectrum management for next-generation DSL systems. *Communications Magazine, IEEE*, 40(10):101 – 109, October 2002.

[142] M. Sorbara, P. Duvaut, F. Shmulyian, S. Singh, and A. Mahadevan. Construction of a dsl-mimo channel model for evaluation of fext cancellation systems in vdsl2. In *Sarnoff Symposium, 2007 IEEE*, 30 2007.

[143] T. Starr, M. Sorbara, J.M. Cioffi, and P. Silverman. *DSL Advances*. Pearson Education, 2002.

[144] R. Stolle. Electromagnetic coupling of twisted pair cables. *Selected Areas in Communications, IEEE Journal on*, 20(5):883 –892, June 2002.

[145] G. Taubock and W. Henkel. Mimo systems in the subscriber line network. In *Fifth International OFDM Workshop, Hamburg, Germany*, pages 18.1 – 18.3, 2000.

[146] Lucent Technologies. Impact of bridged taps on VDSL performance. Tech. Rep. NT-091, ITU-SG15/Q4, Nashville, Tennessee, November 1999.

[147] W. Tiejun, J.G. Proakis, and J.R. Zeidler. Analysis of per-channel equalized filtered multitone modulations over time-varying fading channels. In *Personal, Indoor and Mobile Radio Communications, 2006 IEEE 17th International Symposium on*, pages 1–5, 2006.

[148] A. Tkacenko, P.P. Vaidyanathan, and T.Q. Nguyen. On the eigenfilter design method and its applications: a tutorial. *Circuits and Systems II: Analog and Digital Signal Processing, IEEE Transactions on [see also Circuits and Systems II: Express Briefs, IEEE Transactions on]*, 50(9):497–517, Sept. 2003.

[149] M. Tomlinson. New automatic equaliser employing modulo arithmetic. *Electronics Letters*, 7(5):138 –139, 25 1971.

[150] D. Toumpakaris, Wei Yu, J.M. Cioffi, D. Gardan, and M. Ouzzif. A simple byte-erasure method for improved impulse immunity in DSL. In *Communications, 2003. ICC '03. IEEE International Conference on*, volume 4, pages 2426 – 2430 vol.4, May 2003.

[151] J. A. Tropp. Greed is good: Algorithmic results for sparse approximation. 50:2231–2242, October 2004.

[152] J. A. Tropp. Just relax: Convex programming methods for subset selection and sparse approximation. *ICES Report 04-04*, pages 1–39, February 2004.

[153] J. A. Tropp. Just relax: Convex programming methods for identifying sparse signals in noise. 52:1030–1050, March 2006.

[154] P. Tsiaflakis, J. Vangorp, M. Moonen, J. Verlinden, and K. Van Acker. An efficient search algorithm for the lagrange multipliers of optimal spectrum balancing in multi-user xDSL systems. In *Proc. IEEE International Conference on Acoustics, Speech and Signal Processing*, Toulouse, France, May 2006.

[155] P. Tsiaflakis, J. Vangorp, J. Verlinden, and M. Moonen. Multiple access channel optimal spectrum balancing for upstream DSL transmission. *Communications Letters, IEEE*, 11(4):398 –300, 2007.

[156] A. Vahlin and N. Holte. Optimal finite duration pulses for OFDM. *Communications, IEEE Transactions on*, 44(1):10–14, Jan 1996.

[157] E. van den Berg and M. P. Friedlander. Probing the pareto frontier for basis pursuit solutions. *SIAM Journal on Scientific Computing*, 31(2):890–912, 2008.

[158] L. van der Perre, S. Thoen, P. Vandenameele, B. Gyselinckx, and M. Engels. Adaptive loading strategy for a high speed ofdm-based wlan. In *Global Telecommunications Conference, 1998. GLOBECOM 98. The Bridge to Global Integration. IEEE*, 1998.

[159] K. Vanbleu, G. Ysebaert, G. Cuypers, and M. Moonen. On time-domain and frequency-domain mmse-based teq design for dmt transmission. *Signal Processing, IEEE Transactions on*, 53(8):3311 – 3324, 2005.

[160] K. Vanbleu, G. Ysebaert, G. Cuypers, and M. Moonen. Adaptive bit rate maximizing time-domain equalizer design for dmt-based systems. *Signal Processing, IEEE Transactions on*, 54(2):483 – 498, 2006.

[161] K. Vanbleu, G. Ysebaert, G. Cuypers, M. Moonen, and K. Van Acker. Bitrate-maximizing time-domain equalizer design for dmt-based systems. *Communications, IEEE Transactions on*, 52(6):871 – 876, 2004.

[162] K. Vanbleu, G. Ysebaert, M. Moonen, and P. Vandaele. Combined equalization and alien crosstalk cancellation in ADSL receivers. In *European Signal Processing Conference 2002 (EUSIPCO 2002)*, pages 1–4, Toulouse, France, 2002.

[163] J. Vangorp, M. Moonen, M. Guenach, and M. Peeters. Downstream power backoff in CO/RT-deployed xDSL networks. *Communications, IEEE Transactions on*, 58(2):453 –456, 2010.

[164] F. Vanier. World broadband statistics: Short report, Q3 2010. Point Topic Ltd., December 2010. http://www.point-topic.com.

[165] M.K. Varanasi. Decision feedback multiuser detection: a systematic approach. *Information Theory, IEEE Transactions on*, 45(1):219 –240, January 1999.

[166] Sergio Verdu. *Multiuser Detection*. Cambridge University Press, New York, NY, USA, 1st edition, 1998.

[167] I. Wahibi, M. Ouzzif, J. Le Masson, and S. Saoudi. Stationary interference cancellation in upstream coordinated dsl using a turbo-MMSE receiver. *Digital Multimedia Broadcasting, International Journal of*, 2008:8, 2008.

[168] A. Wang, J. J. Werner, and S. Kallel. Effect of bridged taps on channel capacity at VDSL frequencies. In *Communications, 1999. ICC '99. 1999 IEEE International Conference on*, 1999.

[169] S. Weinstein and P. Ebert. Data transmission by frequency-division multiplexing using the discrete fourier transform. *Communication Technology, IEEE Transactions on*, 19(5):628 –634, 1971.

[170] J.-J. Werner. The HDSL environment [high bit rate digital subscriber line]. *Selected Areas in Communications, IEEE Journal on*, 9(6):785 –800, August 1991.

[171] J.-J. Werner. Tutorial on carrierless am/pm-Part I: Fundamentals and digital CAP transmitter. *ANSI X3T9.5 TP/PMD*, June 1992.

[172] B. Wiese and K.S. Jacobsen. Use of the reference noise method bounds the performance loss due to upstream power backoff. *Selected Areas in Communications, IEEE Journal on*, 20(5):1075 –1084, June 2002.

[173] P.W. Wolniansky, G.J. Foschini, G.D. Golden, and R.A. Valenzuela. V-blast: an architecture for realizing very high data rates over the rich-scattering wireless channel. In *Signals, Systems, and Electronics, 1998. ISSSE 98. 1998 URSI International Symposium on*, 1998.

[174] A. M. Wyglinski, P. Kabal, and F. Labeau. Variable-length subcarrier equalizers for multicarrier systems. In *Proc. IEEE Vehicular Technology Conference*, Los Angeles, California, USA, 2004.

[175] A.M. Wyglinski, M. Cudnoch, F. Labeau, and P. Kabal. Tap loading of subcarrier equalizers for wireless multicarrier transceivers. *Vehicular Technology, IEEE Transactions on*, 57(1):393 –403, 2008.

[176] Wei Yu and J.M. Cioffi. Multiuser detection for vector multiple access channels using generalized decision feedback equalization. In *Signal Processing Proceedings, 2000. WCCC-ICSP 2000. 5th International Conference on*, 2000.

[177] Wei Yu and R. Lui. Dual methods for nonconvex spectrum optimization of multicarrier systems. *Communications, IEEE Transactions on*, 54(7):1310 –1322, 2006.

[178] Chaohuang Zeng and J.M. Cioffi. Crosstalk cancellation in ADSL systems. In *Global Telecommunications Conference, 2001. GLOBECOM '01. IEEE*, 2001.

[179] W. Zhendao and G.B. Giannakis. Wireless multicarrier communications. *Signal Processing Magazine, IEEE*, 17(3):29 –48, May 2000.

[180] Lin Zhiwei, A.B. Premkumar, and A.S. Madhukumar. Matching pursuit-based tap selection technique for uwb channel equalization. *Communications Letters, IEEE*, 9(9):835 – 837, September 2005.

Publication List

Journals

1. P.K. Pandey , M. Moonen , "Resource allocation in ADSL variable length per-tone equalizers", *IEEE Trans. on Signal Processing*, vol. 56, no. 5, May 2008, pp. 2161-2164

2. P.K. Pandey, M. Moonen, and L. Deneire, "MMSE-based partial crosstalk cancellation for upstream VDSL", *Signal Processing*, Submitted in June 2011

3. P.K. Pandey, M. Moonen, and L. Deneire, "Sparse approximation based resource allocation in DMT transmitters with per-tone pulse shaping", *Signal Processing*, Submitted in June 2011

4. P.K. Pandey, M. Moonen, and L. Deneire, "Sparse approximation based resource allocation in DMT receiver with per-tone equalization", *Signal Processing*, to be submitted

5. P.K. Pandey, M. Moonen, and L. Deneire, "Joint transmit power and filter tap allocation in DMT transceivers", to be submitted

6. P.K. Pandey, M. Moonen, and L. Deneire, "Joint MMSE-based partial crosstalk cancellation and spectrum balancing for upstream VDSL", to be submitted

7. P.K. Pandey, M. Moonen, and L. Deneire, "Sparse approximation based linear MMSE partial crosstalk cancellation and spectrum balancing for upstream VDSL", to be submitted

Conferences

1. P.K. Pandey, M. Moonen, and L. Deneire, "Resource allocation in DMT transmitters with per-tone pulse shaping", *in Proc. of the International*

Conference on Acoustics, Speech, and Signal Processing (ICASSP), Las Vegas, USA, Mar. 2008

2. P.K. Pandey, M. Moonen, and L. Deneire, "Joint transmit power and filter tap allocation in DMT transmitters with per-tone pulse shaping", *in Proc. of the Global Communications Conference (GLOBECOM)*, New orleans, USA, Nov. 2008

3. P.K. Pandey, M. Moonen, and L. Deneire, "MMSE-based partial crosstalk cancellation for Upstream VDSL", *in Proc. of the IEEE International Conference on Communications (IEEE-ICC)*, Cape Town, South Africa, May 2010

Internal report

1. P.K. Pandey, M. Moonen, and L. Deneire, "Resource allocation in DMT transmitters with per-tone pulse shaping", *Internal Report 08-225, ESAT-SISTA, K.U.Leuven (Leuven, Belgium)*, 2008., Lirias number: 242631

Poster

1. P.K. Pandey, M. Moonen, and L. Deneire, "MMSE-based partial crosstalk cancellation for upstream VDSL", *Poster presentation, Bell Labs Colloquium*, Antwerp, Belgium, October 20 2009

Curriculum Vitae



Prabin Kumar Pandey was born in Nepal, in 1978. He received his B.E. in Electrical and Electronics Engineering (Distinction) from Kathmandu University, Nepal in 2001 and M.Sc. in Communication Engineering from RWTH Aachen University, Aachen, Germany in 2005. From October 2005 to August 2006, he was a predoctoral student at the Department of Electrical Engineering under the supervision of Prof. Marc Moonen. Since September 2006, he has been pursuing Ph.D under the supervision of Prof. Marc Moonen and Prof. Luc Deneire at the Department of Electrical Engineering, K.U. Leuven, Belgium.

From 2006 to 2009, he was a Marie Curie Fellow involved in the EST-SIGNAL project (Early Stage Training in Signal processing). Since 2009 he is a Research Assistant with K.U.Leuven. In 2009, he was visiting scholar at CAS group TU Delft, Delft, The Netherlands under the supervision of Prof. Geert Leus. In 2010, he was awarded a travel grant by research Foundation Flanders (FWO), Belgium to attend ICC 2010 in Cape town, South Africa. His research interest includes digital signal processing and optimization of digital communication systems.

Arenberg Doctoral School of Science, Engineering & Technology
Faculty of Engineering
Department of Electrical Engineering
Research group ESAT-SCD: SISTA/COSIC/DOCARCH
Kasteelpark Arenberg 10, B-3301 Leuven

KATHOLIEKE UNIVERSITEIT LEUVEN

ASSOCIATIE K.U.LEUVEN